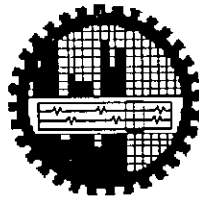


# A STUDY OF ENVIRONMENTAL RADIOACTIVITY IN SOIL SAMPLES

A dissertation submitted in partial fulfillment of the requirement for  
the degree of Master of Philosophy in the Physics Department,  
Bangladesh University of Engineering and Technology, Dhaka

By

**Mohammed Ikbal Kabir**



**Bangladesh University of Engineering and Technology**  
**Dhaka, Bangladesh**  
August 2003

## **DECLARATION**

*This thesis work has been done by the candidate himself and does not contain any material extracted from elsewhere or from a work published by anybody else. The work of this thesis has not been presented elsewhere by the author for any degree or diploma except publication. No other person's work has been used or included without due acknowledgment.*

*Mohammed Ikbal Kabir*  
(Mohammed Ikbal Kabir)

*Candidate*

*Roll No.: 040014002F*

*Registration No: 004572*

*Session: April/2000*

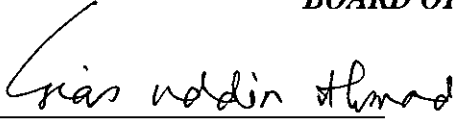




**BANGLADESH UNIVERSITY OF ENGINEERING AND TECHNOLOGY  
DEPARTMENT OF PHYSICS**



***Certification of Thesis work***

*The thesis titled "A Study of Environmental Radioactivity in Soil Samples", submitted by MOHAMMED IKBAL KABIR, Roll No. 040014002F, Registration No. 004572, Session April-2000 has been accepted as satisfactory in partial fulfillment of the requirement for the degree of Master of Philosophy on 4 August 2003.*

**BOARD OF EXAMINERS**

1.   
**Prof. Gias uddin Ahmad (Supervisor)** *Chairman*  
*Professor*  
*Department of Physics, BUET, Dhaka*
2.   
**Dr. Md. Mustafizur Rahman (Co-Supervisor)** *Member*  
*Principal Scientific Officer, BAEC, Dhaka*
3.   
**Dr. Nazma Zaman** *Member*  
*Professor & Head*  
*Department of Physics, BUET, Dhaka*
4.   
**Dr. Md. Feröz Alam Khan** *Member*  
*Associate Professor*  
*Department of Physics, BUET, Dhaka*
5.   
**Prof. M. A. Awal** *Member (External)*  
*Department of Physics*  
*Jahangirnagar University, Savar*  
*Dhaka*

*Dedicated*  
*To*  
*My Parents*

## ACKNOWLEDGEMENT

I express my deepest sense of gratitude to my respected supervisor Dr. Giasuddin Ahmad, Professor, Department of Physics, BUET, and co-supervisor Dr. Md. Mustafizur Rahman, Principal Scientific Officer, Health Physics Division, Atomic Energy Centre (AEC), Dhaka, for their supervision, guidance, encouragement, suggestions and discussions at every stage of this work.

I would like to thank the Director, AEC, Dhaka and Mahfuza Begum, Head, Health Physics Division, Atomic Energy Center (AEC), Dhaka, for allowing me to do the thesis work under the Health Physics Division.

I am thankful to Dr. Nazma Zaman, Head and Professor, Department of Physics, BUET, for giving me permission to carry out this thesis work. I also take this opportunity to thank and express my gratitude to Dr. Mominul Huq, Dr. Md. Abu Hashan Bhuiyan and Dr. Jiban Podder, Professors, Department of Physics, BUET, for their encouragement. I'm also thankful to Dr. Feroz Alam Khan, Dr. Md. Nazrul Islam and all other teachers of Physics Department, BUET, for their encouragement. I am also grateful to the BUET authorities for providing me with the financial grants for this research.

I would like to thank the Chairman, Bangladesh Atomic Energy Commission, for giving me permission to work at the Health Physics Division, Atomic Energy Center (AEC), Dhaka.

I'm grateful to Rubina Rahman, Scientific Officer, Health Physics Division, Atomic Energy Center (AEC), Dhaka, for her sincere help and constructive suggestions during this work.

Further, I would like to express my sincere gratitude to all other members of Health Physics Division, Atomic Energy Center (AEC), Dhaka, for their inspirations and co-operations in successful completion of this work.

I'm thankful to Md. Rafi Uddin, Lecturer, Department of Physics, BUET, and Md, Niyamat Ali, Lecturer in Physics, Sylhet Cadet College, for their co-operation and encouragement.

I like to offer my sincere thanks to Mr. Swapon Kumar Das, Mr. Lutfur Rahman Sarker and all other Laboratory and Office assistants of the Department of Physics, BUET, for their cordial assistance rendered in course of this work.

Finally, warm thanks are also due to Belal Uddin and Ispahani Islam and all other friends and well-wishers for their encouragement.

I am deeply indebted and grateful to my brothers, sisters and parents for their encouragement, sacrifice, affection, and blessing that paved the way to my higher education.

August, 2003

Mohammed Iqbal Kabir

## ABSTRACT

The surface soil samples were collected from 42 different locations in Rangpur and Dinajpur at a depth of 0-5 cm. Total beta activities of the samples were measured using Low Beta Counter. Activity concentrations of the radionuclides  $^{238}\text{U}$ ,  $^{232}\text{Th}$ ,  $^{137}\text{Cs}$  and  $^{40}\text{K}$  were determined from gamma ray spectrum of the soil. The average gross activity was found to be  $38.61 \pm 4.55$  pCi/g with a range of  $30.17 \pm 4.30$  pCi/g to  $50.42 \pm 4.82$  pCi/g for the soil of Rangpur. The average beta activity was found to be  $33.94 \pm 4.21$  pCi/g ranging from  $27.10 \pm 4.41$  pCi/g to  $46.95 \pm 4.60$  pCi/g for the soil of Dinajpur. The mean activities of  $^{238}\text{U}$ ,  $^{232}\text{Th}$ ,  $^{137}\text{Cs}$  and  $^{40}\text{K}$  were  $42.65 \pm 2.34$ ,  $45.58 \pm 5.19$ ,  $6.55 \pm 0.6$  and  $652.91 \pm 50.37$  Bq/kg from the soil of Rangpur and  $37.06 \pm 2.01$ ,  $44.13 \pm 4.66$ ,  $5.05 \pm 0.53$  and  $543.90 \pm 45.36$  Bq/kg from the soil of Dinajpur respectively.  $^{137}\text{Cs}$  was found only in seven samples out of 32 and these were very low. This implies that there is no environmental radiation effect in Bangladesh due to nuclear fallout. Considerably elevated concentrations of  $^{238}\text{U}$ ,  $^{232}\text{Th}$  and  $^{40}\text{K}$  were found compared to countries.

# CONTENTS

<b>CHAPTER-I</b>	<b>TITLES/ SUB-TITLES</b>	<b>Page</b>
<b>INTRODUCTION</b>		
1	General	1
		4
1.1	Radioactivity	6
1.1.1	Types of Radiation	8
1.1.2	Sources of Natural Radiation	11
1.1.3	Sources of Man-Made Radiation	15
1.1.4	Ionising Radiation	17
1.1.5	Non Ionizing Radiation	
1.2	Biological Effects of Radiation	17
1.2.1	Effects of radiation on cell	17
1.2.2	Effects of Radiation on Biological Body	18
1.2.3	Somatic Effects	19
1.2.4	Genetic Effects	19
1.2.5	Stochastic Effects	20
1.2.6	Non-Stochastic Effects	20
1.3	Ionising Radiation Damage and Cancer	21
1.4	Aim and Objectives of the Research Work	22
<b>CHAPTER-II</b>		
<b>LITERATURE REVIEW</b>		
2	Introduction	24
2.1	Review of Previous Works	24
<b>CHAPTER-III</b>		
<b>EXPERIMENTAL SET-UP</b>		
3.1	Overview of Radiation Detectors	41
3.1.1	The Ordinary Photographic Film	41
3.1.2	The Gas Filled Detectors	41
3.1.3	Proportional Counter	42
3.1.4	Scintillation Method	42
3.1.5	Thermoluminescence Detector	42
3.1.6	Cerenkov Detectors	43
3.1.7	Semiconductor Radiation Detectors	43
3.2	The Principles of Operation of a Gas-Filled Detector	44
3.3	The Operation of a Proportional Counter	47
3.4	G5000 Automatic Low Level Counting System	50
3.4.1	Introduction	50

3.4.2	System Description	51
3.4.2.1	Detector Assembly	51
3.4.2.2	Changer Assembly	51
3.4.2.3	System Electronics	51
3.4.2.4	Processor Control Section	52
3.4.2.5	Sample Changer Front Panel Description	52
3.4.2.6	System Performance	52
3.4.3	Theory of Operation	53
3.4.3.1	Proportional Counters	53
3.4.4	Factors Affecting the Count Rate	54
3.4.4.1	Background counts	54
3.4.4.2	Cosmic Radiation	55
3.4.4.3	Noise	55
3.4.4.4	Count Rate Loss	55
3.4.4.5	Sample Distance	56
3.4.4.6	Window Absorption	56
3.4.4.7	Detector Efficiency	56
3.4.4.8	Detector Area	57
3.4.4.9	Sample Preparation	57
3.4.5	Statistics of Measurement	57
3.4.5.1	Pico-Curies Per Volume Calculation	57
3.4.5.2	Standard Deviation	57
3.4.5.3	Background Subtraction	59
3.4.5.4	Background Checks	59
3.5	High Purity Germanium (HPGe) Detectors	61
3.5.1	Advantages of the HPGe Detectors	62
3.6	A Brief Description of HPGe	63
3.6.1	Liquid nitrogen (LN <sub>2</sub> ) Dewar	63
3.6.2	Cryostat	63
3.6.3	Preamplifier	64
3.6.4	Amplifier	65
3.6.5	High Voltage Power Supply	65
3.6.6	Personal Computer Analyser (PCA)	65
3.6.7	Lead Shielding Arrangement of the HPGe Detector	66
3.7	Calibration of Detector Parameters	68
3.7.1	Energy calibration	68
3.7.2	Counting Efficiency of the HPGe Detector	69
3.7.3	Energy Resolution	69



## **CHAPTER-IV METHODS AND MATERIALS**

4.1	Sample Collection	71
4.2	Sample Preparation	71
4.3	Standard Beta Source	72
4.4	Beta Activity Measurement	75
4.5	Error Calculation	76
4.6	Efficiency of HPGe Detector	79
4.7	Activity of Gamma	79

## **CHAPTER-V RESULTS AND DISCUSSION**

5.1	Introduction	85
5.2	Gross Beta Activity of the Soil of Rangpur	85
5.3	Gross Beta Activity of the Soil of Dinajpur	85
5.4	Gamma Activity for the Soil of Rangpur	85
5.5	Gamma Activity for the Soil of Dinajpur	86
5.6	Conclusion	87

<b>REFERENCES</b>	<b>88</b>
-------------------	-----------

<b>APPENDIX</b>	<b>96</b>
-----------------	-----------

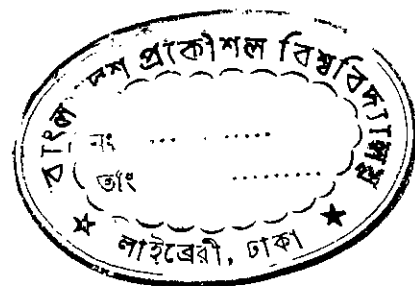
## LIST OF FIGURES

<b>FIGURE No.</b>	<b>TITLE</b>	<b>Page</b>
Figure 1.1	Presents Some Naturally Occurring Radioactive Isotopes	10
Figure 1.2	Atmospheric Nuclear Tests	13
Figure 1.3	Average Individual Global Radiation Dose In The 1990s From Nuclear Explosions	14
Figure 3.1	Shows A Schematic Diagram Of A Gas-Filled Chamber With A Central Electrode	45
Figure 3.2	Proportional Counter	47
Figure 3.3	Gas Ionization Curve	48
Figure 3.4	General Specifications Of A Proportional Counter.	61
Figure 4.1	Efficiency curve of Low Beta Counter using Potassium Chloride (KCl)	73

## LIST OF TABLES

TABLE No.	TITLE	Page
Table 1.1	Examples of primordial, cosmogenic, and artificial radionuclides with their half-lives and radiation emitted	5
Table 4.1	Efficiency calculation of the low beta counter using different weight of potassium chloride (KCl)	72
Table 4.2	Efficiency of low beta counter corresponding to different weight of soil samples collected from Rangpur	74
Table 4.3	Efficiency of low beta counter corresponding to different weight of soil samples collected from Dinajpur	75
Table 4.4	Total beta activity of the soil samples collected from different locations of Rangpur	77
Table 4.5	Total beta activity of the soil samples collected from different locations of Dinajpur	78
Table 4.6	Efficiency calculation of High Purity Germanium (HPGe) detector for different energy	79
Table 4.7	Activity concentration of different radionuclides in soil samples collected from different locations of Rangpur district	81
Table 4.8	Activity concentration of different radionuclides in soil samples collected from different locations of Dinajpur district	82
Table 4.9	Distribution of $^{238}\text{U}$ , $^{232}\text{Th}$ , $^{137}\text{Cs}$ and $^{40}\text{K}$ in soil samples collected from different locations of Rangpur	83
Table 4.10	Distribution of $^{238}\text{U}$ , $^{232}\text{Th}$ , $^{137}\text{Cs}$ and $^{40}\text{K}$ in soil samples collected from different locations of Dinajpur	84
Table-A	Quality factors of various types of radiation	97
Table -B	Radiation output in mGy/h at 1 meter from the source of gamma emitting radionuclide	99
Table- C	Relationship between radiation units	100

## CHAPTER-I INTRODUCTION



### 1 General

Man is always exposed to radiation from natural and artificial radiation sources in his environment. While there have been natural nuclides since the beginning of earth existence. The main source comes from natural sources in space, rocks, soil, water and even the human body itself. This is called background radiation and its levels vary from place to place, though the average dose is fairly constant. The radiation which is of most concern is artificial radiation which results from human activities. Sources of this include the medical use of radioactive materials, fallout and contamination from nuclear bomb tests, discharges from the nuclear industry, and the storage and dumping of radioactive waste. For the safe use of artificial radiation, careful monitoring of the environment around us is essential<sup>[1]</sup>.

With a half-life of 29 years, strontium-90 loses its radioactivity slowly. It is also highly toxic because of its ability to mimic calcium in the body, becoming part of the bone marrow tissue and damaging blood-producing cells. Uranium-238 is a heavy metal that is chemically toxic in certain doses. It is also a long-lived alpha and gamma particle emitter with isotopes of concern.

If strontium-90 or uranium-238 is present in soil, either will produce highly energized beta particles. Although strontium-90 and uranium-238 produce energetic betas that are indistinguishable from one another, the two elements are rarely found in the same location; the former is a fission product and the latter occurs in nature. In a case where the two are found together, such as in regions contaminated as a result of the Chernobyl catastrophe<sup>[2]</sup>.

The radiobiological hazard of worldwide fallout is essentially a long-term one due to the potential accumulation of long-lived radioisotopes, such as strontium-90 and cesium-137, in the body as a result of ingestion of foods which had incorporated these radioactive materials. This hazard is much less serious than those which are associated with local fallout.

In addition, atoms of environmental material, such as soil, air, and water, may be activated, depending on their composition and distance from the burst. For example, a small area around ground zero may become hazardous as a result of exposure of the minerals in the soil to initial neutron radiation. This is due principally to neutron capture by sodium (Na), manganese, aluminum, and silicon in the soil. This is a negligible hazard because of the limited area involved.

While artificial radiation accounts for a small proportion of the total, its effects can be disproportionate. Some of the radioactive materials discharged by human activity are not found in nature, such as plutonium, while others that are found naturally may be discharged in different physical and chemical forms, allowing them to spread more readily into the environment, or perhaps accumulate in the food-chain.

To estimate the dose that a person may receive, we need to look at all the possible ways in which the radionuclides can get into the body, and in what form. If the radionuclides are deposited on the ground, some will be transferred to the food plants in the same way that the plants take in other nutrients. When those plants are eaten, some of the radioactivity is transferred to the person. As well as food, people also eat dust, either unintentionally by poor hygiene or food preparation, or deliberately because of a medical condition, although this is rare. To take account of this, the calculations used to estimate doses normally allow for a certain percentage of soil to be eaten. The concentration of radionuclides in the soil is sometimes much higher than in the food. Consequently, even if only small quantities of soil are eaten, this process can account for much of the activity that is eaten. The soils used were loam, peat and sand, which had been deliberately contaminated with caesium-137, americium-241, plutonium-239 and strontium-90 some years ago. The measured availability of caesium-137, americium-241, plutonium-239 and strontium-90 associated with loam, sand and peat soils were about 3%, 3%, 10% and 50% respectively. These soils have very different characteristics than most other types of soil <sup>[3]</sup>.

For all these reasons, simple comparisons of background and artificial radioactivity may not reflect the relative hazards. Equally important, it has never been shown that there is such a thing as a safe dose of radiation and so the fact that we are progressively

raising global levels should be of as much concern to us as the possibility of another major nuclear disaster like Chernobyl. Every nuclear test, nuclear reactor or shipment of plutonium means an additional and unnecessary health risk.

In general, the effects of radiation can be divided into those which affect the individuals exposed and those which affect their descendants. Somatic effects are those which appear in the irradiated or exposed individual. These include cancer and leukaemia. Hereditary or genetic effects are those which arise in subsequent generations<sup>[4]</sup>.

Many of the elements which our bodies need are produced by the nuclear industry as radioactive isotopes or variants. Some of these are released into the environment, for example iodine and carbon, two common elements used by our bodies. Our bodies do not know the difference between an element which is radioactive and one which is not. So radioactive elements can be absorbed into living tissues, bones or the blood, where they continue to give off radiation. Radioactive strontium behaves like calcium—an essential ingredient in our bones. Strontium deposits in the bones, where the blood cells are formed, causing leukaemia<sup>[5]</sup>.

There are three principal effects which radiation can have on cells: firstly the cell may be killed; secondly the way the cell multiplies may be affected, resulting in cancer; and thirdly damage may occur in the cells of the ovaries or testes, leading to the development of a child with an inherited abnormality.

In most cases, cell death only becomes significant when large numbers of cells are killed, and the effects of cell death therefore only become apparent at comparatively high dose levels. If a damaged cell is able to survive a radiation dose, the situation is different. In many cases the effect of the cell damage may never become apparent. A few malfunctioning cells will not significantly affect an organ where the large majority are still behaving normally.

However, if the affected cell is a germ cell within the ovaries or testes, the situation is different. Ionising radiation can damage DNA, the molecule which acts as the cell's 'instruction book'. If that germ cell later forms a child, all of the child's cells will carry

the same defect. The localized chemical alteration of DNA in a single cell may be expressed as an inherited abnormality in one or many future generations<sup>16</sup>.

In the same way that a somatic cell in body tissue is changed in such a way that it or its descendants escape the control processes which normally control cell replication, the group of cells formed may continue to have a selective advantage in growth over surrounding tissue. It may ultimately increase sufficiently in size to form a detectable cancer and in some cases cause death by spreading locally or to other parts of the body.

While there is now broad agreement about the effects of high-level radiation, there is controversy over the long-term effect of low-level doses. This is complicated by the length of time it takes for effects to show up, the fact that the populations being studied (bomb survivors, people exposed to nuclear tests or workers in the nuclear industry) are small and exact doses are hard to calculate<sup>17</sup>.

All that can be said is that predictions made about the effects of a given dose vary. A growing number of scientists point to evidence that there is a disproportionately high risk from low doses radiation. Others assume a directly proportionate link between the received dose and the risk of cancer for all levels of dose, while there are some who claim that at low doses there is a disproportionately low level of risk<sup>18,91</sup>.

### **1.1 Radioactivity**

Radioactivity is a special attribute recognized more by its outward effect rather than its cause. That effect is the spontaneous and irrepressible emission of radiation. The majority of the chemical elements that make up the natural world are now known to exist as mixtures of isotopes. Less than 25% of the elements occur in a single isotopic form. A few chemical elements in the Periodic Table exist with isotopes in which the arrangement of protons and neutrons is less than ideal. Because of this, these elements exhibit a degree of nuclear instability which manifests itself as radioactivity. The phenomenon of radioactivity is not only exhibited by elements at the extreme top end of the Periodic Table (e.g., uranium, thorium, radium and lead). Indeed isotopes of potassium, some rare earths (neodymium, samarium and gadolinium), and hafnium, osmium and platinum have also been found to be slightly radioactive. Isotopes which spontaneously emit radiation are called radio-isotopes.

Radioactivity has existed since the beginning of the universe. The earth contained radioactive isotopes long before life started to develop. Even human beings contain radioactive atoms, so-called radioisotopes or radionuclides. Natural radionuclides, either have existed since the beginning of the universe (primordial radionuclides), or are being formed continuously by cosmic radiation (cosmogenic radionuclides). Nuclear reactor has created many artificial radionuclides, which are also detectable in the environment today.

Table 1.1: Examples of primordial, cosmogenic, and artificial radionuclides with their half-lives and radiation emitted <sup>[10]</sup>:

<b>Primordial radionuclides</b>	<b>Half-life (years)</b>	<b>Radiation emitted</b>
Potassium 40	1,280,000,000	$\beta^+$ and $\beta^-$
Rubidium 87	47,000,000,000	$\beta^-$
Thorium 232	14,100,000,000	$\alpha$
Uranium 235	704,000,000	$\alpha$
Uranium 238	4,470,000,000	$\alpha$

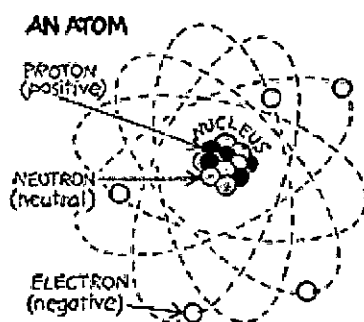
<b>Cosmogenic radionuclides</b>	<b>Half-life (years)</b>	<b>Radiation emitted</b>
Tritium (3H)	12.3	$\beta^-$
Beryllium 7	57 days	Electron capture decay + gamma
Beryllium 10	1,600,000	$\beta^-$
Carbon 14	5736	$\beta^-$
Silicium 32	172	$\beta^-$



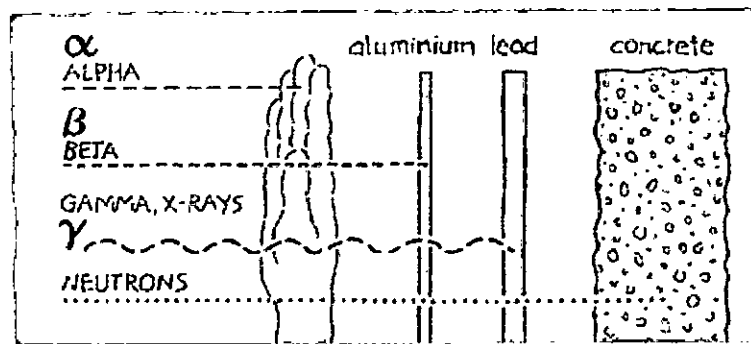
Artificial radionuclides	Half-life (years)	Radiation emitted
Tritium (3H)	12.3	$\beta^-$
Cobalt 60	5.3	$\beta^-$ and $\gamma$
Strontium 90	29	$\beta^-$
Technetium 99	213,000	$\beta^-$
Ruthenium 106	1.01	$\beta^-$ and $\gamma$
Antimony 125	2.77	$\beta^-$ and $\gamma$
Caesium 134	2.04	$\beta^-$ and $\gamma$
Caesium 137	30	$\beta^-$ and $\gamma$
Plutonium 238	87.8	$\alpha$
Plutonium 239	24,390	$\alpha$
Plutonium 241	14.9	$\beta^-$
Americium 241	433	$\alpha$

### 1.1.1 Types of Radiation

Nuclear radiation arises from hundreds of different kinds of unstable atoms. Many exist in nature, the majority are created in nuclear reactions. Ionising radiation which can damage living tissue is emitted as the radioisotopes change ('decay') spontaneously to become different kinds of atoms. Ionising radiation produces electrically charged particles called ions in the materials it strikes. This process is called ionisation. In the large chemical molecules of which all living things are made the changes caused may be biologically important. The principal kinds of ionising radiation are listed below.



There are several types of ionising radiation:



Alpha particles consist of two protons and two neutrons, in the form of atomic nuclei. They thus have a positive electrical charge and are emitted from naturally occurring heavy elements such as uranium and radium, as well as from some man-made elements. Because of their relatively large size, alpha particles collide readily with matter and lose their energy quickly. They therefore have little penetrating power and can be stopped by the first layer of skin or a sheet of paper.

However, if alpha sources are taken into the body, for example by breathing or swallowing radioactive dust, alpha particles can affect the body's cells. Inside the body, because they give up their energy over a relatively short distance, alpha particles can inflict more severe biological damage than other radiations. People everywhere are typically exposed to up to 3 mSv/yr from inhaled radon without apparent ill-effect. However, in industrial situations its control is a high priority.

Beta particles are fast-moving electrons ejected from the nuclei of atoms. These particles are much smaller than alpha particles and can penetrate up to 1 to 2 centimetres of water or human flesh. Beta particles are emitted from many radioactive elements. They can be stopped by a sheet of aluminium a few millimetres thick.

X-rays and gamma rays, like light, represent energy transmitted in a wave without the movement of material, just as heat and light from a fire or the sun travels through space. X-rays and gamma rays are virtually identical except that X-rays are generally produced artificially rather than coming from the atomic nucleus. Unlike light, X-rays and gamma rays have great penetrating power and can pass through the human body. Radiation dose badges are worn by workers in exposed situations to detect them and hence monitor exposure. All of us receive about 0.5 - 1 mSv per year of gamma

radiation from cosmic rays and from rocks, and in some places, much more. Thick barriers of concrete, lead or water are used as protection from them.

Cosmic radiation consists of very energetic particles including protons which bombard the earth from outer space. It is more intense at higher altitudes than at sea level where the earth's atmosphere is most dense and gives the greatest protection.

Neutrons are particles which are also very penetrating. On Earth, they mostly come from the splitting, or fissioning, of certain atoms inside a nuclear reactor. Neutrons are not normally a problem outside nuclear plants. However, fast neutrons can be very destructive to human tissue. Public dose limits for exposure from uranium mining or nuclear plants are usually set at 1 mSv/yr above background. Water and concrete are the most commonly used shields against neutron radiation from the core of the nuclear reactor.

It is important to understand that alpha, beta, gamma and X-radiation does not cause the body to become radioactive. However, most materials in their natural state (including body tissue) contain measurable amounts of radioactivity <sup>[11, 12]</sup>.

### **1.1.2 Sources of Natural Radiation**

We are all immersed in naturally occurring ionizing radiation. Radiation reaches us from outer space and it comes from radionuclides present in rocks, buildings, air, and even our own bodies. Each flake of snow, each grain of soil, every drop of rain—and even every person on this planet—emits radiation. And every day, at least a billion particles of natural radiation enter our bodies <sup>[11]</sup>.

Natural sources of radiation are cosmic radiation and terrestrial radiation arising from the decay of naturally occurring radioactive substances. Most radiation exposure is from natural sources. These include: radioactivity in rocks and soil of the earth's crust; radon, a radioactive gas from the earth and present in the air; and cosmic radiation. About one quarter of natural radiation comes from the human body itself. The human environment has always been radioactive. These natural radionuclides are background loads, distributed over great areas. They enter the human body through foodstuffs,

drinking water and air. This background level in the world varies depending on the geological nature of soils and the altitude of residency.

The element potassium, a normal constituent of the human body, exists in three isotopic forms- potassium-39, potassium-40, and potassium-41. Potassium-39 and potassium-41 are stable isotopes and together constitute 99.99% of potassium. Although only present in the low concentration of 0.01%, in contrast to the other potassium isotopes, potassium-40 emits radiation and therefore must be considered as a radioisotope of potassium. The relative abundances of the three isotopes of potassium are constant, regardless of source. Therefore, as a consequence of there being 150 to 200 grams of potassium in the adult human body, some 15 to 20 milligrams of it must always exist as the radioisotope  $^{40}\text{K}$ .

Another source of natural radioactivity is the air we breathe. Bombarded by radiation from the sun and outer space, atmospheric nitrogen undergoes nuclear reactions to produce the carbon radioisotope, carbon-14 and radioactive hydrogen (tritium,  $^3\text{H}$ ).

During our lifetime, we participate in natural processes involving  $^{14}\text{C}$  absorption and excretion and, as a result, the  $^{14}\text{C}$  in our tissues gradually increases to an equilibrium level. On a much longer scale, the levels of  $^{14}\text{C}$  in our tissues decrease due to radioactive decay. Because the half-life of  $^{14}\text{C}$  is 5730 years, the effect of decay is not noticeable while we are alive. Only after we are dead and have stopped assimilating the radioisotope is an age effect measurable. Then an accurate measure of the residual  $^{14}\text{C}$  becomes a very sensitive gauge of the age of an object that was once alive.

The most significant of the naturally occurring radioisotopes are radon-222 and radon-220. These radioactive gases seep out from rocks containing uranium and thorium to be responsible for between 50 and 80% of the background radiation exposure. Thorium is present in soil, rocks, surface water, groundwater, plants, and animals at low concentrations, on the order of ten parts per million. It is about three times as abundant as uranium and about as abundant as lead or molybdenum. Higher levels are present in certain geological materials such as monazite sands. The chief commercial source is monazite sands in the United States as well as Brazil, India, Australia, and South Africa. The concentration of thorium oxide in monazite sands is about 3 to 10%.

Essentially all naturally occurring thorium is present as thorium-232. Thorium-230 is a radioactive decay product of uranium-238 and is found in low concentrations in uranium deposits and mill tailings. The concentration of thorium in plants is typically about 0.0042 (or 0.42%) of the soil. The concentration of radon in air is highest in localities where igneous rocks are prevalent. It can be trapped in poorly ventilated buildings.

Much higher levels of natural radioactivity have existed throughout the history of the earth. Fortunately, the planet is old enough to have allowed the original intense radioactivity to all but disappear. **Figure 1.1** presents some naturally occurring radioactive isotopes.

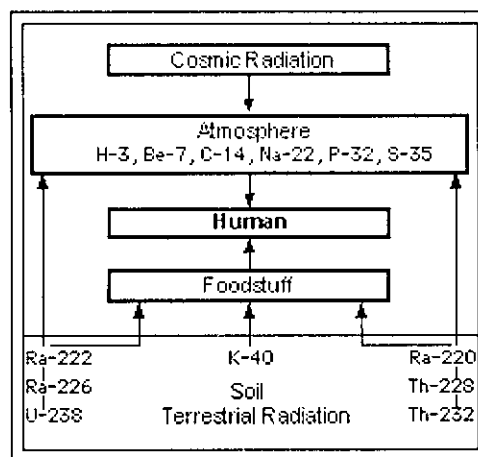


Fig. 1.1: Sources of Natural Radioactivity (H = hydrogen, Be = beryllium, C = carbon, Na = sodium, P = phosphorus, S = sulfur, K = potassium, Ra = radium, U = uranium, Th = thorium).

The individual dose rate of natural radiation that the average inhabitant of Earth receives is about 2.2 mSv per year but this varies depending on the geology and altitude where people live. In some regions—for example, parts of India, Iran, Brazil and Bangladesh—the natural dose rate is up to a hundred times higher. In Bangladesh, the average dose rate due to the external background radiation was found to be 13 mSv.y<sup>-1</sup> with a range of 2.6-44.0 at Cox’s Bazar sea beach sand areas. And no adverse genetic, carcinogenic, or other malign effects of those higher doses have ever been observed among the people, animals, and plants that have lived in those parts since time immemorial [13, 14, 15, 16].

### 1.1.3 Sources of Man-Made Radiation

Radiation arising from human activities typically accounts for up to 25% of the public's exposure every year. This radiation is no different from natural radiation except that it can be controlled. X-rays and other medical procedures account for most exposure from this quarter. The most familiar and, in national terms, the largest of these sources of exposure is medical X-rays. The rest comes from coal burning, electrical appliances, and sundry sources. Less than 1% of exposure is due to the fallout from past testing of nuclear weapons or the generation of electricity in nuclear, as well as coal and geothermal power plants<sup>1171</sup>.

#### **Radioisotopes in nuclear medicine:**

In Nuclear Medicine, a radioisotope is administered to a patient either to aid the diagnosis of disease or for the treatment of disease. The radioisotopes used in diagnostic nuclear medicine are selected on the basis of their ability to provide useful clinical information (usually by providing an image of an internal structure in the human body or by visualizing various stages in the function of an organ) while exposing the patient to only minimal radiation. Reactor produced technetium-99m ( $^{99m}\text{Tc}$ ) is pre-eminent, being used in more than 80% of the estimated 100,000 patient studies that are performed world-wide each day. After ( $^{99m}\text{Tc}$ ), a series of cyclotron produced radioisotopes, such as thallium-201 ( $^{201}\text{Tl}$ ), gallium-67 ( $^{67}\text{Ga}$ ), indium-111 ( $^{111}\text{In}$ ) and iodine-123 ( $^{123}\text{I}$ ), are the next most popular.

A different group of radioisotopes are used for therapeutic purposes. Well-established examples are iodine-131 ( $^{131}\text{I}$ ), phosphorous-32 ( $^{32}\text{P}$ ) and yttrium-90 ( $^{90}\text{Y}$ ) but several other are being investigated for possible application. Examples of these are samarium-153 ( $^{153}\text{Sm}$ ), rhenium-186 and rhenium-188 ( $^{186}\text{Re}$ ,  $^{188}\text{Re}$ ), dysprosium-165 ( $^{165}\text{Dy}$ ) and holmium-166 ( $^{166}\text{Ho}$ )<sup>1101</sup>.

#### **Nuclear weapons and reactor:**

The atmospheric nuclear weapons tests of the 50's and 60's were the primary causes of high levels of global fallout. Radioactive materials were diffused depending on the extent and form of the emissions, and are found even in areas otherwise uninfluenced by human activity. The reactor accident at Chernobyl on 26 April 1986 dramatically demonstrated the dangers involved in man-made radioactivity. The Chernobyl

catastrophe was incomparably larger than the reactor accident in Harrisburg, USA in 1979. Chernobyl released enormous amounts of radioactive substances. Wind and weather dynamics transported these substances and deposited them onto the earth as radioactive dust and rain (fallout, washout).

Nuclear fission in a nuclear reactor produces a range of radioactive matter, the fission products. The exact nature and composition of these often long-lived products depends on the type of reactor, its operational life, and its rate of utilization. Knowledge of these factors enable clear statements to be made about the emissions from the Chernobyl accident. The primary emissions were radioactive iodine and cesium. Other emissions were strontium, molybdenum, barium, and a less familiar element, ruthenium.

# Radiation Risk and Ethics

by *Zbigniew Jaworowski*

---

*FIGURE 1.2*



*FIGURE 1.2* ATMOSPHERIC NUCLEAR tests, like the one shown here (XX-27 Charlie, a 14 kiloton device exploded over Yucca Flats, Nevada, on 30 October 1951), released radioactive fallout but did not lead to high average doses of radiation—even for the inhabitants of Nevada. (Photo courtesy of US Department of Energy.)

---



**FIGURE 1.3**

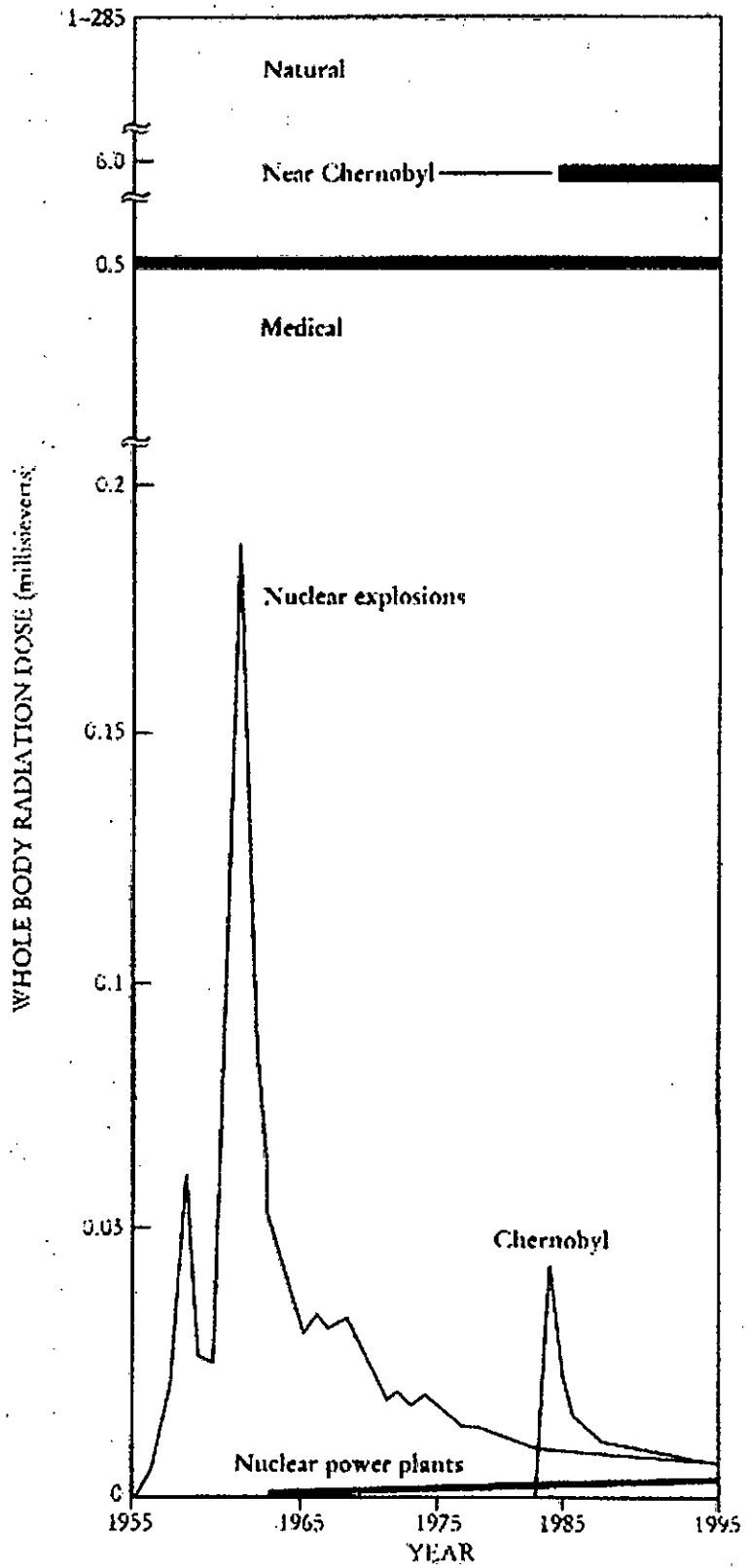


**Figure 1.3 Average individual global radiation dose** in the 1990s from nuclear explosions, the Chernobyl accident, and commercial nuclear power plants combined was about 0.4% of the average natural dose of 2.2 mSv per year. In areas of Belarus, Ukraine, and Russia that were highly contaminated by Chernobyl fallout, the average individual dose was actually much lower than that in the regions with high natural radiation. The greatest man-made contribution to radiation dose has been irradiation from x-ray diagnostics in medicine, which accounts for about 20% of the average natural radiation dose. Natural exposure is assumed to be stable. The temporal trends in medical and local Chernobyl exposures are not presented. (Based on data from UNSCEAR.)<sup>11</sup>.

#### **1.1.4 Ionising Radiation**

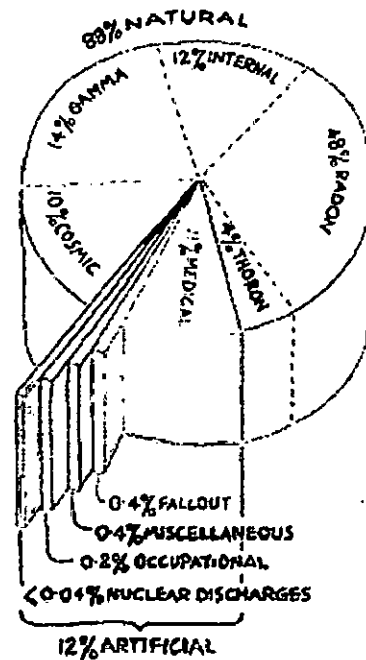
Ionising radiation is the energy produced from natural and man-made radioactive materials. It is present in the environment because of naturally occurring radioactive minerals remaining from the very early formation of the planet. This leads to exposure to gamma rays and radioactive radon gas from certain rocks and from radioactive material in our food and drink. We are also exposed to natural ionising radiation that comes from outer space and passes through the atmosphere of the planet – so-called cosmic radiation.

There are three main sources of man-made ionising radiation. First, it is used in medicine for treating cancer and for the diagnosis of many diseases. Second, radioactive materials are also used in industry, primarily for measurement purposes and for producing electricity. Both medical and industrial uses of radiation produce radioactive waste. Third, it is present as fallout from previous nuclear weapon explosions and other accidents/incidents world-wide.

Naturally occurring background radiation is the main source of exposure for most people. Levels typically range from about 1.5 to 3.5 millisievert per year but can be more than 50 mSv/yr. The highest known level of background radiation affecting a substantial population is in Kerala and Madras States in India where some 140,000 people receive doses which average over 15 millisievert per year from gamma radiation

in addition to a similar dose from radon. Comparable levels occur in Brazil and Sudan, with average exposures up to about 40 mSv/yr to many people.

Several places are known in Iran, India and Europe where natural background radiation gives an annual dose of more than 50 mSv and up to 260 mSv (at Ramsar in Iran). Lifetime doses from natural radiation range up to several thousand millisievert. However, there is no evidence of increased cancers or other health problems arising from these high natural levels. A typical breakdown between natural background and artificial sources of radiation is shown in the pie chart.



Natural radiation contributes about 88% of the annual dose to the population and medical procedures most of the remaining 12%. Natural and artificial radiations are not different in kind or effect.

The damaging effects of ionising radiation come from the packages of high energy that are released from radioactive material. Although different types of ionising radiation have different patterns of energy release and penetrating power there is no general property that makes man-made ionising radiation different and more damaging than the ionising radiation that comes from natural radioactive material. This means that we can make direct comparisons between doses from man-made sources of ionising radiation and those from natural sources<sup>[12]</sup>.

### 1.1.5 Non Ionizing Radiation

Finally it is important to know that the radiations in the environment that come from sunlight, power-lines, electrical equipment and mobile phone systems do not have enough energy to produce these ionisations. Therefore, they are called non-ionising radiations.

## 1.2 Biological Effects of Radiation

### 1.2.1 Effects of radiation on cell

Cell is a basic unit of life. The tissues and organs are made up of such cells. It is estimated that the adult human body consists of about  $10^{14}$  cells. The biological effects of radiation are the manifestations of the interaction between radiation and biological cells.

Biological tissues comprise of 70% of water, the remaining composition being special macro-molecules and other elements. The size of the cells varies from tissue to tissue and from species to species. In human body, the smallest cell is the special leukocyte (white blood cell) and has a diameter of 3 to 4 microns. The cell consists of a central nucleus and surrounding cytoplasm.

The effects on cell can be explained in terms of direct and indirect action of radiation. In direct action, the sensitive volumes (e.g., molecules, atoms) in the cells are affected by direct absorption of energy from radiation. The sensitive volume is treated as the target and each ionization as a hit, where a single hit can inactivate the target.

In indirect action, the sensitive volume is inactivated by transfer of energy from another volume, which has absorbed energy from radiation, either directly or indirectly.

The processes leading to radiation damage to cells are often considered in four stages:

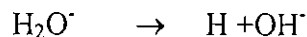
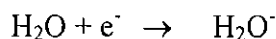
(i) The initial physical stage, lasting only a minute fraction ( $\sim 10^{-16}$ ) of a second in which energy is deposited in the cell and causes ionization. In water, the process may be written as:



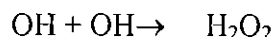
(ii) The physico-chemical stage, lasting about  $10^{-6}$  seconds, in which, the ions interact with water molecules resulting in several new products. For example, the positive ion dissociates:



The negative ion, which is the electron, attaches to a neutral water molecule which then dissociates:



$\text{H}^+$  and  $\text{OH}^-$  take no part in subsequent reactions while H and  $\text{OH}^-$  have an unpaired electron and are chemically highly reactive



and  $\text{H}_2\text{O}_2$  is a strong oxidizing agent.

(iii) The chemical stage, lasting a few seconds in which the reaction products interact with the important organic molecules of the cell. The free radicals and oxidizing agents may attack the complex molecules which form the chromosomes.

(iv) The biological stage, in which the time scale varies from tens of minutes to tens of years depending on the particular symptoms. The chemical changes discussed above can effect an individual cell in a number of ways resulting in: (a) the early death of the cell, (b) the prevention or delay of cell division, (c) a permanent modification passed on to daughter cells.

### 1.2.2 Effects of Radiation on Biological Body

The interaction of ionizing radiation with the human body, arising from external sources outside the body or from internal contamination of the body by radioactive substances, leads to biological effects, which may later show up as clinical symptoms. The nature of these symptoms depend on the amount of radiation absorbed and the rate at which it is received.

The damage caused by the irradiation of human tissue derives from atomic and molecular interactions, such as ionization, excitation and dissociation, which lead eventually to cellular damage. The resulting biological effects of exposure of man to radiation are well known from experiments, accidents, medical treatment, nuclear bomb explosion at Hiroshima and Nagasaki. They are subdivided into somatic effects, which are manifest in the exposed individual itself and into genetic effects, which in general are transmitted to descendants [18].

### 1.2.3 Somatic Effects

The somatic effects due to different levels of radiation received can be classified as:

(a) Early (immediate) effects, (b) Late (delay) effects.

(a) Early effects which occur in the period from a few hours up to a few weeks after an acute exposure, (i.e., a large dose received over a few hour or less). The effects are due to major depletion of cell populations in a number of body organs due to cell killing and the prevention or delay of cell division. The main effects are attributable to bone marrow, gastrointestinal or neuromuscular damage depending on the dose received. Certain effects are common to all categories; these include: (i) Nausea and vomiting, (ii) Malaise and fatigue, (iii) Increase in temperature, (iv) Blood changes.

Another effect which shows up soon after an acute over-exposure to radiation is erythema, (i.e., reddening of the skin).

(b) Late effects which manifest themselves in exposed individuals years after the original exposure. Delayed radiation effects may result from previous acute, high dose exposures or from chronic, low level exposures over a period of years. Long-term effects of ionizing radiation on human are cancer, leukemia, shortening of life span, embryological defects and cataract formation in the lens of the eye. As radiation interacts with human cells, the large molecules which are somewhat flexible in structure can show, 'Degradation' or breaking into smaller units, as well as 'Crosslinking' between themselves. The hydrogen bonds are the weakest and, thus are the first to be broken by radiation. Such structural change can lead to severe alteration in the biochemical properties of the molecule <sup>[18]</sup>. Effects, visible to the human eye, can range from death due to cancer or leukemia to genetic mutations.

### 1.2.4 Genetic Effects

Genetic effects can cause the radiation damage to the chromosome of a germ cell (a sperm or an ovum). During the cellular division, the chromosomes are exactly duplicated, so that all the cells in the body contain the same genetic information. The units of information carrier in chromosomes are called the genes. Nucleic acids (RNA and DNA) are molecules of which the RNA's are found primarily in the cytoplasm of cells and DNA's are major constituents of chromosomes. DNA's have 2-deoxy-D-

ribose as their sugar, adenine, guanine, cytosine and thymine as bases. The DNA exists as a double-stranded helix, i.e., two strands, each of which have the base-sugar-phosphate configuration, are linked by hydrogen bonds between the bases, and the entire structure is coiled into a helical configuration. Since the order and composition of the bases on a DNA molecule are thought to determine the genetic code which is carried by the molecules, an alteration in the base sequence can potentially give rise to a change in genetic composition, or mutation. This in turn may produce gross biochemical or physical alteration in an entire cell or organism. The information which is passed on to the succeeding generations of cells when the DNA replicate itself in cell division and the information that it transcribed into messenger ribonucleic acid (RNA) copies. Genetic effects from the studied children born to survivors of the atomic bombings of Hiroshima and Nagasaki revealed untoward pregnancy outcomes such as stillbirth, major congenital defect, death during first postnatal week, occurrence of death in life-born children, through an average life expectancy of 17 years, children with sex aberration and mutations<sup>[19]</sup>. The studies suggest that the genetic effects of radiation are inversely dependent on dose rate over range of  $8\text{-mGy min}^{-1}$  to  $0.9\text{ Gy min}^{-1}$ <sup>[20]</sup>.

Presently, ICRP has introduced another term to distinguish between effects for which the probability of occurrence depends on the dose received and those for which the severity is related to the dose as:

### **1.2.5 Stochastic Effects**

Defined as the probability of an effect occurring rather than its severity, is regarded as a function of dose, without threshold. The most important somatic stochastic effect is induction of cancers, for which the risk must be regarded as increasing progressively with increasing dose received, without threshold.

### **1.2.6 Non-Stochastic Effects**

Defined as the severity of the effects varies with the dose, and for which a threshold may therefore exist. Example of non-stochastic injuries are cataract of the lens, damage to blood vessels and impairment of fertility.

### **1.3 Ionising Radiation Damage and Cancer**

There is very strong scientific evidence that the energy from radioactive material affects the cells of the body, mainly because of the damage it can cause to cellular genetic material known as DNA. DNA controls the way in which each individual cell behaves. At high doses enough cells may be killed by damage to DNA and other parts of the cell to cause great injury to the body and even rapid death. At lower doses there will be no obvious injury but a number of the cells that survive will have incorrectly repaired the DNA damage so that they carry mutations. Some specific mutations leave the cell at greater risk of being triggered to become cancerous in the future. The body will already carry cells with these mutations from other causes but the ionising radiation exposure increases the number of these mutant cells. It therefore increases the chance of cancer development, usually after many years.

From the early 1900s, it has been known that ionizing radiation (IR) impairs hematopoiesis through a variety of mechanisms. IR exposure directly damages hematopoietic stem cells and alters the capacity of bone marrow stromal elements to support and/or maintain hematopoiesis *in vivo* and *in vitro*. Exposure to IR induces dose-dependent declines in circulating hematopoietic cells not only through reduced bone marrow production, but also by redistribution and apoptosis of mature formed elements of the blood. Recently, the importance of using lymphocyte depletion kinetics to provide a "crude" dose estimate has been emphasized, particularly in rapid assessment of large numbers of individuals who may be exposed to IR through acts of terrorism or by accident. A practical strategy to estimate radiation dose and triage victims based upon clinical symptomatology is presented. An explosion of knowledge has occurred regarding molecular and cellular pathways that trigger and mediate hematologic responses to IR. In addition to damaging DNA, IR alters gene expression and transcription, and interferes with intracellular and intercellular signaling pathways. The clinical expression of these disturbances may be the development of leukemia, the most significant hematologic complication of IR exposure among survivors of the atomic bomb detonations over Japan. Those at greatest risk for leukemia are individuals exposed during childhood. The association of leukemia with chronic, low-dose-rate exposure from nuclear power plant accidents and/or nuclear device testing has been more difficult to establish, due in part to lack of precision and sensitivity of methods to



assess doses that approach background radiation dose. Nevertheless, multiple myeloma may be associated with chronic exposure, particularly in those exposed at older ages [21].

The scientific information that has been obtained worldwide leads NRPB to believe that even the lowest dose of ionising radiation, whether natural or man-made, has a chance of causing cancer. The extra cancer risk from very low doses will be extremely small and, in practice, undetectable in the population. However the extra cancer risk at higher doses may be detectable using statistical methods. Even after high dose exposure it is rarely possible to be certain that radiation was directly responsible for a cancer arising in an individual.

Our knowledge of radiation effects derives primarily from groups of people who have received high doses. Radiation protection standards assume that any dose of radiation, no matter how small, involves a possible risk to human health [9].

#### **1.4 Aim and Objectives of the Research Work**

It has been reported earlier that the environmental radiation level of some of the areas of Bangladesh is higher than the world average; these areas are mainly Chittagong, Cox's Bazar, Sylhet and some other districts of Rajshahi division. The radioactivity of  $^{238}\text{U}$ ,  $^{232}\text{Th}$ , and  $^{40}\text{K}$  in soil of these areas were analyzed by different workers [16, 22-25], but the results of their analysis of radionuclides in soil in different areas of Bangladesh showed that the activity concentration level of  $^{238}\text{U}$ ,  $^{232}\text{Th}$ , and  $^{40}\text{K}$  in soil are not much higher than the range and mean results of natural background radioactivity level of other countries of the world. In order to further investigate the cause of high environmental background radiation in Bangladesh, the present work has been undertaken. Previously, no research work had been carried out on beta activity measurement and beta dose level calculation of the soil of Bangladesh. There has been a few research works on beta activity measurement in soils in various parts of the world [2, 26-27]. Gamma activity measurements of soil have been done in various countries including Bangladesh. Most of these analyses indicate higher activity in the surface soil [16, 28-31].

There is no real measurement of the effect of beta on the population of Bangladesh and gamma radiation from soil contamination. This results would be helpful to assess the radiation exposure to human, animal, and plants.

Man has been exposed to radiation from the environment in which he lives and this natural background radiation comes from various sources i.e., terrestrial sources. Total beta activity measurement will be useful for assessment of radioactive contamination level. The ultimate goal of the present study is to control the environmental radiation hazard, which is contributed by soil sources. The main task of the control system is to find out unusual levels of contamination in Bangladesh in due time and to alert the authorities about the possible radiological hazard to people.

If it is possible to control this hazard, it will reduce the radiation effect on population, which in the long run will reduce economic burden on the country.

## CHAPTER-II LITERATURE REVIEW

### 2 Introduction

Human body is incapable of sensing any type of ionizing radiations. As there was no sensor to measure and detect radiation naturally, these measurements were done by different methods using different instruments. Methods and results of some of the recent works that are most relevant to the present work are described below in brief.

### 2.1 Review of Previous Works

Z. Papp\*, Z. Dezső, S. Daróczy<sup>[32]</sup> made a study on the activity concentrations of  $^{238}\text{U}$ ,  $^{226}\text{Ra}$ ,  $^{232}\text{Th}$ ,  $^{137}\text{Cs}$ , and  $^{40}\text{K}$  in soil samples collected from around a coal-fired power plant from different depths of 81 different locations at Ajka in Hungary. A laboratory method has been developed by the authors to determine the activity concentrations of the nuclides  $^{238}\text{U}$ ,  $^{226}\text{Ra}$ ,  $^{232}\text{Th}$ ,  $^{137}\text{Cs}$ , and  $^{40}\text{K}$ , respectively, in soil samples by direct Ge(Li)  $\gamma$ -ray spectrometry. Considerably elevated concentrations of  $^{238}\text{U}$  and  $^{226}\text{Ra}$  have been found in most samples collected within the populated area. Concentrations of  $^{238}\text{U}$  and  $^{226}\text{Ra}$  in soil decreased regularly with increasing depth at many locations, which can be explained by fly-ash fallout. Concentrations of  $^{238}\text{U}$  and  $^{226}\text{Ra}$  in the top (0-5 cm depth) layer of soil in public areas inside the town of Ajka are 4.7 times higher, on average, than those in the uncontaminated deeper layers, which means there is about  $108 \text{ Bq.kg}^{-1}$  surplus activity concentration above the geological background. A high emanation rate of  $^{222}\text{Ra}$  from the contaminated soil layers and significant disequilibrium between  $^{238}\text{U}$  and  $^{226}\text{Ra}$  activities in some kinds of samples have been found. The mean activities of  $^{238}\text{U}$ ,  $^{226}\text{Ra}$ ,  $^{232}\text{Th}$ ,  $^{137}\text{Cs}$ , and  $^{40}\text{K}$  for the surface soils (0-5 cm) were found to be  $159.72 \pm 58.14 \text{ Bq.kg}^{-1}$ ,  $198.36 \pm 4.37 \text{ Bq.kg}^{-1}$ ,  $29.63 \pm 3.32 \text{ Bq.kg}^{-1}$ ,  $31.76 \pm 2.54 \text{ Bq.kg}^{-1}$  and  $325.72 \pm 35.43 \text{ Bq.kg}^{-1}$  respectively.

S. Selvasekarapandian, R. Sivakumar, N. M. Manikandan, V. Meenakshisundaram, V. M. Raghunath, and V. Gajendran<sup>[33]</sup> measured the concentration of primordial radionuclides in soil samples of Gudalore Taluk in the district of Udagamandalam from the gamma ray spectrum of the soil. The mean activities of  $^{232}\text{Th}$ ,  $^{238}\text{U}$  and  $^{40}\text{K}$  are  $75.3 \pm 44.1$ ,  $37.7 \pm 10.1$  and  $195.2 \pm 85.1 \text{ Bq.kg}^{-1}$  dry weight, respectively. The average outdoor absorbed dose rate in air at a height of 1 m above ground is  $74.3 \pm 27.8 \text{ nGyh}^{-1}$ ,

corresponding to an annual effective dose equivalent of 455.6  $\mu\text{Sv}$ . The dose equivalent ranges from 168.3 to 1250.5  $\mu\text{Sv}$ .

C. A. Papachristodoulou, P. A. Assimakopoulos, N. E. Patronis, and K. G. Ioannides<sup>[34]</sup> have used HPGe  $\gamma$ -ray spectrometry to determine uranium activity and investigate the presence of depleted uranium in soil samples collected from camping sites of the Greek expeditionary team in Kosovo. Assessment of  $^{238}\text{U}$  concentrations was based on measurements of the 63.3 KeV and 92.38 KeV emissions of its first daughter nuclide,  $^{234}\text{Th}$ . To determine the isotope ratio of  $^{238}\text{U}/^{235}\text{U}$ , secular equilibrium along the two radioactive series was first ensured and thereby the contribution of  $^{235}\text{U}$  under the 186 KeV peak was deduced. The uranium activity in the samples varied from 48 to 112  $\text{Bq.kg}^{-1}$ , whereas the activity ratio of  $^{238}\text{U}/^{235}\text{U}$  averaged  $23.1 \pm 4.3$ .

J. Sannappa, M. S. Chandrashekar, L. A. Sathish, L. Paramesh, and P. Venkataramaiah<sup>[35]</sup> made a study of background radiation level in Mysore city, Karnataka State, India. The activities of  $^{226}\text{Ra}$ ,  $^{232}\text{Th}$ , and  $^{40}\text{K}$  in soil were measured using HPGe  $\gamma$ -ray spectrometry. The mean activities of  $^{226}\text{Ra}$ ,  $^{232}\text{Th}$ , and  $^{40}\text{K}$  were found to be 14.22  $\text{Bq.kg}^{-1}$ , 22.55  $\text{Bq.kg}^{-1}$  and 258.32  $\text{Bq.kg}^{-1}$  respectively.

Z. Papp\*, Z. Dezső, S. Daróczy<sup>[36]</sup> made a study on the activity concentrations of  $^{238}\text{U}$ ,  $^{226}\text{Ra}$ ,  $^{232}\text{Th}$ ,  $^{137}\text{Cs}$ , and  $^{40}\text{K}$  in soil samples collected from 80 different places of different depths in Ajka town, Hungary, which is a mining and industrial town having coal-fired power plant. A laboratory method has been developed by the authors to determine the activity concentrations of the nuclides  $^{238}\text{U}$ ,  $^{226}\text{Ra}$ ,  $^{232}\text{Th}$ ,  $^{137}\text{Cs}$ , and  $^{40}\text{K}$ , respectively, in soil samples by direct Ge(Li)  $\gamma$ -ray spectrometry. The average activity concentrations of uranium in this coal-fired power plant nowadays is about 300-500  $\text{Bq.kg}^{-1}$  but reached the value of 800-900  $\text{Bq.kg}^{-1}$  40 years ago. The concentration of  $^{238}\text{U}$  and  $^{226}\text{Ra}$  increased significantly in the upper layers of the soil compared with the lower layers. The mean activities of  $^{238}\text{U}$ ,  $^{226}\text{Ra}$ ,  $^{232}\text{Th}$ ,  $^{137}\text{Cs}$ , and  $^{40}\text{K}$  for the surface soil (0-5 cm) were found to be  $209.33 \pm 52.67 \text{ Bq.kg}^{-1}$ ,  $292.67 \pm 5.67 \text{ Bq.kg}^{-1}$ ,  $24.33 \pm 4 \text{ Bq.kg}^{-1}$ ,  $33.33 \pm 2.67 \text{ Bq.kg}^{-1}$  and  $283.67 \pm 36 \text{ Bq.kg}^{-1}$  respectively.

During the period of 1975 to 1979, Bangladesh Atomic Energy Commission had carried out a countrywide environmental radioactivity-monitoring programme by M. A. Rab Molla, A. Jalil, F. Nasreen, and S. F. Mahal<sup>1151</sup>. It was found that the external background radiation levels lie between 1.0 and 3.9 mSv.y<sup>-1</sup> with an average value of 2 mSv.y<sup>-1</sup> excluding Cox's Bazar sea beach sand areas where an average value of 13 mSv.y<sup>-1</sup> with a range of 2.6 – 44.0 mSv.y<sup>-1</sup> was observed.

M.A. Rab Mollah and A.F.M. Salahuddin Chowdhury<sup>1281</sup> studied the environmental radioactivity of <sup>137</sup>Cs in some soil sample of Bangladesh in 1975 by  $\gamma$ -spectrometry. They found that the range of concentration of <sup>137</sup>Cs in the studied soil samples varied from 2.02 pCi.g<sup>-1</sup> (1.32 mCi.km<sup>-2</sup>) to 2.03 pCi.g<sup>-1</sup> (134.06 mCi.km<sup>-2</sup>). The lowest concentration of <sup>137</sup>Cs was found in the soil sample of Rangamati collected from a depth of 11"-13" and the highest concentration was found in the sample collected from Cox's Bazar at a depth of 0 "-2 ". In most of the analyzed samples, they found that there was a random variation of <sup>137</sup>Cs activities with depth of the soil from where the samples were collected.

M.A. Rab Molla<sup>1371</sup> made a study on the activity of <sup>137</sup>Cs in soil samples collected from different depths of 29 different sampling stations at Cox's Bazar, Chuandi, and Rangamati. They found that the activity level ranged from 5.17 to 479.93 mCi.km<sup>-2</sup>. In most of the analyzed samples, they found a definite indication of decreasing <sup>137</sup>Cs activity with increasing soil depth, having higher activity in the surface soil.

In Finland, M.Asikainen and H. Kahlos<sup>1381</sup> measured the natural radioactivity in drinking water with the help of scintillation detectors. They analyzed the water samples for <sup>222</sup>Rn, <sup>226</sup>Ra, gross  $\alpha$ - and gross  $\beta$ - activity. They found that the mean concentrations were 670 pi.L<sup>-1</sup> for <sup>222</sup>Rn and 0.1 pCi.L<sup>-1</sup> for <sup>226</sup>Ra in the water samples of drilled wells. They found the radioactivity to be very high in the water samples of drilled wells. Some of the drilled wells also had abnormally high concentrations of uranium, up to 2100  $\mu$ g.L<sup>-1</sup> and even higher in some wells in the Helsinki region.

Using gamma spectrometry technique, C.S. Chong and G.U. Ahmad<sup>1391</sup> measured the gamma activity of <sup>40</sup>K, <sup>226</sup>Ra, and <sup>232</sup>Th in building materials in Penang, Malaysia. In

sand samples, they found the average activities of  $^{40}\text{K}$ ,  $^{226}\text{Ra}$ , and  $^{232}\text{Th}$  to be 11.5  $\text{pCi.g}^{-1}$ , 1.9  $\text{pCi.g}^{-1}$  and 0.9  $\text{pCi.g}^{-1}$  respectively.

T.E. Myrick et al. <sup>[40]</sup> made a study to determine the concentrations of selected radionuclides viz.  $^{226}\text{Ra}$ ,  $^{232}\text{Th}$ , and  $^{238}\text{U}$  in surface soil in the US. The sampling programme provided background information at 356 locations in 33 states. The nationwide average concentrations of  $^{226}\text{Ra}$ ,  $^{232}\text{Th}$ , and  $^{238}\text{U}$  in surface soil were found to be  $1.1 \pm 0.48 \text{ pCi.g}^{-1}$  (range-0.23 – 4.2  $\text{pCi.g}^{-1}$ ),  $0.98 \pm 1.46 \text{ pCi.g}^{-1}$  (range-0.10-3.4  $\text{pCi.g}^{-1}$ ), and  $1.0 \pm 0.83 \text{ pCi.g}^{-1}$  (range- 0.12- 3.8  $\text{pCi.g}^{-1}$ ) respectively.

Malcolm E. Cox and Barry L. Fankhauser <sup>[41]</sup> determined the concentration of  $^{137}\text{Cs}$  in soils and surface-deposited volcanic sublimates from various climatic locations on the islands of Hawaii, Oahu and Maui by gamma spectrometry. Samples of undisturbed soil were taken from approximately  $5(\pm 0.5)$  cm in depth and from locations where vegetation did not form an overhanging canopy. Gamma-ray detection was performed with a 7.6 x 7.6 cm Bicron well-type NaI (TI) crystal detector. In the soil samples, the range of the concentrations of  $^{137}\text{Cs}$  measured varied from 0.04 – 1.93  $\text{pCi.g}^{-1}$ , with an average for windward samples of 0.87  $\text{pCi.g}^{-1}$  and 0.17  $\text{pCi.g}^{-1}$  for leeward samples.

J.G. Ackers et al. <sup>[42]</sup> analyzed about 140 samples of building materials in the Netherlands in the period 1982- 1984 by gamma spectrometry for their  $^{226}\text{Ra}$ ,  $^{232}\text{Th}$ , and  $^{40}\text{K}$  concentrations. They also measured the radon exhalation rate from concrete slabs of different composition including fly ash components. They found that the mean activities of  $^{226}\text{Ra}$ ,  $^{232}\text{Th}$ , and  $^{40}\text{K}$  in sand samples to be 8.1  $\text{Bq.kg}^{-1}$ , 10.6  $\text{Bq.kg}^{-1}$ , and 200  $\text{Bq.kg}^{-1}$  respectively.

G. Keller and H. Muth <sup>[43]</sup> estimated the radiation exposure in German dwelling. They found that in indoors, the median  $^{222}\text{Rn}$  concentration was approximately four times higher than that of outdoors. A correlation analysis of the data obtained showed that in indoors the equilibrium factor  $F$  is almost independent of ventilation,  $^{222}\text{Rn}$  concentration, and other parameters. The mean effective dose equivalent by residence in dwelling amounted to 0.2- 0.8  $\text{mSv.y}^{-1}$  for  $^{222}\text{Rn}$  daughters, and approximately 0.1  $\text{mSv.y}^{-1}$  for  $^{220}\text{Rn}$  daughters.

R. Van Dongen and J. R. D. Stoute <sup>[44]</sup> measured the outdoor natural background radiation with the help of an ionization detector at more than 1000 locations evenly distributed throughout the country (Netherlands). They showed that the gamma radiation originating from the soil in the Netherlands varies between 1.1 and 1.2  $\mu\text{R}\cdot\text{h}^{-1}$ . They also found that, 'high' values of exposure rates correspond to areas with silty deposits and the 'low' exposure rates correspond to areas with sandy deposits. Gamma spectrometric analysis of the radiation at some location showed that the terrestrial radiation is mainly caused by natural radionuclides.

A representative sample of over 2000 UK dwellings was monitored for a year using thermoluminescent and etchable plastic dosimeters to measure gamma-ray dose rates and radon concentrations by B. M. R. Green et al. <sup>[45]</sup>. The mean gamma-ray dose rates were 0.062 and 0.057  $\mu\text{Gy}\cdot\text{h}^{-1}$  in air for living areas and bedrooms respectively. They also conducted more detailed surveys in areas where the local geology indicated that elevated exposure to natural radiation might occur. They visited over 800 dwellings and made measurements of several parameters. The mean gamma-ray dose rates varied from 0.05 to 0.10  $\mu\text{Gy}\cdot\text{h}^{-1}$  in air. The gamma-ray dose rates and radon gas concentrations were measured in over 2000 dwellings with LiF, TLD-100 and diethylene glycol bis (allyl carbonate) polymer (CR-39) etched-track dosimeters respectively.

A. Rannou et al. <sup>[46]</sup> conducted a survey of natural radiation in France since 1981 with the assessment of the components resulting from external sources (ground and building materials) using thermoluminescent dosimeters. Moreover, the internal exposure to  $^{222}\text{Rn}$  and the potential alpha energy due to radon daughters were estimated by passive track detectors in the first case and the active dosimeters in the second case. In order to estimate the terrestrial component and the one due to building materials, each chosen location had two detectors: an indoor TLD and an outdoor TLD, the second one being used only in case of natural soil. The arithmetic mean values obtained after subtraction of the component due to cosmic rays (assumed to be 0.032  $\mu\text{Gy}\cdot\text{h}^{-1}$ ) were as follows: Indoors (5798 measurements): 0.075  $\mu\text{Gy}\cdot\text{h}^{-1}$  and Outdoors (5142 measurements): 0.068  $\mu\text{Gy}\cdot\text{h}^{-1}$ .

A. S. Mollah et al. <sup>1471</sup> measured the natural radioactivity level of some building materials in Bangladesh. All samples were ground to powder and then oven-dried at 110°C for 24h. 1 kg of each sample was placed in a Marinelli beaker (1-L capacity) which was sealed and stored for 4 week before counting to allow time for <sup>238</sup>U and <sup>232</sup>Th to reach equilibrium with their respective daughters. For activity measurements, they used semiconductor detector technique. In soil samples they found the average activity concentrations of <sup>238</sup>U, <sup>232</sup>Th, and <sup>40</sup>K to be  $88.1 \pm 4.8$  Bq.kg<sup>-1</sup>,  $68.2 \pm 5.2$  Bq.kg<sup>-1</sup> and  $256.4 \pm 16.3$  Bq.kg<sup>-1</sup> respectively. For sand samples the corresponding values were  $248.2 \pm 17.8$  Bq.kg<sup>-1</sup>,  $219.0 \pm 19.2$  Bq.kg<sup>-1</sup>, and  $389.2 \pm 22.8$  Bq.kg<sup>-1</sup> respectively.

Thirty-seven soil samples representing the major soil types were collected from various sites around the Louisiana state, for estimation of radionuclide concentrations, by R.D. Delaune et al. <sup>1481</sup>. For this purpose, they used a Ge(Li) detector which was connected to a multi-channel analyzer. The averages of the mean concentrations of <sup>228</sup>Ac( <sup>232</sup>Th ), <sup>214</sup>Pb( <sup>238</sup>U ), <sup>137</sup>Cs, and <sup>40</sup>K in the analyzed samples were found to be  $36 \pm 4$  Bq.kg<sup>-1</sup>,  $14 \pm 2$  Bq.kg<sup>-1</sup>,  $23 \pm 1$  Bq.kg<sup>-1</sup>, and  $472 \pm 13$  Bq.kg<sup>-1</sup> respectively.

Yu-Ming Lin et al. <sup>1301</sup> studied Taiwan's natural background radiation for a period of 3 years (1981- 1983) which included the ambient exposure rate and radionuclides in soil and rock samples. They also compared the observed exposure rate and the exposure rate calculated from the concentrations of radioactive elements mainly <sup>228</sup>U, <sup>232</sup>Th and <sup>40</sup>K in soil and rock samples and found that a good correlation exists. For this purpose, they used a survey meter equipped with a 2.5 cm diameter by 2.5 cm long cylindrical NaI (TI) detector, and a Ge(Li) detector of 23.5% relative efficiency for measuring the activities of soil and rock samples. They found that the exposure rate ranged from  $2 \times 10^{-8}$  to  $9 \times 10^{-8}$  Gy.h<sup>-1</sup>, with an average of  $5.4 \times 10^{-8}$  Gy.h<sup>-1</sup>. Taking into account the cosmic-ray contribution of  $2.8 \times 10^{-8}$  Gy.h<sup>-1</sup> the average absorbed dose rate in Taiwan due to terrestrial  $\gamma$ -rays and cosmic-rays was  $8.2 \times 10^{-8}$  Gy.h<sup>-1</sup>. The K content ranged from 265-607 Bq.kg<sup>-1</sup>, Th content ranged from 30-71 Bq.kg<sup>-1</sup>, and U content ranged from 22-45 Bq.kg<sup>-1</sup>. The average specific activities of K, Th, and U were 431 Bq.kg<sup>-1</sup>, 44 Bq.kg<sup>-1</sup> and 30 Bq.kg<sup>-1</sup>.



P. Corvisiero et al. <sup>1491</sup> measured the radioactivity in food and environment in Italy immediately after the Chernobyl reactor accident of 1986. They used a 3" x 3" NaI detector for this purpose. They also estimated the internal dose from inhalation (assuming an average inhalation rate of about 20 m<sup>3</sup>.d<sup>-1</sup>) external irradiation and ingestion as follows: (i). Inhalation dose equivalents in the target organs thyroid, lungs, and gonads were 120 µSv, 2.5 µSv and 2.2 µSv respectively; (ii). External irradiation-estimated total body dose equivalent was 8.8 µSv (iii) Ingestion-dose equivalent in the target organs thyroid, lungs and gonads were 1000 µSv, 20 µSv, and 20 µSv respectively.

C. Papastefanou et al. <sup>1501</sup> measured the <sup>137</sup>Cs and <sup>40</sup>K content in soil samples immediately after the chernobyl explosion, in Thessaloniki, North Greece. They used high resolution (1.9- 2.0 KeV at 1.33 MeV of <sup>60</sup>Co) and high efficiency (42%) spectrometers consisting of a Ge-Li and a high purity Ge detector for <sup>137</sup>Cs and <sup>40</sup>K measurements (total 56 samples). The concentration of <sup>137</sup>Cs in soils ranged between 290 Bq.kg<sup>-1</sup> and 7670 Bq.kg<sup>-1</sup>, while the <sup>40</sup>K specific activity ranged between 226 Bq.kg<sup>-1</sup> and 1604 Bq.kg<sup>-1</sup>. The <sup>137</sup>Cs concentrations were inversely proportional with <sup>40</sup>K concentration of K content of soils.

Tieh-Chi Chu et al. <sup>1511</sup> worked on the changes in per capita and collective dose equivalent in Taiwan in three decades (1950-1983) based on the measured terrestrial and cosmic radiation levels and the population distribution as well. The population had increased 2.5 times in that 33 years and reached to 1.9 x 10<sup>7</sup> people, yet the migration of population had been from the rural areas where the natural radiation was usually high to the urban areas where the natural radiation was usually low. The resulting collective dose equivalent had been increasing, yet the per capita dose equivalent, on the contrary, had been decreasing. In 1983, over 50% of the population in Taiwan was living in a radiation level interval of 50-60 nGy.h<sup>-1</sup>. Another 30% was living in the interval of 60-70 nGy.h<sup>-1</sup>. The rest was living either above or below the radiation intervals mentioned above. The population fraction in the radiation intervals of 50-60 nGy.h<sup>-1</sup> was 51.7% in 1950 and increased to 58.7% in 1980. On the contrary, the population fraction in the radiation interval of 60-70 nGy.h<sup>-1</sup> was 31.1% in 1950 and decreased to 28.8% in 1980. Similarly, the population fraction in the radiation interval

of 70-80 nGy.h<sup>-1</sup> was 0.45% in 1960 and decreased to 0.37% in 1980. The female per capita dose equivalent had been about 0.15% higher than that for males. This might account for the females who stay in the countryside while the males were working in the urban areas.

Olafur Arnalds et al. <sup>[52]</sup> measured the fallout of <sup>137</sup>Cs levels in soil samples of 11 diverse sites throughout Montana, US. Soil samples were collected from 11 undisturbed native vegetation sites in the state. The sampling was performed during the summer of 1982. Most of the samples were taken in 10 cm depth increments, although sampling-depth increments differed at some sites. For the radioactivity measurements, they used Li-drifted Ge or intrinsic Ge  $\gamma$ -ray detectors coupled to a Nuclear Data 6620 analyzer system. Concentrations of <sup>137</sup>Cs in near surface samples ranged from 20-200 mBq.g<sup>-1</sup> (0.51-5.41 pCi.g<sup>-1</sup>). Most of the <sup>137</sup>Cs was found in the top 10 cm of soil. Deeper occurrences were attributed to disturbances by animals and to interstitial flow of small sediment particles within saturated soils. The areal concentrations ranged from 130-748 mBq.cm<sup>-2</sup> (3.6-20.2 pCi.cm<sup>-2</sup>) and was highly correlated with annual precipitation.

T. Yesin and N. Cakir <sup>[53]</sup> used gamma-ray scintillation spectrometry in order to measure the <sup>137</sup>Cs and <sup>134</sup>Cs levels and depth distributions in soil of a tea plantation in the eastern black sea region in Turkey. Soil samples were collected in November 1987. The depth distribution was found to be exponential with  $\alpha = 0.16 \text{ cm}^{-1}$  and the exposure rate arising there from was calculated as 17.46  $\mu\text{R.h}^{-1}$  over the ground surface.

S.E. Simopoulos <sup>[54]</sup> collected 1242 soil samples, over Greece, during the period May-Nov. 1986 for <sup>137</sup>Cs analysis of the Chernobyl fallout in Greece. These samples were analyzed for <sup>137</sup>Cs and the counting was performed using a NaI detector on-line to a inter-microcomputer, moreover, 252 of the samples were also analyzed by using Ge detectors, for inter-comparison and also for the assessment of other long-lived isotopes in the fallout. The results showed that <sup>137</sup>Cs fallout from Chernobyl present a remarkable geographical variability. The evaluated ground activity due to <sup>137</sup>Cs depositions ranged between 0.01 and 137 kBq.m<sup>-2</sup>.

R. J. de Meijer et al. <sup>[55]</sup> measured the concentrations of radionuclides originating from the Chernobyl reactor accident as a function of time in air, rainwater, grass, cow's milk,

vegetables, and dust by means of high-resolution  $\gamma$ -ray spectroscopy and found the high level of concentrations of fission product elements. They also found the concentrations of  $^{137}\text{Cs}$  in rainwater samples (collected total 31 samples of different stations and mixed samples, from May 03 to July 01, 1986), ranged between  $0.8 \text{ Bq.L}^{-1}$  and  $210 \text{ Bq.L}^{-1}$ .

H. Florou and P. Kritidis <sup>[56]</sup> analyzed the environmental samples viz. soil, sediment, ores, and marine organisms collected from Milos Island ( $36^{\circ}42' \text{N}$ ,  $24^{\circ}27' \text{E}$ ) located in the Volcanic arc of the Cyclades Archipelago in the south-eastern Aegean sea, Greece for estimating the natural radioactivity levels in the island. They used an HPGe detector and a car-borne scintillometry for this purpose. The results of radiometry indicated that the existence of some areas in Milos where the exposure rate exceeds  $20 \mu\text{R.h}^{-1}$ , which corresponded to dose rate of  $123 \text{ nSv.h}^{-1}$ . In soil samples, the average concentrations of  $^{226}\text{Ra}$ ,  $^{232}\text{Th}$  and  $^{40}\text{K}$  were found to be  $50 \pm 21 \text{ Bq.kg}^{-1}$ ,  $57 \pm 21 \text{ Bq.kg}^{-1}$ , and  $877 \pm 332 \text{ Bq.kg}^{-1}$  respectively.

M. Brai et al. <sup>[57]</sup> estimated the population exposure to those living on the island of Pantelleria, Italy, by measuring the natural gamma background. They analyzed the gamma spectra of natural rocks and measured absorbed dose in air. They used an HPGe detector for gamma spectrometric measurements and thermoluminescent dosimeters LiF (Mg, Cu, and P) for measurements of absorbed dose due to natural gamma terrestrial radiation. They found a correlation between the gamma exposure rate and the mean values of natural radionuclide concentrations in the investigated rocks. They found the ranges of specific activities of  $^{232}\text{Th}$ ,  $^{238}\text{U}$ , and  $^{40}\text{K}$  in different rock samples respectively as 11.6 to  $165.5 \text{ Bq.kg}^{-1}$ , 12.1 to  $168.5 \text{ Bq.kg}^{-1}$ , and 27.7 to  $1295 \text{ Bq.kg}^{-1}$ . The minimum activity had been found for Basalts and the minimum for Pumice (Rhyolitic rocks). They further estimated the population-absorbed dose to be  $1.4 \text{ mGy.y}^{-1}$ .

Ching –Jiang Chen et al. <sup>[58]</sup> investigated the natural radiation in houses built with black schist slabs located at an altitude of 1 km in the mountainous southern part of Taiwan by studying the naturally occurring radionuclides present in the black schist. In the mountainous area of southern Taiwan, houses owned by aborigines, such as the Lukai tribe, are commonly built with locally produced black schist slabs. Gamma-ray

spectroscopy was performed using an HPGe detector coupled to a multichannel analyzer. In-situ measurements were carried out using a survey meter coupled to a sodium iodide detector. Cellulose nitrate films, ZnS(Ag) scintillation cells, and alpha spectroscopy were used to study radon and radon daughters. They furthermore calculated the radiation dose due to all natural sources. In the black schist, concrete and soil samples, they found the ranges of  $^{40}\text{K}$ ,  $^{232}\text{Th}$  and  $^{238}\text{U}$  to be  $432\text{-}911\text{ Bq.kg}^{-1}$ ,  $33.2\text{-}59.2\text{ Bq.kg}^{-1}$  and  $26.8 - 57.0\text{ Bq.kg}^{-1}$ .  $^{137}\text{Cs}$  was found only in soil samples and its level was  $0.48\text{ Bq.kg}^{-1}$ . The total natural radiation doses received by the Lukai tribe were  $1.50\text{ mSv.y}^{-1}$ , while the corresponding value for average Taiwanese was  $1.47\text{ mSv.y}^{-1}$ .

P. Schuller et al. <sup>[59]</sup> collected soil, prairie plants, and milk samples from 39 dairy farms in southern Chile ( $38^{\circ}44' - 41^{\circ}08' \text{S}$ ) during the green -feed periods (September to March) between 1982 and 1990. They analyzed the samples with the help of a Ge(Li) detector and an HPGe detector for  $^{137}\text{Cs}$  assay. In soil samples, the concentration of  $^{137}\text{Cs}$ , was found to range from  $3.8 \pm 0.2$  to  $17.1 \pm 0.7\text{ Bq.kg}^{-1}$ . The reason for the increment of  $^{137}\text{Cs}$  in soil samples was explained as due to higher average rainfall, latitudinal positions (which corresponds to the maximal radionuclide deposit bands of the southern hemisphere, according to UNSCEAR- 1982 <sup>[60]</sup>), and the long term influence of radioactive fallout caused by the French and British atmospheric nuclear weapons testing undertaken within the southern hemisphere.

Using a hyperfine germanium spectrometer, N. M. Ibrahim et al. <sup>[61]</sup> measured the concentrations of radionuclides  $^{40}\text{K}$ ,  $^{137}\text{Cs}$ ,  $^{232}\text{Th}$ , and  $^{238}\text{U}$  in surface soil across the Nile Delta, the north coast of Egypt. They collected the samples by either the template or the core method. In the template method, a 25-cm x 25-cm area sample was cut out using a template for guidance to a depth of 10 cm. In the core method, core of either 10.5 cm or 7.35 cm diameter and 7 cm of 25 cm in depth was used to take the samples. They found the activities of  $^{40}\text{K}$ ,  $^{238}\text{U}$  series,  $^{232}\text{Th}$  series, and  $^{137}\text{Cs}$  ranged from  $29 \pm 1.3$  to  $653 \pm 12.9\text{ Bq.kg}^{-1}$ ,  $5.2 \pm 2.1$  to  $63.7 \pm 6.2\text{ Bq.kg}^{-1}$ ,  $1.1 \pm 0.3$  to  $95.6 \pm 26\text{ Bq.kg}^{-1}$ , and below detectable limit to  $2644\text{ Bq.m}^{-2}$  respectively for dry weight of 162 soil samples. They also calculated the absorbed dose rate at a height of 1 m above the ground surface for each location from the wet weight concentrations of natural radionuclides measured by using the standard conversion factors. The average value of

the total dose rate at 1 m above the ground due to  $^{40}\text{K}$ , the  $^{238}\text{U}$  series in soil was  $31.5 \text{ nGy.h}^{-1}$  (excluding cosmic radiation and  $^{137}\text{Cs}$  contribution the range of which was 7.6 to  $93.2 \text{ nGy.h}^{-1}$ ).

A. P. Radhakrishna et al. <sup>[62]</sup> made a systematic study on the background radiation and the distribution of radionuclides in the environment of coastal Karnataka, South India, and an industrialized area endowed with nuclear and thermal power plants in addition to others. They measured the ambient gamma radiation dose in the environment by using a  $5 \text{ cm} \times 5 \text{ cm}$  NaI (TI) scintillator and by using TLD ( $\text{CaF}_2$ ), and measured the concentrations of radionuclides in soil and sand samples by employing an HPGe detector coupled with MCA. Mangalore, a major industrial city of coastal Karnataka, revealed significantly high gamma dose in air. The measured gamma dose in air in high background area was in the range  $44\text{-}2102 \text{ nGy.h}^{-1}$ . The average activities of  $^{232}\text{Th}$ ,  $^{238}\text{U}$  and  $^{40}\text{K}$  in soil samples (collected from the Bhagawathi temple area of Ullal beach, the area of highest radiation dose level) were found to be  $2,971 \text{ Bq.kg}^{-1}$ ,  $546 \text{ Bq.kg}^{-1}$ , and  $268 \text{ Bq.kg}^{-1}$  respectively.

During the period of 1989 –1992, L. S. Quindos et al. <sup>[63]</sup> collected soil samples nationwide from 952 sampling sites for assessment of natural radioactivity in the 17 autonomous regions of Spain. They made gamma spectrometry measurements of  $^{226}\text{Ra}$ ,  $^{232}\text{Th}$  and  $^{40}\text{K}$  activities in soil samples by using a high-purity germanium co-axial detector with an efficiency of 20%, a resolution of 1.86 KeV, and surrounded with shielding material to reduce the background-counting rate. The detector was calibrated using standard solutions  $^{226}\text{Ra}$ ,  $^{232}\text{Th}$  and  $^{40}\text{K}$  in the same geometry as the measured soil samples. The ranges of concentrations of radionuclides  $^{226}\text{Ra}$ ,  $^{232}\text{Th}$  and  $^{40}\text{K}$  in 952 samples was found to be  $8 - 310 \text{ Bq.kg}^{-1}$  (average  $39 \text{ Bq.kg}^{-1}$ ),  $5\text{-}258 \text{ Bq.kg}^{-1}$  (average  $41 \text{ Bq.kg}^{-1}$ ) and  $31\text{-}2040 \text{ Bq.kg}^{-1}$  (average  $578 \text{ Bq.kg}^{-1}$ ) respectively for dry weight of samples. For the whole Spain, an overall population-weighted mean outdoor terrestrial gamma dose rate of  $53.3 \text{ nGy.h}^{-1}$  was also calculated from the measurements of the  $^{226}\text{Ra}$ ,  $^{232}\text{Th}$  and  $^{40}\text{K}$  concentrations in soil. This value was comparable with that of  $47.1 \text{ nGy.h}^{-1}$  derived from absorbed dose rates in air measured experimentally outdoors throughout the country (correlation co-efficient  $r = 0.979$ ) and was similar to the world average value of  $55 \text{ nGy.h}^{-1}$  reported in UNSCEAR-1988 <sup>[64]</sup>.

Man-yin W. Tso et al.<sup>[65]</sup> measured the concentrations of radionuclides of  $^{226}\text{Ra}$ ,  $^{232}\text{Th}$ , and  $^{40}\text{K}$  in building materials in Hong Kong. They also estimated the indoor  $^{222}\text{Rn}$  level released from the building materials simultaneously. They further calculated the emanation coefficients and  $^{222}\text{Rn}$  diffusion coefficients. The effect of surface coating on  $^{222}\text{Rn}$  exhalation rate was also studied. The radionuclides contents of typical building materials used locally in Hong Kong was determined by  $\gamma$ -spectrometry method using an HPGe detector with MCA, and the results indicated that the average contents of  $^{226}\text{Ra}$ ,  $^{232}\text{Th}$ , and  $^{40}\text{K}$  in Hong Kong concrete were the highest known in the world. The average concentration of the mentioned radionuclides was the highest for granite chip. The average activities of  $^{226}\text{Ra}$ ,  $^{232}\text{Th}$ , and  $^{40}\text{K}$  in granite chips were  $180 \pm 31 \text{ Bq.kg}^{-1}$ ,  $122 \pm 5 \text{ Bq.kg}^{-1}$  and  $1248 \pm 15 \text{ Bq.kg}^{-1}$  respectively, having Radium Equivalent (Ra-eq) of  $451 \text{ Bq.kg}^{-1}$ . The sea sand, river sand, aggregate, and concrete blocks had average Ra-eq as  $38 \text{ Bq.kg}^{-1}$ ,  $162 \text{ Bq.kg}^{-1}$ ,  $395 \text{ Bq.kg}^{-1}$ , and  $293 \text{ Bq.kg}^{-1}$  respectively.

External  $\gamma$ -ray dose rates in air were measured by Y. Narayana et al.<sup>[66]</sup>, by using a sensitive plastic scintillator in the environment of coastal Karnataka, on the south-west coast of India, where intensive industrial activities including a nuclear power plant, a super thermal power station, and a petrochemical complex were envisaged. The gamma dose rates in air were found to range from 26 to 174  $\text{nGy.h}^{-1}$  with a geometric mean of  $74 \text{ nGy.h}^{-1}$  and a geometric standard deviation of 1.4. The activity of primordial radionuclides in soil samples of the region were measured by using an HPGe gamma-ray spectrometer and resulting doses in air were calculated. The mean absorbed dose rate due to primordial radionuclides was  $41.4 \text{ nGy.h}^{-1}$  with a geometric standard deviation of 1.4. A correlation was found between doses measured using scintillometer and doses estimated from the measured activity of primordial radionuclides when the cosmic-ray component was taken into account. The concentration of primordial radionuclides in soil and sand showed considerable variation in their vertical depth distribution in the high background area of the region.

A. S. Mollah et al.<sup>[29]</sup> studied the radioactivity in soil samples at AERE, Savar, Dhaka, using an HPGe detector of volume 53 cc and of resolution 2.1. KeV at 1332 KeV line of  $^{60}\text{Co}$  source. The samples were collected from a circular area having a radius of 10

km with the research reactor TRIGA-MARK-II of AERE as the centre, from two different depths, namely: - 2.5 – 5.0 cm, and 15-18 cm, at each sampling spot. They analyzed the samples for assessment of the concentrations of  $^{208}\text{Tl}$ ,  $^{214}\text{Bi}$ ,  $^{40}\text{K}$  and  $^{137}\text{Cs}$ . In the superficial (2.5-5.0 cm) soil samples, they found the ranges of the concentrations of the mentioned radionuclides as- 21.55 – 25.98  $\text{Bq.kg}^{-1}$ , 32.43 – 48.73  $\text{Bq.kg}^{-1}$ , 322.10 – 526.51  $\text{Bq.kg}^{-1}$ , and from below detectable limit to 3.17  $\text{Bq.kg}^{-1}$  respectively.

John R. Meriwether et al.<sup>[67]</sup> developed a new protocol for soil sampling named “Pedologically Based Sampling Technique” and applied successfully in determining the concentration of radionuclides in Louisiana, US. For determining the concentrations of naturally occurring radionuclides in Louisiana’s soil samples, they used an HPGe detector associated with necessary electronics and a computer based MCA. The ranges of the concentrations of  $^{226}\text{Ra}$  ( $^{214}\text{Bi}$ ), and  $^{232}\text{Th}$  ( $^{228}\text{Ac}$ ) was found to be from  $14.4 \pm 1.44$  to  $53.6 \pm 5.36$   $\text{Bq.kg}^{-1}$  and from  $10.8 \pm 1.08$  to  $61.16 \pm 6.16$   $\text{Bq.kg}^{-1}$  respectively. They also showed that the concentration levels of primordial radionuclides are dependent on the depth from where the samples had been collected, the activity levels differ significantly with the variation of the depth of soil samples of same place.

Masayoshi Yamamoto et al.<sup>[68]</sup> made a survey on the residual radioactivity in the soil at the “Semipalatinsk Nuclear Test Site (SNTS)” and at off-site areas in Kazakhstan. The soil was sampled in October 1994 from four locations in SNTS and the cities of Kurchatov and Almaty. The concentrations of different fission product radionuclides were assessed by using non-destructive  $\gamma$ -spectrometric analysis on ordinary Ge detector. During soil sampling, they also measured the radiation dose level above 1m from the ground surface by portable type survey meters PDR-101 & PDR-102. The radiation dose level was found to be ranged between 0.1  $\mu\text{Sv.h}^{-1}$  (headquarters and research centre for SNTS) to 30  $\mu\text{Sv.h}^{-1}$  (near hypocentre where the first Soviet nuclear explosion was tested on 29 August 1949).

Kiyoshi Shizuma et al.<sup>[31]</sup> performed low background gamma-ray measurement to determine the  $^{137}\text{Cs}$  content in soil samples collected in a very early survey of Hiroshima atomic bomb. Those soil samples had been collected just 3 day after the

explosion within 5 km from the hypocentre and had not been exposed to the global fallout from nuclear weapon test. In their research work, soil samples were repackaged in plastic containers instead of glass vials to eliminate the  $^{40}\text{K}$  gamma-ray background from the vial itself. Out of 22 samples,  $^{137}\text{Cs}$  was detected in 11 samples, and their activities found to be ranged from 0.16 to 10.6  $\text{mBq}\cdot\text{g}^{-1}$  at the time of the measurement (1994-1995). Cumulative exposure by the fallout was estimated to be  $0.12 \pm 0.02 \text{ R}$  ( $0.031 \pm 0.004 \text{ mCi}\cdot\text{kg}^{-1}$ ) in Hiroshima city except for the heavy fallout area and where it was  $4.0 \pm 0.4 \text{ R}$  ( $1.03 \pm 0.11 \text{ mCi}\cdot\text{kg}^{-1}$ ).

Shu-Ying Lai et al. <sup>1691</sup> measured the fallout of  $^{137}\text{Cs}$  activities in soils and trees from samples taken in mountainous areas and along three-cross island highways in Taiwan. Typical concentration in near surface samples was about  $5 \text{ Bq}\cdot\text{kg}^{-1}$  depending on soil density. No correlation was found between the concentrations of  $^{137}\text{Cs}$  and stable elements in soils. Mechanical disturbance and soil density were identified as major causes for redistribution of  $^{137}\text{Cs}$  in both forest soils and trees. The transfer coefficient of  $^{137}\text{Cs}$  from soil to Bastard banyan was estimated to be 0.23. Each sample was counted by a Ge(Li) detector of 23.5% relative efficiency which was housed with a heavy shield to reduce background activity. The detector had a resolution of 1.86 KeV full width at half maximum (FWHM) 1.33 MeV, MCA 4096, PCA coupled.

By means of in-situ gamma-spectrometry with semiconductor detectors, J. Uyttenhove et al. <sup>1701</sup> measured the residual radiocaesium concentration, nearly 10 years after the Chernobyl accident at different sites on the Belgian territory. They also investigated a possible link between the rainfall at the beginning of May 1986 and the actual cesium concentration. The concentration of  $^{137}\text{Cs}$  in Belgian surface soil samples was found to range between 400 and 5600  $\text{Bq}\cdot\text{m}^{-2}$ . The measured radiocaesium activity was the sum of the Chernobyl accident contribution and the residual activity from previous contamination. The radiological impact of that contamination, even in the most affected regions in the Ardennes, was very small ( $5.6 \mu\text{Sv}\cdot\text{y}^{-1}$ ).

E. Gomez et al. <sup>1711</sup> studied the radioactive concentrations of the man-made radionuclides  $^{137}\text{Cs}$ ,  $^{89}\text{Sr}$ , and  $^{90}\text{Sr}$ ; in calcareous soils of the island of Majorca (Spain),



by analyzing the top 5 cm of the surface layer. The activity of  $^{137}\text{Cs}$  was determined by  $\gamma$ -ray spectrometry and found to range between 10 to 60  $\text{Bq.kg}^{-1}$ .

By using gamma-spectrometry technique with an HPGe, F. K. Miah et al. <sup>[72]</sup> measured the concentrations of natural radionuclides of the uranium and thorium series, and  $^{40}\text{K}$  and a fission product  $^{137}\text{Cs}$  in soil samples collected from Dhaka city and its neighbouring environs. Activities of the radionuclides present in the soil samples were greatly influenced by the geomorphologic conditions in the area from where samples were collected. In their study, the average concentrations of the radionuclides  $^{226}\text{Ra}$ ,  $^{228}\text{Ra}$ , ( $^{228}\text{Ac}$ ),  $^{232}\text{Th}$  ( $^{208}\text{Tl}$ ),  $^{40}\text{K}$ , and  $^{137}\text{Cs}$  were found to be  $33 \pm 7 \text{ Bq.kg}^{-1}$  (range-  $21 \pm 6$  to  $43 \pm 7 \text{ Bq.kg}^{-1}$ ),  $55 \pm 14 \text{ Bq.kg}^{-1}$  (range-  $34 \pm 12$  to  $81 \pm 15 \text{ Bq.kg}^{-1}$ ),  $16 \pm 4 \text{ Bq.kg}^{-1}$  ( range-  $9 \pm 2$  to  $22 \pm 2 \text{ Bq.kg}^{-1}$ ),  $574 \pm 111 \text{ Bq.kg}^{-1}$  (range-  $402 \pm 78$  to  $750 \pm 82 \text{ Bq.kg}^{-1}$ ), and  $7 \pm 2 \text{ Bq.kg}^{-1}$  ( range-  $3 \pm 1$  to  $10 \pm 1 \text{ Bq.kg}^{-1}$ ) respectively.

N. N. Jibiri and I. P. Farai <sup>[73]</sup> determined the average annual effective dose equivalent and the collective effective dose equivalent from measurements of the concentrations of  $^{40}\text{K}$ ,  $^{238}\text{U}$ , and  $^{232}\text{Th}$  in the top soil in and around the city of Lagos using in-situ  $\gamma$ -spectrometry. The average outdoor absorbed dose rate was  $0.041 \pm 0.012 \mu\text{Gy.h}^{-1}$  resulting in an annual average effective dose equivalent of  $50 \mu\text{Sv.y}^{-1}$ . The collective effective dose equivalent to the population in the city was  $2.84 \times 10^2 \text{ man-Sv.y}^{-1}$ .

B. Baggoura et al <sup>[74]</sup> carried out a national environmental sampling programme during 1993 to determine natural and artificial radionuclide content in the (0-15 cm) upper layer of the soil, in Algeria. Soil samples were analyzed with the help of direct counting by gamma-ray spectrometry (an HPGe detector associated with necessary accessories). In addition, terrestrial gamma-ray dose rates in air had been measured out of doors throughout Algeria at the time of sample collection, at each of the sampling locations, by means of a pressurized argon ionization chamber; type RSS-112, at 1m above the top soil. In each of the 48 administrative divisions of the country, selected sites were chosen to collect soil samples and to measure gamma-ray dose rates simultaneously. Radioactivity concentrations in  $\text{Bq.kg}^{-1}$  dry mass of  $^{226}\text{Ra}$ ,  $^{214}\text{Pb}$ ,  $^{214}\text{Bi}$ ,  $^{212}\text{Pb}$ ,  $^{228}\text{Ac}$ ,  $^{40}\text{K}$ , and  $^{137}\text{Cs}$  were found to range between (5-176), (2-107 ), (3-65 ), (2-97), (3-144),

(36-1405), and (0.3-0.41) respectively. The dose rates in air measured over the whole country were found to range between 20 and 133 nGy.h<sup>-1</sup>.

R. H. Higgy and M. Pimpl<sup>1751</sup> measured the specific radioactivities of U-series, <sup>232</sup>Th, <sup>137</sup>Cs and <sup>40</sup>K in soil samples around the Inshass reactor in Cairo (Egypt), using a  $\gamma$ -ray spectrometer with an HPGe detector. The specific activities of <sup>238</sup>U, <sup>232</sup>Th, <sup>40</sup>K and <sup>137</sup>Cs obtained from direct  $\gamma$ -spectrometric measurements for soil samples were found to range between 5.3 and 7.7 (average 6.3), 10.7 and 17.0 (average 13.3), 152 and 202 (average 163), and from 1.6 to 19.1 (average 5.5) respectively in Bq.kg<sup>-1</sup> dry weight.

Using an HPGe  $\gamma$ -ray detector, M. M. Rahman<sup>1761</sup> analyzed soil (sand) samples collected from the sea-beaches of Cox's Bazar, Potenga, Fauzdarhat (Chittagong), and Harinbaria (Borguna); and rock samples collected from Fultala (Sylhet) for determining the concentrations of <sup>208</sup>Tl, <sup>214</sup>Bi, <sup>228</sup>Ac, <sup>40</sup>K, and <sup>137</sup>Cs. He collected the sand samples at a depth of 20-25 cm from each of the beaches. The average concentrations of the mentioned radionuclides in sand samples were found to be  $31.31 \pm 12.98$  Bq.kg<sup>-1</sup>,  $29.55 \pm 11.43$  Bq.kg<sup>-1</sup>,  $39.95 \pm 13.26$  Bq.kg<sup>-1</sup>,  $454.08 \pm 96.59$  Bq.kg<sup>-1</sup>, and  $2.28 \pm 0.59$  Bq.kg<sup>-1</sup> respectively.

The outdoor environmental background radiation was measured by thermoluminescence dosimetry, gamma spectrometry of soil samples, and ionization chamber ( $\beta$ - $\gamma$  survey meter); by Tutul Kanti Saha<sup>1231</sup>. The study was carried out for 2 and 4 months periods in the region of Chittagong City. The average environmental radiation dose rate during the monitoring period was found to be  $1321.93 \pm 223.20$   $\mu$ Sv.y<sup>-1</sup> with TL dosimeters and  $1847.35 \pm 171.33$   $\mu$ Sv.y<sup>-1</sup> with a  $\beta$ - $\gamma$  survey meter. The average environmental radiation dose rate due to natural <sup>238</sup>U, <sup>232</sup>Th, and <sup>40</sup>K radionuclides in surface soil of Chittagong obtained by the measurement with an HPGe detector was  $559.34 \pm 115.34$   $\mu$ Sv.y<sup>-1</sup>. The variation in these three dose levels was explained as the  $\beta$ - $\gamma$  survey meter measured the  $\beta$  &  $\gamma$  radiation of all energies, the TL dosimeters measured only  $\gamma$ -radiation (the perspex holder of TL-chips absorbed  $\beta$ -radiation), and the last one was only due to <sup>238</sup>U series, <sup>232</sup>Th series, and <sup>40</sup>K radionuclides without considering the impact of other (cosmic and natural) sources of radiation.

Michelle Huelskamp<sup>1261</sup> conducted an investigation on background radiation in soil and water samples near Albuquerque in U.S.A. Liquid Scintillation Counter (LSC) was used for measuring gross beta activity levels. The average gross beta activities of soil samples from Albuquerque, outside city limits and sandia laboratory complex were  $12.44 \pm 6.41$ ,  $14.17 \pm 7.33$  and  $10.76 \pm 6.54$  pCi/g respectively.

D.S. Sill, C.W. Sill<sup>1271</sup> made a study on radioactive concentrations in the environmental samples from different locations in U.S.A. The average gross beta activity of soil samples was found to be  $24.33 \pm 0.77$  pCi/g.

## **CHAPTER-III**

### **EXPERIMENTAL SET-UP**

#### **3.1 Overview of Radiation Detectors**

Radiation cannot be detected by human senses. A variety of hand-held and laboratory instruments are available for detecting and measuring radiation. The most common hand-held or portable instruments are:

(1) The photographic emulsion, (2) The cloud chamber (3) Gas filled detectors. (4) The electroscopes, (5) Cerenkov detectors, (6) Scintillation detectors, (7) Semiconductor detectors, (8) Thermoluminescent crystals etc<sup>[77]</sup>.

##### **3.1.1 The Ordinary Photographic Film**

It consists of an emulsion of silver bromide grains suspended in gelatin matrix and supported with a backing of glass or cellulose acetate film. Ionizing radiation on passing through the emulsion sensitizes the grains of silver halide molecules. In the subsequent development process, the entire sensitized grain is converted to metallic silver, the degree of blackening of emulsion, which can be determined photometrically after development, is roughly proportional to the radiation dose received. The photographic method provides a permanent record of the passage of radiations and cloud chambers make it possible to assess the track of individual particles<sup>[77]</sup>.

##### **3.1.2 The Gas Filled Detectors**

These are termed as ionization chamber, Proportional counter and Geiger-Muller (GM) counter depending upon the ionization characteristics with increasing operational Voltage. It consists of a tube filled with inert gas (such as argon/methane) at a reduced pressure with a central electrode well insulated from the chamber walls. Radiation passing through the cylinder produces ions which flow towards respective electrodes where the central wire is maintained at a high +Ve Voltage with respect to cylinder<sup>[78]</sup>.

### **3.1.3 Proportional Counter**

A common laboratory instrument is the standard proportional counter with sample counting tray and chamber, and argon/methane flow as a counting gas. Most units employ a very thin ( $\text{microgram/cm}^2$ ) window, while some are windowless. Shielding and identical guard chambers are used to reduce background, and in conjunction with electronic discrimination, these instruments can distinguish between alpha and beta radiation, and achieve low minimum detectable activities (MDA). Similar to the liquid scintillation counter (LSC) units, these proportional counters have multiple sample capability, and automatic data acquisition, reduction and storage. Such counters are often used to count smear / wipe or air filter samples. Additionally, large area gas flow proportional counters with thin ( $\text{milligram/cm}^2$ ) mylar windows are used for counting the whole body and extremities of workers for external contamination when exiting a radiological control area.

### **3.1.4 Scintillation Method**

It is one of the most interesting and widely used detection methods. When ionizing radiation passes through certain materials called scintillators, flashes of light are emitted. These light flashes are picked up by a photomultiplier tube which amplifies the initial output of photoelectrons from a suitable cathode by secondary emission of further electrons at successive dynodes resulting in a final gain of about  $10^6$  to  $10^7$  electrons per incident electron. These electrons produce electronic pulses in the external circuit and the size of pulse is proportional to the energy deposited in the crystal by a charged particle or a photon<sup>[79]</sup>.

### **3.1.5 Thermoluminescence Detector**

Thermoluminescent detectors utilize the electron trapping process; traps are imperfections or impurity atoms in the crystal structure which cause electrons to be caught in the forbidden band. The material is selected so that electron trapped as a result of exposure to ionizing radiation is stable at normal temperatures. If, after irradiation, the material is heated to a suitable temperature, usually about  $200^\circ\text{C}$ , the trapped electrons are released and return to the valance band with the emission of a light photon. Thus if the device is heated in the dark under a photomultiplier tube, the light output can be measured and this is proportional to the radiation dose which the

detector has received. The most common material used is lithium fluoride (LiF). This system measures the total dose accumulated over the period of exposure<sup>[80]</sup>.

### **3.1.6 Cerenkov Detectors**

Cerenkov detectors are those category of radiation detectors based on the light which is emitted by a fast charged particle passing through an optically transparent medium with index of refraction greater than one. The light emitted is converted into an electrical signal by a photomultiplier tube in an optical contact with Cerenkov medium<sup>[81]</sup>.

### **3.1.7 Semiconductor Radiation Detectors**

Ge detectors are commonly used in gamma-ray spectroscopy, but they also have applications in x-ray and charged-particle spectroscopy. Ge detectors operate at liquid-nitrogen temperature and provide excellent energy resolution and good gamma-ray detection efficiency. Unequaled flexibility in the design and fabrication of Ge detectors has been achieved at Berkeley Lab through development of a variety of contact technologies such as lithium diffusion, ion implantation, metal surface barriers, and amorphous/crystalline semiconductor junctions. A wide range of device configurations such as planar, coaxial, and multi-element strip and pixel detectors have been produced with detector Volumes ranging from  $<1 \text{ cm}^3$  to several hundred  $\text{cm}^3$ . A complete Ge detector systems, which typically include vacuum, cryogenic, and electronics subsystems. Applications include gamma-ray astronomy, medical imaging, x-ray spectroscopy using synchrotron radiation, nuclear physics, and nuclear material detection.

A semiconductor is a material that can act as an insulator or as a conductor. Semiconductor detectors are fabricated from either elemental or compound single crystal materials having a band gap in the range of 1-5 eV. The group IV elements, silicon and germanium are by far the most widely used semiconductors.

Charged particles or gamma rays when pass through the charge free regions of these detectors, a large number of ion pairs are produced which are collected by applying a high Voltage across the region. The resultant collected charge is integrated by a charge

sensitive preamplifier and converted to a Voltage pulse with amplitude proportional to the photon energy <sup>[77,82]</sup>.

### **Ge(Li) & Si(Li) Detectors:**

In silicon and germanium, the material with highest available purity tends to be P-type, in which there is predominance of acceptor impurities. Interstitial donor atom like lithium must therefore be added to the crystal of silicon or germanium to serve as a practical compensating impurity. The fabrication is done by diffusing an excess of lithium through one surface of the P-type crystal so that the lithium donors greatly outnumber the original acceptors, creating an N-type region near the exposed surface. The resulting P-N junction is then reversed biased while the temperature of the crystal is elevated to enhance the mobility of the ionized lithium donors. The lithium ion mobility is such greater in germanium and remains high enough at room temperature to permit an undesirable redistribution of the lithium from the compensated situation achieved during the drift. The lithium profile must therefore be preserved immediately after the drift in germanium at 77<sup>0</sup> K. In silicon, the ion mobility is low enough at room temperature to permit storage and use of lithium – drifted silicon detectors without cooling <sup>[77]</sup>.

### **3.2 The Principles of Operation of a Gas-Filled Detector**

- a. How the electric field affects ion pairs
- b. How gas amplification occurs

The pulsed operation of the gas-filled detector illustrates the principles of basic radiation detection. Gases are used in radiation detectors since their ionized particles can travel more freely than those of a liquid or a solid. Typical gases used in detectors are argon and helium, although methane is utilized when the detector is to be used to measure beta's.

Figure 3.1 shows a schematic diagram of a gas-filled chamber with a central electrode.

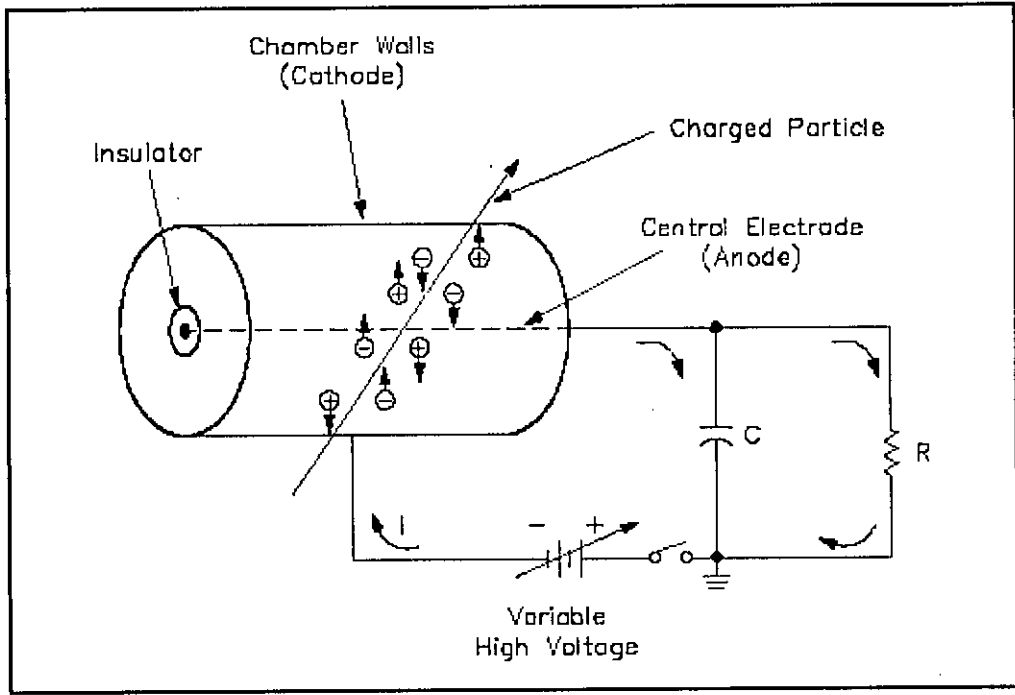


Figure 3.1 Schematic Diagram of a Gas-Filled Detector.

The central electrode, or anode, collects negative charges. The anode is insulated from the chamber walls and the cathode, which collects positive charges. A Voltage is applied to the anode and the chamber walls. The resistor in the circuit is shunted by a capacitor in parallel, so that the anode is at a positive Voltage with respect to the detector wall. As a charged particle passes through the gas-filled chamber, it ionizes some of the gas (air) along its path of travel. The positive anode attracts the electrons, or negative particles. The detector wall, or cathode, attracts the positive charges. The collection of these charges reduces the Voltage across the capacitor, causing a pulse across the resistor that is recorded by an electronic circuit. The Voltage applied to the anode and cathode determines the electric field and its strength.

As detector Voltage is increased, the electric field has more influence upon electrons produced. Sufficient Voltage causes a cascade effect that releases more electrons from the cathode. Forces on the electron are greater, and its mean-free path between collisions is reduced at this threshold. Calculating the change in the capacitor's charge yields the height of the resulting pulse. Initial capacitor charge  $Q$ , with an applied Voltage  $V$ , and capacitance  $C$ , is given by Equation (3.1).

$$Q = CV \text{ -----(3.1)}$$



A change of charge  $\Delta Q$  is proportional to the change in Voltage  $\Delta V$  and equals the height of the pulse, as given by Equation (3.2) or (3.3).

$$\Delta Q = C\Delta V \text{-----}(3.2)$$

$$\Delta V = \frac{\Delta Q}{C} \text{-----}(3.3)$$

The total number of electrons collected by the anode determines the change in the charge of the capacitor  $\Delta Q$ . The change in charge is directly related to the total ionizing events which occur in the gas. The ion pairs (n) initially formed by the incident radiation attain a great enough velocity to cause secondary ionization of other atoms or molecules in the gas. The resultant electrons cause further ionizations. This multiplication of electrons is termed gas amplification. The gas amplification factor (A) designates the increase in ion pairs when the initial ion pairs create additional ion pairs. Therefore, the height of the pulse is given by Equation (3.4).

$$\Delta V = \frac{ANe}{C} \text{-----}(3.4)$$

where,

$\Delta V$  = pulse height (Volts)

A = gas amplification factor

N = initial ionizing events

e = charge of the electron ( $1.602 \times 10^{-19}$  coulombs)

C = detector capacitor (farads)

The pulse height can be computed if the capacitance, detector characteristics, and radiation are known. The number of ionizing events may be calculated if the detector size and specific ionization, or range of the charged particle, are known. The only variable is the gas amplification factor that is dependent on applied Voltage.

The operation of gas-filled detectors is summarized below.

The central electrode, or anode, attracts and collects the electron of the ion-pair.

The chamber walls attract and collect the positive ion.

When the applied Voltage is high enough, the ion pairs initially formed accelerate to a high enough velocity to cause secondary ionizations. The resultant ions cause further ionizations. This multiplication of electrons is called gas amplification<sup>1781</sup>.

### 3.3 The Operation of a Proportional Counter

- a. Radiation detection
- b. Quenching
- c. Voltage variations

A proportional counter is a detector which operates in the proportional region. Figure 3.2 illustrates a simplified proportional counter circuit.

To be able to detect a single particle, the number of ions produced must be increased. As Voltage is increased into the proportional region, the primary ions acquire enough energy to cause secondary ionizations (gas amplification) and increase the charge collected. These secondary ionizations may cause further ionization.

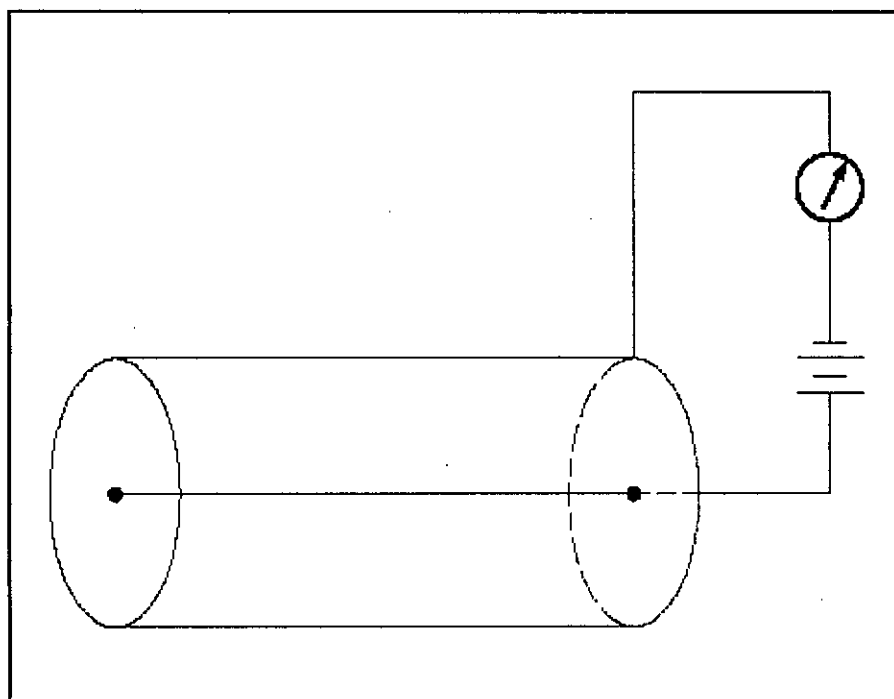


Figure 3.2 Proportional Counter

In this region, there is a linear relationship between the number of ion pairs collected and applied Voltage. A charge amplification of  $10^4$  can be obtained in the proportional region. By proper functional arrangements, modifications, and biasing, the proportional counter can be used to detect alpha, beta, gamma, or neutron radiation in mixed radiation fields.

To a limited degree, the fill-gas will determine what type of radiation the proportional counter will be able to detect. Argon and helium are the most frequently used fill gases and allow for the detection of alpha, beta, and gamma radiation.

The simplified circuit, illustrated in Figure (3.2), shows that the detector wall acts as one electrode, while the other electrode is a fine wire in the center of the chamber with a positive Voltage applied.

Figure 3.3 illustrates how the number of electrons collected varies with the applied Voltage<sup>[83]</sup>.

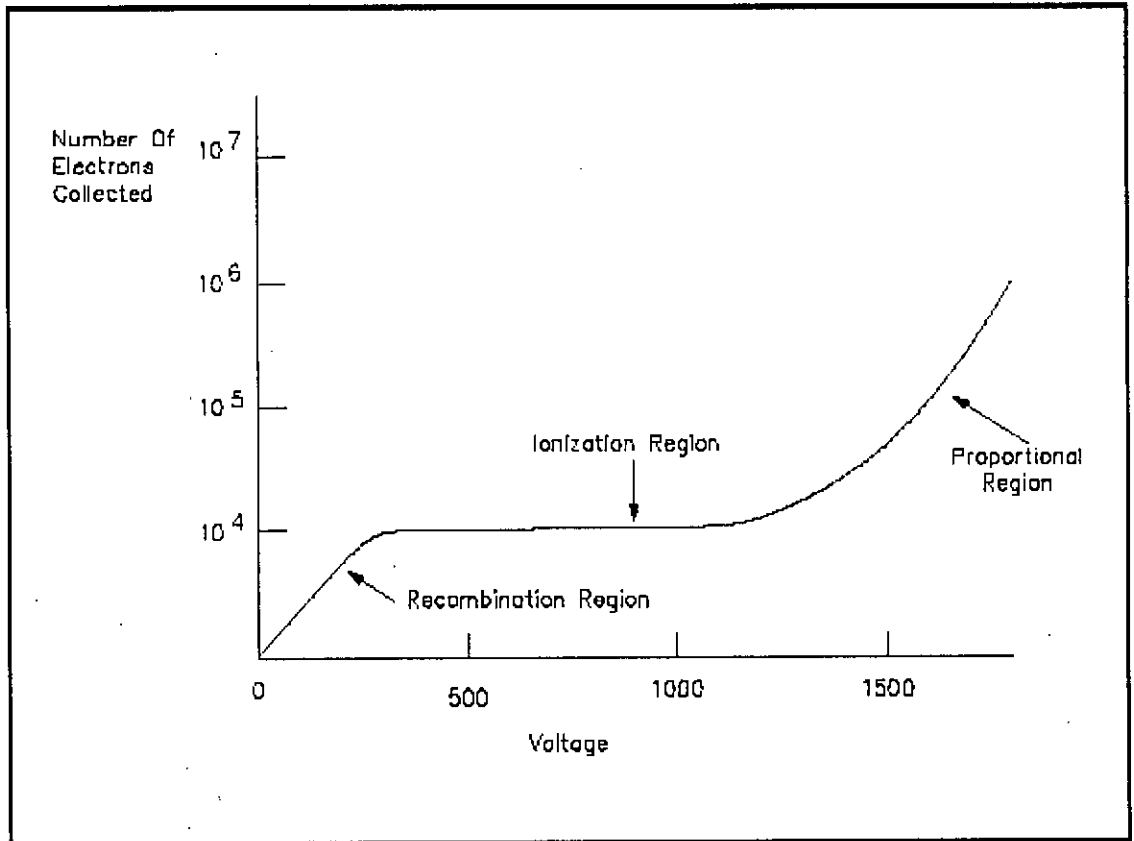


Figure (3.3) Gas Ionization Curve

When a single gamma ray interacts with the gas in the chamber, it produces a rapidly moving electron which produces secondary electrons. About 10,000 electrons may be formed depending on the gas used in the chamber. The applied Voltage can be increased until the amount of recombination is very low. However, further increases do not appreciably increase the number of electrons collected. This region in which all 10,000 electrons are collected is the ionization region.

As applied Voltage is increased above 1000 V, the number of electrons becomes greater than the initial 10,000. The additional electrons which are collected are due to gas amplification. As Voltage is increased, the velocity of the 10,000 electrons

produced increases. However, beyond a certain Voltage, the 10,000 electrons are accelerated to such speeds that they have enough energy to cause more ionization. This phenomenon is called gas amplification.

As an example, if the 10,000 electrons produced by the gamma ray are increased to 40,000 by gas amplification, the amplification factor would be 4. Gas amplification factors can range from unity in the ionization region to  $10^3$  or  $10^4$  in the proportional region. The high amplification factor of the proportional counter is the major advantage over the ionization chamber. The internal amplification of the proportional counter is such that low energy particles ( $< 10$  KeV) can be registered, whereas the ion chamber is limited by amplifier noise to particles of  $> 10$  KeV energy.

Proportional counters are extremely sensitive, and the Voltages are large enough so that all of the electrons are collected within a few tenths of a microsecond. Each pulse corresponds to one gamma ray or neutron interaction. The amount of charge in each pulse is proportional to the number of original electrons produced. The proportionality factor in this case is the gas amplification factor. The number of electrons produced is proportional to the energy of the incident particle.

For each electron collected in the chamber, there is a positively charged gas ion left over. These gas ions are heavy compared to an electron and move much more slowly. Eventually the positive ions move away from the positively charged central wire to the negatively charged wall and are neutralized by gaining an electron. In the process, some energy is given off, which causes additional ionization of the gas atoms. The electrons produced by this ionization move toward the central wire and are multiplied route. This pulse of charge is unrelated to the radiation to be detected and can set off a series of pulses. These pulses must be eliminated or "quenched."

One method for quenching these discharges is to add a small amount ( $\sim 10\%$ ) of an organic gas, such as methane, in the chamber. The quenching gas molecules have a weaker affinity for electrons than the chamber gas does; therefore, the ionized atoms of the chamber gas readily take electrons from the quenching gas molecules. Thus, the ionized molecules of quenching gas reach the chamber wall instead of the chamber gas. The ionized molecules of the quenching gas are neutralized by gaining an electron, and

the energy liberated does not cause further ionization, but causes dissociation of the molecule. This dissociation quenches multiple discharges. The quenching gas molecules are eventually consumed, thus limiting the lifetime of the proportional counter. There are, however, some proportional counters that have an indefinite lifetime because the quenching gas is constantly replenished. These counters are referred to as gas flow counters.

*Proportional counters are summarized below.*

When radiation enters a proportional counter, the detector gas, at the point of incident radiation, becomes ionized.

The detector Voltage is set so that the electrons cause secondary ionizations as they accelerate toward the electrode.

The electrons produced from the secondary ionizations cause additional ionizations.

This multiplication of electrons is called gas amplification.

Varying the detector Voltage within the proportional region increases or decreases the gas amplification factor.

A quenching gas is added to give up electrons to the chamber gas so that inaccuracies are not introduced due to ionizations caused by the positive ion.

### **3.4 G5000 Automatic Low Level Counting System**

In the present work, this gas flow proportional counter was used to calculate only the gross beta activity of soil samples of Rangpur and Dinajpur Districts. Outstanding low level alpha/beta radiation counting with Gamma detector, MCA option and Advanced Computer Controlled Operation, multiple laboratory functions in one system.

#### **3.4.1 Introduction**

The Gamma Products Inc. G5000 low level alpha beta counting system is the most advanced alpha-beta counting system available today. It features state of the art microprocessor technology which provides for complete sample measurement programmability and a total complement of counting functions including a multichannel analyzer option for complete gamma counting analysis. Time proven detector and sample changer technology produce unsurpassed reliability in the G5000 system.

A user friendly menu driven display in the G5000 system provides the operator with function statements for automatic sample selection and control, detector bias selection, user requested sample calculation and operator definable counting sequences.

The higher resolution twelve inch video monitor puts all sample data in front of the operator. Calculations, sample ID's, data analysis, concentration, background subtractions, or user defined equations are all displayable. All sample data is retained in memory or floppy disks for later retrieval and reported, Printout capability is also provided for permanent hard copy data reporting.

### **3.4.2 System Description**

#### **3.4.2.1 Detector Assembly**

The G5000 detector assembly consists of an ultra stable gas flow proportional sample and cosmic guard detector enclosed within oxygen free high conductivity (OFHC) copper and surrounded by a four inch thick low background lead shield. The lead blocks the "Soft" cosmic rays. The copper shields the detector from contaminants in the lead. A precisely machined shielding drawer assembly accurately positions the counting sample within the detector area.

#### **3.4.2.2 Changer Assembly**

The G500 series sample changer incorporates the fewest possible number of moving parts in order to decrease wear problems and insure a high system reliability. The changer mechanism consists of two precision lead screws driven by stepping motors. All moving parts are protected from damage by the automatic disengagement of the drive motors.

The sample changer is controlled automatically by the processor which provides changer movement commands to the motors through the G5000 multifunction controller. Both sequential and random sample selections are provided by the system processor. A manual sample changer mode provides for single sample insertion and user control of the changer mechanism if necessary.

#### **3.4.2.3 System Electronics**

The G5000 system features a personal computer (PC) keyboard programmable microprocessor which controls all sample count functions. The PC utilizes a disk

operating system (DOS) which permits the user to store a multiple number of operating programs. Designed into the G5000 system are buffers and registers which hold programmed preset information and actual sample data. Easy user operation of the system is accomplished through the use of display menus. Sample changer movement is controlled by the G5000 multifunction controller. This unit receives commands from the PC processor to change samples and detector Voltages. Signal analyzing electronics consists of alpha, beta, and guard circuits which accurately interpret sample information from the detectors while the system automatically corrects for system dead time. Analyzed data and keyboard information are displayed on the monitor. The system printer is a dot matrix printer with graphics capability.

#### **3.4.2.4 Processor Control Section**

The PC microprocessor controls all the operations of the G5000 system. The PC control section consists of a color display monitor capable of displaying 25 lines of 80 text characters. The monitor shows all phases of the system operation and all operator input commands. Sample movements, fault and error indications are all displayed on the PC monitor.

The keyboard section of the PC contains an ASCII type keyboard which allows the user to enter alpha/numeric commands into the processor.

#### **3.4.2.5 Sample Changer Front Panel Description**

The G5000 sample changer front consists of an elevator and slide driver mechanism. Sample cartridges are loaded onto the elevator for automatic sample holder insertion under the detector. A gas flow meter is mounted on the panel to the right of the elevator and slide mechanism. The flow meter gives a visual indication of the gas flow and by the adjustment of its needle valve, the gas flow through the detectors can be regulated

#### **3.4.2.6 System Performance**

Background performance (alpha plus beta)

diameter, detector 1 1/4" < 0.5 cpm,

diameter, detector 2 1/4" < 1.3 cpm.

Detector efficiency:

Alpha > 35% for  $^{210}\text{Po}$ , Beta > 30% for  $^{14}\text{C}$  and > 40% for  $^{90}\text{Sr}$  using 80 microgram/cm<sup>2</sup> window.

Alpha > 20% for  $^{210}\text{Po}$ , Beta > 20% for  $^{14}\text{C}$  and > 40% for  $^{90}\text{Sr}$  using 500 microgram/cm<sup>2</sup> window.

Guard efficiency: > 99% cosmic detection.

Detector Uniformity:  $\pm 5\%$  over 90% of window surface.

Detector operation: p/o or methane gas.

Sample count rate: >500,000 cpm

Count limit: >10,000, 000 counts

Timer limit: > 10,000 minutes (to the nearest 0.1sec.)

Time base accuracy: Crystal time base.

### **3.4.3 Theory of Operation**

#### **3.4.3.1 Proportional Counters**

The Gamma Products G5000 gas flow proportional counting systems use the traditional guard sample detector arrangement for the detection and analysis of incoming radiation to the detectors. The sample and guard detectors are p/o or methane gas filled proportional counters. The sample detector incorporates a thin mylar window for particle enters into the detector. Lead and copper shielding surround the detectors to reduce the affects of environmental radiation on the counting statistics. The gas flows through the detectors while a Voltage is applied to the detectors in order to create a detecting medium. When a charged particle enters the proportional detector, it collides with gas molecules and gas ionization occurs. This ionization creates positive ions and free electrons which travel in opposite directions at a velocity that is directly dependent upon the electric field strength (bias applied to the detector) and inversely dependent upon the gas pressure. A charged pulsed proportional in size to the amount of energy released within the detector by the incident nuclear particle results from the collection of free electrons at the electrode. This charge is converted to an electronic pulse by a charge sensitive preamplifier, amplifier and shaped for analysis by a main amplifier and then analyzed as to radiation type. This analyzed data is then stored in the PC system memory for later display, calculation or printout requirements.



If a cosmic event is detected in the guard detector, all sample detector pulses which occur simultaneously with these pulses are rejected.

When a sample counting period has elapsed, the analyzed data is displayed on the PC screen monitor or on printer output. The data may also be stored on floppy disks for later report generation. The sample changer will engage and change samples when a preset condition is reached.

The G5000 utilizes the processor to handle all counting operations. The user enters all operation instructions into the PC keyboard, even the detector Voltage.

### **3.4.4 Factors Affecting the Count Rate**

Various factors can affect the counting results. Spurious counts from background activity can affect counting results, cosmic events and electrical noise can alter system counting results. A brief description of some of the factors which can affect counting results follows.

#### **3.4.4.1 Background Counts**

All proportional counters exhibit background counts. These are counts which occur when no sample is present under the sample detector. For proportional counters these background radiations may come from contamination of system materials, environmental radiation and cosmic radiation.

The G5000 low background counting system uses four inches of lead shielding to reduce the effects of environmental gamma radiation. The lead itself is contaminated to a certain extent by natural radioactivity from heavy elements such as Uranium and Thorium. To counteract this radiation, the detector cavity is used with oxygen free high conductivity copper (OFHC). This copper lining shields the detector from the natural radiation occurring in the lead.

Alpha and beta radiation is present in all materials and if it is inherent in the detector material. This radiation will be counted with 99% efficiency.

Gamma products proportional counters are made of oxygen free high conductivity copper which is machined etched, cleaned and electroplated with gold to give excellent shielding and conduction characteristics.

#### **3.4.4.2 Cosmic Radiation**

The earth is being continually bombarded with cosmic radiation; this radiation produces a large spectrum of secondary particles consisting of electrons, protons, mesons, etc at the earth surface.

The four inches of lead shielding in the G5000 system removes the less energetic components of cosmic radiation. However, mu-meson type of cosmic activity is very penetrating (up to several feet of lead) and is easily detected with almost 100% efficiency in the sample detector.

To counteract this background radiation, a cosmic detector (guard) is placed directly above the sample detector in the G5000 system. All cosmic rays causing a count in the sample detector will also produce a count in the guard detector. Electronic coincidence gating circuits in the system analyzer blank the cosmic ray pulses from being analyzed as true counts.

#### **3.4.4.3 Noise**

Another source of background counts is electrical noise. Electronic noise is present in every environmental laboratory. Power line noise, noise from electrical motors, fluorescent lightings, changing electrical loads, such as communication, elevators and motor controllers, can create system background noise.

To guard against outside noise interference, the G5000 system incorporates extensive noise filtering and lines noise monitoring in order to reduce the effects of environmental electrical noise.

#### **3.4.4.4 Count Rate Loss**

In addition to the background counts other factors can enter into sample count rate determination. These factors include detector window energy absorption, sample to detector distance, detector efficiency, detector active area and sample preparation. The

presence of an absorbing substance in the path of the radiation can greatly affect the sensitivity of a proportional counter detector medium. This occurrence is of most importance for alpha and beta radiation. Charged particles (alpha and beta) are easily detected if they are allowed to enter the detector.

Absorption can be of several type, sample self absorption, absorption in the medium between the sample and counter, and window absorption.

#### **3.4.4.5 Sample Distance**

The solid angle effect and the absorption in the air between the sample and detector window can become significant for low energy beta and alpha emitters. For carbon-14, air absorption affects become significant above 25 millimeters sample to window spacing. For beta emitters above 0.3 MeV, the air absorption does not become significant until 10 MeV, or above the solid angle effect can be quite large due to sample to detector distance, especially if the sample diameter equals the detector diameter.

#### **3.4.4.6 Window Absorption**

Window absorption is very critical for low energy beta emitters. The G5000 system standard window thickness is 500 micrograms/cm<sup>2</sup> of mylar with gold film. This window thickness is recommended for counting .03 MeV or greater beta emitters. For softer beta emitters such as carbon-14 at .01 MeV, a thin 80 microgram/cm<sup>2</sup> thick mylar with gold film is recommended.

#### **3.4.4.7 Detector Efficiency**

The probability that radioactivity penetrating proportional detector window will create enough ion parts to produce a count is the intrinsic efficiency of the detector. Gas flow counters can achieve intrinsic efficiencies approaching 100% when plateau slopes are better than 3% per 100 Volts. Poor plateaus are an indication of a scattered electric field distribution with subsequently lower detector intrinsic efficiencies. This lower efficiency will make reproducible counting results difficult to achieve.

Gamma products flow proportional counters typically have detectors plateau slopes of 1.2% to 2.0 % per 100 Volts.

#### **3.4.4.8 Detector Area**

The sensitive area of a detector varies directly as the square of the detector diameter and is the most important factor affecting sample count rate. The sample count rate for a given sample thickness varies as the sample area; therefore the sample count rate is proportional to the square of the detector diameter. It is important to match the detector diameter to the size of the sample for best counting results.

#### **3.4.4.9 Sample Preparation**

Another factor affecting sample counting is sample preparation. Samples whose thickness approach or exceed self absorption limits of the material will produce low counting yields and erroneous data. Sample should be prepared in a manner consistent with reasonable self absorption effects.

#### **3.4.5 Statistics of Measurement**

This section provides a basic outline of some of the statistical calculations used in low activity level counting and which are necessary to determine counting errors and to test the system counting integrity.

##### **3.4.5.1 Pico-Curies Per Volume Calculation**

In many applications it is necessary to determine the total level of sample activity in pico-curies for the detected sample Volume. This requires the counting of the sample counts back to pico-curies per Volume.

The G5000 system does this automatically by calculating the net CPM and then corrects for the detector counting efficiency, sample Volume, sample collection efficiency, DPM or other user defined parameters. The user enters as a defined statement the variables pertaining to the sample. The processor then computes the pico-curies per Volume for each sample counted.

##### **3.4.5.2 Standard Deviation**

The standard deviation is used as a basis for most error calculation in radiation counting. Simply stated the standard deviation is the square root of the observed counts and is expressed as sigma.

Standard Deviation ( $\sigma$ ) = Square root of observed counts

( $\sigma$ ) = Square root of N,

Where N counts are observed for a period of time (T), a standard deviation of the counting rate (R) may be taken.

**Standard Deviation of the Count Rate:**

Square root of observed counts/time.

For example, if 10,000 counts are observed in ten minutes then:

The count rate R or  $N/T = 10,000/10$  or 1000 cpm.

The standard deviation of R = square root of  $N/T$

$10,000/10 = \pm 10$  cpm.

The true count rate will be expressed as the count rate  $R \pm$  the standard deviation which in this case is

$1000 \text{ cpm} \pm 10 \text{ cpm}$ .

The standard deviation in the above example expresses the range of the values about the average count for which about two thirds of all similar counts are outside of this range, we have a measure of the reproducibility of the type of count taken.

This is referred to as an error of one standard deviation. Statistical principles show that the distribution of errors for a random process follow a bell shaped curved. If we can increase the number of standard deviations, we can increase the probability that the observed count rate will fall within the calculated range.

For an error of two standard deviations, the true count rate will fall within the error limits 95% of the time. Two standard deviations or 2 sigma is expressed as:

2 sigma = times the square root of observed count rate  $N/T$ .

Where an error of three standard deviations has been assigned, the true count rate will fall within error limits 99.9% of the time.

It is standard practice to use a 2 sigma or 95% confidence level in radiation counting. If a 2 sigma error is used consistently and the equipment is reproducing counts accurately one can be confident that the observed counts will lie within the stated limits 95% of the time.

The G5000 incorporate a programmed calculation for the 2 sigma standard deviation of the observed count rate.

### **3.4.5.3 Background Subtraction**

Background concentrations affect the calculation of reduced data by contributing counts that are not due to the source being counted. If the sample count rate is very low, the background may mask the source count rate. It is therefore necessary to correct for counting results by taking into consideration the background contribution. Longer counting periods are necessary for good counting statistics when the background rate approaches the sample count rate. The G5000 system has provisions for automatic background subtraction during sample counting.

### **3.4.5.4 Background Checks**

Background checks should be made periodically and plotted in order to indicate trends in counter operation. If a two-sigma error is applied to background checks and the background falls outside the error limits, the system should be service checked. Possible changes in background may be due to contamination of the slide mechanism or sample window. High Voltage drift contaminated gas or electronic instrument malfunctions may also cause changes in background.

If a new background level has occurred due to system contamination which cannot be corrected, a new two-sigma limit should be determined for this background level.

### **System Operation:**

#### General Information

The initial setup and run operations for the G5000 system can be accomplished quickly once all the system controls and functions are understood.

Setting up the G5000 for initial system operations requires five main operator functions:

1. Setting the detector gas flow rate.
2. Initializing the system
3. Loading the sample changer with sample.
4. Entering the counting routines to be performed.
5. Starting the Count Operation:

Activating and setting the proper gas flow rate requires that all gas pressure valves and regulators are correctly set and that the detectors have been purged for at least 30 minutes.

Initializing the system requires that all system AC power and signal cords are properly connected and that the G5000 system diskette has been installed into the sample cartridge and placing the cartridge in the sample changer mechanism. A disk drive or the default drive before system power has been switched on. Loading samples for counting involves the placing of the samples into the sample cartridge and placing the cartridge in the sample changer mechanism.

Initiating the counting operation involves entering user defined operating routines into the G5000 processor control menus and starting the count operation.

General specifications <sup>[84]</sup>

Gas Filling	Methane
Path Length (inch/mm)	0.35 / 9.0
Cathode Material	OFHC Copper
Maximum Length (inch/mm)	3.72 / 94.5
Effective Length (inch/mm)	1.72 / 43.7
Maximum Diameter (inch/mm)	2.25 / 57.2
Effective Diameter (inch/mm)	1.25 / 31.8
Connector	Pin
Operating Temperature Range 0C	0 to +50

Window specifications

Material	Aluminized Mylar
Areal Density (mg/cm <sup>2</sup> )	0.2
Diameter (inch/mm)	1.25 / 31.8

Electrical specifications

Recommended Operating Voltage (Volts) – Alpha	1000
Recommended Operating Voltage (Volts) - Beta / Gamma	1450

Operating Voltage Range (Volts) – Alpha	900 – 1150
Operating Voltage Range (Volts) - Beta / Gamma	1350 – 1600
Background (Anticoincidence +4 inches Pb (CPM))	1.0
Capacitance (pf)	3

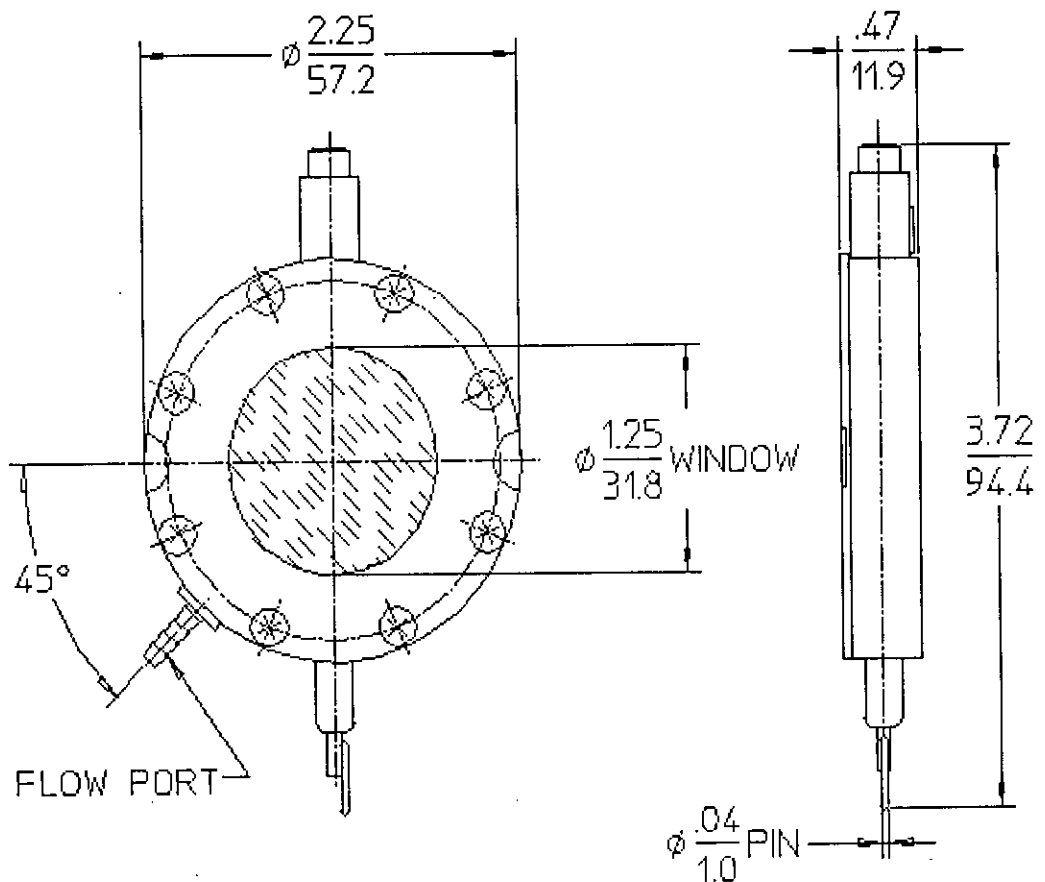


Figure 3.4 General specifications of a proportional counter.

### 3.5 High Purity Germanium (HPGe) Detectors

HPGe detector is a high quality precision instrument and is used in gamma ray spectroscopy above about 100 KeV for its high efficiency and good resolution. The basic element of an HPGe detector is a single crystal of germanium with P-N diode structure. If the impurity concentration in germanium can be reduced to about  $10^{10}$  atoms/cm<sup>3</sup> a depletion depth of about 10 mm can be obtained. These large-Volume



germanium diode detectors are usually called “intrinsic “or “high purity” germanium detectors. The bulk of the high purity materials is generally P-type, due either to residual acceptor impurities (such as aluminum ) or to acceptor centre associated with lattice defects within the germanium itself, the configuration is sometimes referred to as  $N^+ -P-P^+$  diode structure. The  $N^+$  contact is usually formed by lithium evaporation onto a lapped surface of the germanium followed by a short period of diffusion at elevated temperature. The detector depletion region is formed by reverse biasing this  $N^+ -P$  junction. The  $P^+$  contact at the opposite face is a typically diffused gold surface barrier junction. The outer N-type diffused Li contact is about 300 mm thick. The inner surface barrier contact is about  $40 \text{ mg/cm}^2$  of evaporated gold<sup>[77]</sup>.

### 3.5.1 Advantages of the HPGe Detectors

The widespread popularity of germanium as semiconductor radiation detector is attributable to the excellent charge transport properties, which allows the use of large crystals without excessive carrier losses due to trapping or recombination. The greater efficiency, larger photofraction, and lower cost of sodium iodide may well tip the balance in its favour when only a few gamma ray energies are involved. Germanium detectors are clearly preferred for the analysis of complex gamma ray spectra involving many energies and peaks, it also aids in the detection of weak sources of discrete energies when superimposed on a broad continuum. Germanium must always be operated at low temperature ( $77^0\text{K}$ ) to reduce thermally generated leakage current. The reason for the attractiveness of the semiconductor detectors lies in the improved energy resolution compared to scintillation detectors (NaI, ZnS etc.) and in the increased stopping power of a solid material instead of a gas. About 3 eV is needed for the production of one electron –hole pair in a semiconductor detector, 100 eV in a solid-state scintillation detectors and 34 eV in a gaseous ionization detector to form an ion pair. So the number of carriers produced for a given energy absorption is large in the case of semiconductors, and the statistical fluctuations in that number are small when expressed as a percentage of the total number. A 100 KeV photon will only give rise to a statistical spread in the number of carriers of about 180 in a semiconductor detector (or  $s = 0.55 \text{ KeV}$  on energy spread). In the case of gas ionization detector, it is about 2 KeV. Since about 300 V is needed to create an electron-ion pair and so the energy spread is 20 KeV for these detectors<sup>[85]</sup>.

### **3.6 A Brief Description of HPGe**

In the present work, the measurements were made with HPGe detector for gamma counting. The main parts of this detector coupled with other accessories are.

1. Liquid Nitrogen (LN<sub>2</sub>) Dewar;
2. Cryostat;
3. A preamplifier connected just below the detector,
4. Spectroscopy amplifier;
5. High Voltage power supply;
6. Personal computer analyser (PCA);
7. Shielding arrangement of the detector.

A brief description of these parts are given bellow:

#### **3.6.1 Liquid Nitrogen (LN<sub>2</sub>) Dewar**

The detector must be cooled sufficiently in order to reduce the thermal generation of charge carriers to an acceptable level; otherwise, the noise due to leakage current would destroy the energy resolution of the detector. Liquid nitrogen, which has temperature 77<sup>0</sup>K, is the common cooling medium of the detector. The liquid nitrogen Dewar serves as a reservoir of liquid nitrogen, while the cryostat provides a path via the copper stem for heat transfer from the detector to liquid nitrogen reservoir.

#### **3.6.2 Cryostat**

Typical detectors are mounted in a vacuum cryostat with a copper coldfinger immersed in liquid nitrogen. The crystal is clamped on the other end of the copper coldfinger. The cryostat provides a path via the copper stem for heat transfer from the detector to liquid nitrogen reservoir and heat is pumped out of the system by the nitrogen. The cryostat is a sealed vacuum chamber, and usually the vacuum is maintained by a passive system, a molecular sieve, and placed in the bottom of the cold finger assembly. This molecular sieve adsorbs any gaseous molecules, which come loose inside the cryostat, and prevents them from depositing on the surface of the crystal. Otherwise, the increasing

surface contamination on the crystal would result in increased surface currents, which, in turn, elevates the noise and broadens the resolution.

### **3.6.3 Preamplifier**

The preamplifier associated with radiation detector performs three essential functions:

1. Conversion of charge to Voltage pulses,
2. Signal amplification,
3. Pulse shaping.

There are only two basic types of preamplifiers used in Germanium detectors: Charge sensitive that employs either dynamic charge restoration (RC feed back) or pulse charge restorer type (pulse optical or transistor reset) for discharging the integrator. Absorption of a photon by detector produces a current pulse at the preamplifier input. These pulses are too small to measure without amplification into a measurable electric signal. Therefore, the first element in a signal-processing cabin is a preamplifier that provides interference between the detector and pulse processing and analyzing electronics. The preamplifier has been located as close as possible to the detector to minimise the signal from noise and capacitive loading. It also serves as an impedance matcher, presenting high impedance to the detector or to minimize loading, while providing a low impedance output to drive succeeding components. In the present work, PGT preamplifier of model RG-15 was used for its following characteristics:

#### **Characteristics of RG-15 preamplifier:**

- (a) Charge sensitivity (nominal): 100 mV/MeV
- (b) Input pulse polarity: Positive
- (c) Input open loop gain: <20000
- (d) Output polarity: Negative
- (e) Delay time constant: 100  $\mu$  sec
- (f) Output impedance: 93 ohm
- (g) Maximum cable length: 30 m
- (h) Energy rate produce: 50000 MeV/sec.

### **3.6.4 Amplifier**

The amplifier is a key unit in gamma-ray spectrometry. It performs the following function:

1. It amplified the weak signals from the preamplifier to level suitable for pulse height analysis.
2. It improves the signal to noise ratio.

A good amplifier should have low input noise and high amplification or gain factor. In the present work ORTEC Model-570 amplifier was coupled with HPGe detector <sup>[86]</sup>:

Coarse gain: 100

Fine gain: 1

Time constant: 4  $\mu$ sec

Out put polarity: unipolar

Output shape: Gaussian

### **3.6.5 High Voltage Power Supply**

In order to collect the charges produced in the detector, an external high Voltage bias must be placed across the detector. This Voltage is conventionally called "Detector Bias Supply". In our present experiment, the positive Voltage of 1900V was selected from the detector bias supply (Nucleus Model- ORTEC 495). For the case of electricity failure, the output Voltage is dropped and restored back slowly to the applied value; otherwise the sudden reverse polarity of high Voltage to a detector may destroy the FET inside the cryostat and also may damage the preamplifier. Some important characteristics of detector bias supply are furnished below:

Bias control: 5 turns direct reading precession potentiometer range 0- 5000 Volts.

Bias polarity: The polarity was positive selected by internal switch.

Voltage selection: + 1900 Volts <sup>[87]</sup>.

### **3.6.6 Personal Computer Analyser (PCA)**

The analyzer is used for recording pulses from the output of the spectroscopy amplifier falling within selected Voltage amplitude. A device that is capable of digitizing and analysing these pulses according to the channel numbers is called a multichannel analyzer (MCA).

A personal computer analyzer (PCA) card (APTEC PCMCA/WIN version 5.30) with software's was installed in the central processing unit of the IBM. PC supplied by the APTEC Nuclear Instruments Co. U.S.A., contains 100 MHz Wilkinson analogue to digital converter (ADC), single channel analyzer (SCA), multichannel scaler (MCS) and a dualported memory<sup>[88]</sup>. The pulses from the amplifier enter into the MCA and display the data in the monitor for various purposes. The display provides a graphic representation of the accumulated data. The channel numbers is the memory address and is proportional to the input signal Voltage. The horizontal scale is adjustable over a range of memory channels. The spectrum may be examined in details by expanding the horizontal scale. Groups of adjacent channels may be defined as a region of interest and these channels are intensified on the display for identification. An intensified region can represent the boundary of a peak and the average of its end points is used in the calculation of peak area. Cursor positions are used in setting up the regions of interest and specify the points of scale expansion as peak location. The PCA has the following features:

- a. Memory: 8192 channel acquisition memory (optional 1024, 2048, 4096 channel)
- b. Conversion gain: Selectable from 256 to 8192 channels in binary increments.
- c. Digital offset: Selectable in 256-channel blocks to 7936 channels.
- d. Display: In the present work a high-resolution live display colour monitor has been used.

Here, there is an IBM video graphics adapter (VGA) and an IBM CGA card # 15120 installed inside the central processing unit (CPU) of personal computers.

**Printer:** Printer (both dot and laser) was coupled with the personal computer. The necessary print out of data has been taken from it.

### **3.6.7 Lead Shielding Arrangement of the HPGe Detector**

The shielding of the detector from the environmental radiation is an absolute necessary for low-level measurement of activity. The shielding not only reduces the background resulting from cosmic radiation and from natural radioactive traces in the building materials or in the surface of the earth, but also from nearby nuclear facilities and other radiation sources like the ambient air, which presumably contains trace of radioactive

gases such as, Radon ( $^{22}\text{Rn}$ ) and Thoron ( $^{22}\text{Th}$ ) etc. In the present experiment, the shielding arrangement was fabricated by using locally available lead and steel materials. Theoretically, the shielding arrangement was found to attenuate 95%-99.99% of unwanted gamma flux of energy ranging from 303 KeV to 1332 KeV, where most of the gamma lines from background radiation (Thorium, Uranium, Actinium series) were found to decrease by 74% - 96%.

The following are the specifications for the shielding of the HPGe detector:

**Shielding material around the detector (lead):**

- (a) Internal diameter: 33.02 cm
- (b) External diameter: 43.18 cm
- (c) Wall thickness: 5.08 cm
- (d) Shielding height: 33.02 cm

Steel ring outside lead shielding:

- (a) Height: 40.00 cm
- (b) Thickness: 0.4 cm

Circular top cover of the shielding:

- (a) Diameter: 43.18 cm
- (b) Thickness: 5.08 cm
- (c) Diameter of sample inserting hole: 12.70 cm

Table (Steel Material):

- (a) Height: 58.09 cm
- (b) Top area: 66.04 cm<sup>2</sup>
- (c) Top steel thickness: 1.27 cm

Distance between the detector and the shielding wall: 13 cm

As a whole, the following are the specifications of the HPGe detector (Model IGC-3019):

Detector: High purity Germanium (HPGe)

- Detector model: IGC
- Model number: 3019
- Serial number: 2743
- Crystal geometry: P-type coaxial
- Crystal diameter: 62 mm

Crystal length: 47 mm

Crystal active Volume: 132 cm<sup>3</sup>

Dead layer: > 1 mm

Crystal/Window distance: 5 mm

Detector window thickness: 51 mm

Dewar capacity: 30 litres

Cooling temperature of the Ge crystal: 77<sup>0</sup> K (i.e., LN<sub>2</sub> temperature)

Energy resolution of the detector: (FWHM at 1332 KeV of <sup>60</sup>Co gamma rays)= 1.83 KeV (specified by manufacturer)

Relative efficiency (relative to 3" x 3" NaI) = 356%

Peak to Compton ratio: 60.1:1 (or 60.1)

### 3.7 Calibration of Detector Parameters

#### 3.7.1 Energy Calibration

In gamma spectrometry, radiation pulses are recorded by a multichannel analyzer (MCA) and the location of the peak depends on the gamma ray energy. For identifying a particular radionuclide of unknown sample, it is necessary to calibrate the MCA by the observed gamma energy against the channel number. Here the channel number has no significance until it can be calibrated in terms of energy.

For a detector the output pulse height is proportional to the gamma ray energy i.e., channel numbers. Therefore two or more known point sources of sufficiently different energy will serve to establish the energy calibration. Let E<sub>1</sub> and E<sub>2</sub> are the known energies of peaks and let X<sub>1</sub> and X<sub>2</sub> are the peak locations in channel numbers. Thus energy per channel number can be calculated as:

$$E = mX + b$$

where; X is any channel number.

$$\text{Energy per channel} = m = (E_2 - E_1) / (X_2 - X_1)$$

$$\text{Constant, } b = E_1 - mX_1$$

In the present study calibration of the MCA was carried out by using good geometry point sources placed close to the detector inside the shield. The gamma spectra obtained on the PCA monitor after the equipment set up of live time, high Voltage power supply

(3500 Volts), Amp. Gain (8.84) lower level discriminator (LLD), adjustment of spectroscopy amplifier such as course gain (100), fine gain (1), time constant (4  $\mu$ sec). The energies of the calibration source in KeV were entered in the MCA to convert all 4096 channel to respective energies.

### 3.7.2 Counting Efficiency of the HPGe Detector

The efficiency of a detector is a measure of the number of gamma rays detected out of the number of gamma rays that are actually emitted by the source. The full energy peak efficiency is defined as:

$$\epsilon(E) = \frac{n(E)}{R(E)} \text{-----(3.5)}$$

where, n (E)= net count rate in the peak energy for the standard source,

R (E) = rate at which photon of energy E are emitted from the source.

Thus, equation (3.5) becomes,

$$\epsilon(E) = \frac{n(E)}{A \times I} \text{-----(3.6)}$$

Where, A = activity,

I= intensity of gamma energy

The determination of detector efficiency by using Eq<sup>n</sup>. (3.6) requires a standard source that has similar chemical composition and geometry as the studied samples but higher concentration than the studied samples. Usually the deviations are below 10%, which could be acceptable for many applications<sup>[89]</sup>.

### 3.7.3 Energy Resolution

The resolution of a spectrometer is a measure of its ability to resolve two peaks that are fairly closed together in energy. The resolution is defined as the Full Width at Half Maximum (FWHM) to the pulse height produced in channel numbers, which is directly proportional to the gamma-ray energy. Thus resolution,

$$R = \frac{FWHM}{H_0} \text{----- (3.7)}$$

FWHM= full width at half maximum of the full energy peak

H<sub>0</sub> = mean pulse height for the corresponding peak.



The measurement of FWHM was done by placing the specific radioisotope source on the top of the detector and the peak counts were accumulated for a reasonable time. The width of the peak at the point halfway between the peak maximum and the baseline was taken in channel numbers. This observed channel numbers could be expressed in energy often knowing the energy calibration term i.e., energy per channel. A better resolution means a narrow and sharp peak, which is above the natural background signal<sup>[90]</sup>.

## CHAPTER-IV METHODS AND MATERIALS

### 4.1 Sample Collection

Soil samples were collected from different locations at the sites of Rangpur and Dinajpur districts to measure the radioactivity level. For this purpose, sites were selected in several directions and at various distances from each sampling spot and samples were collected at a depth of 0-5 cm from the surface of the soil. Each site was selected on the basis that the soil appeared, or was known to have been, undisturbed for a number of years. Sixteen soil samples were collected from different locations in Rangpur from 9 to 10 July 2001 and twenty-three samples were collected from different locations in Dinajpur from 11 to 12 July 2001. These samples were packed in polythene bags tightly in such a way that no fraction of the soil could normally escape from the bags. All the collected samples were stored in Health Physics Laboratory, BAEC of Dhaka.

### 4.2 Sample Preparation

These samples were air dried under laboratory temperature and relative humidity condition. Each sample was cleaned and crushed to fine powder with mortar and pestle. These samples were transferred to cylindrical plastic containers, measured individually by a sensitive balance, marked with identification number and net weight. In this way, 16-sample from Dinajpur of weight 420-538 g and 16 from Rangpur of weight 350-500 g were prepared for gamma activity measurement.

For beta activity measurement, samples were made moisture free by keeping it overnight in an oven at a temperature of 100°C. The dried samples were ground by grinder and then homogeneously spread out on a planchette. The sample on that planchette covered with 5% UHU-glue and 95% acetone mixture for fixing the sample. This sample was kept in a desiccator for further analysis. In this way, 16-sample of Rangpur prepared for the mass ranging from 204.20 mg to 294.10 mg and 26-sample of Dinajpur with the mass ranging from 200.40 mg to 298.0 mg. These samples were analyzed by using the low-beta (G5000 series, gamma products, inc.) connecting system where locally produced Methane gas (99%) is used <sup>191</sup>.

### 4.3 Standard Beta Source

The determination of detector counting efficiency requires standard source that have similar chemical composition, comparable concentration, geometry and counting configuration as the real samples. In the present study, Potassium Chloride (KCL) was used as a standard source for the determination of efficiency of the detector. By keeping the standard source within the detector, the sample and background counts for 30 minutes were recorded. Efficiency changes with physical changes of counting system and the environment surrounding it. For low-level activity of environmental samples, it is desirable to increase the efficiency as much as possible to increase the minimum level of detection <sup>[92]</sup>. Efficiency was measured using the formula:

$$\% \text{Efficiency} = \frac{CPM}{DPM} \times 100 \text{-----(4.1)}$$

where, CPM → Counts per minute

DPM → Disintegrations per minute

Results are shown in table below:

Table 4.1: Efficiency calculation of the Low Beta Counter using different weight of Potassium Chloride (KCl).

Sample Identity	Sample Weight (g)	Sample cpm	Background cpm	Net cpm	dpm	% Efficiency
1	0.05	12.767	3.2	9.567	43.325	22.0819
2	0.1	26.967	3.167	23.8	86.65	27.4668
3	0.5	106.45	3.133	103.317	433.25	23.847
4	1	189.855	3.4	186.455	866.5	21.5182
5	1.5	252.85	3.267	249.583	1299.75	19.2024
6	2	307.967	3.533	304.434	1733	17.5669
7	2.5	352.333	3.467	348.866	2166.25	16.1046
8	3	389.567	3.2	386.367	2599.5	14.8631
9	3.5	409.6	3.5	406.1	3032.75	13.3905
10	4	416.5	3.667	412.833	3466	11.9109

From the above table, a graph of weight against %efficiency was plotted.

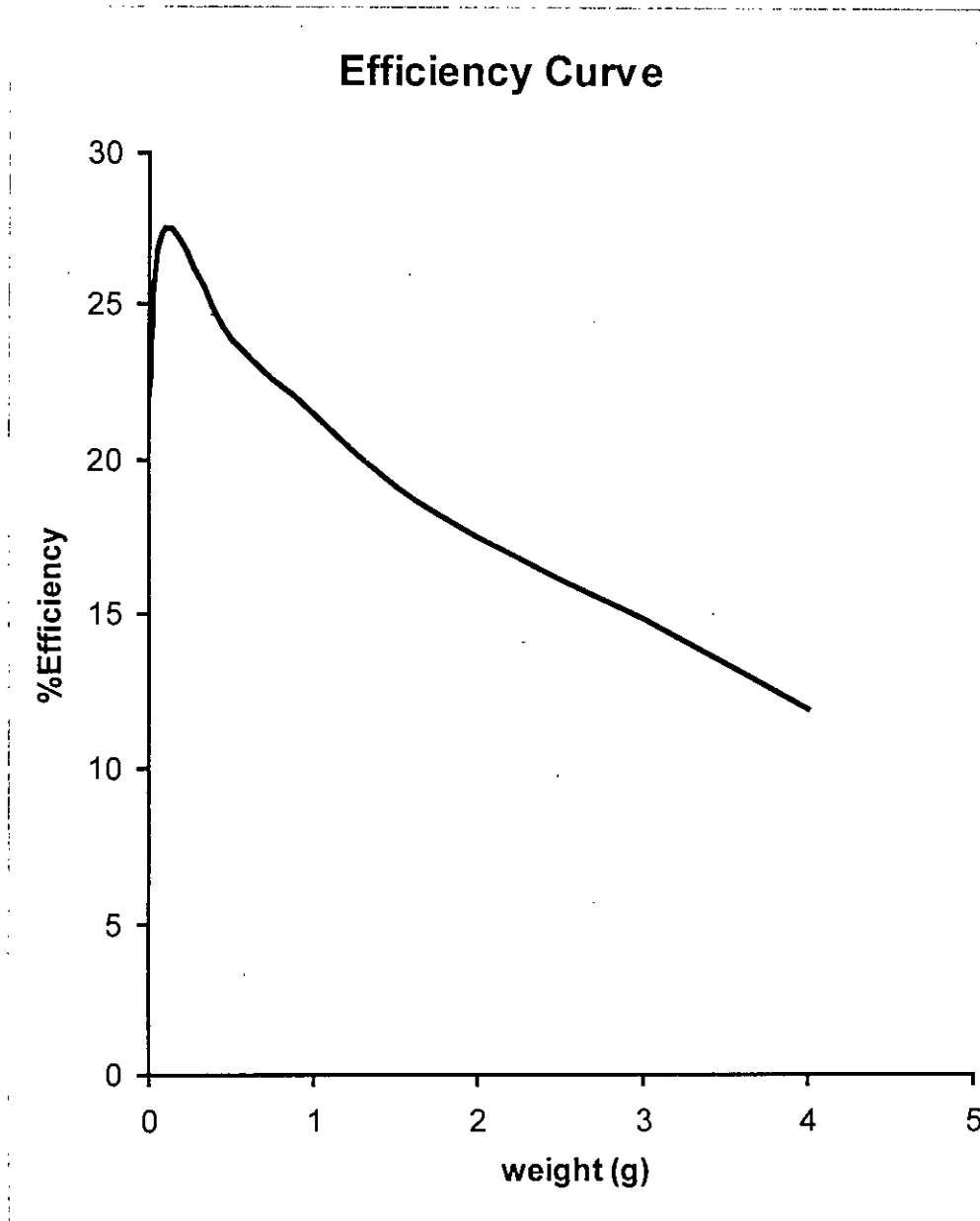


Fig. 4.1: Efficiency curve of Low Beta Counter using Potassium Chloride (KCl).

Using origin 41 program, the efficiency for corresponding samples were calculated from the graph, shown in Table 4.2-4.3.

Table 4.2: Efficiency of Low Beta Counter corresponding to different weight of soil samples collected from Rangpur

Sample Identity	Weight of Sample (mg)	%Efficiency
RS-1	222.6	26.42
RS-2	231.1	26.27
RS-3	207.7	26.56
RS-4	294.1	26.62
RS-5	204.2	26.4
RS-6	249.7	26.12
RS-7	252.6	26.13
RS-8	216.9	26.5
RS-9	225.2	26.45
RS-10	269.6	25.98
RS-11	285.9	25.84
RS-12	248.6	26.1
RS-13	229.3	26.2
RS-14	236.5	26.22
RS-15	243.9	26.13
RS-16	276.9	25.9

Table 4.3: Efficiency of Low Beta Counter corresponding to different weight of soil samples collected from Dinajpur

Sample Identity	Weight of Sample (mg)	%Efficiency
DS-1	239.2	26.25
DS-2	225.9	26.45
DS-3	265.1	26.98
DS-4	235.7	26.27
DS-5	229.98	26.2
DS-6	282.1	26.8
DS-7	271.17	26.95
DS-8	217.5	26.5
DS-9	214.2	26.5
DS-10	267	26.98
DS-11	268.3	26.98
DS-12	251.9	26.13
DS-13	279.7	26.92
DS-14	222.6	26.42
DS-15	256.2	26.3
DS-16	238.9	26.22
DS-17	298	26.85
DS-18	227.9	26.45
DS-19	276.4	26.9
DS-20	260.6	26.4
DS-21	245.6	26.23
DS-22	252.5	26.13
DS-23	209	26.56
DS-24	200.4	26.44
DS-25	217.4	26.5
DS-26	270.2	26.95

#### 4.4 Beta Activity Measurement

Each sample was put into the detector and counted for 30-minute duration. Background was also counted for the same duration. Activity of the samples was measured by using the formula:

$$A = \frac{CPS}{\%efficiency \times weight(g)} Bq/g \text{-----(4.2)}$$

where, A → Activity of the sample

CPS → Net counts per second (cps for sample-cps for background)

E → Counting efficiency (in percentage) of the detector

W → Weight of the sample (g)

#### 4.5 Error Calculation

Each sample was counted three times for the 30-minute duration and one count for background for the same duration. The average cps for each sample was:

$$CPS_{avg} = \frac{cps(1) + cps(2) + cps(3)}{3} \text{-----(4.3)}$$

The errors in the measurements have been expressed in terms of standard deviation ( $\pm 1\sigma$ ) which is expressed as:

$$\pm 1\sigma = \left[ \frac{CPS_{avg}}{T_s^2} + \frac{CPS_b}{T_b^2} \right]^{\frac{1}{2}} \text{-----(4.4)}$$

where,  $CPS_{avg}$  → Average counts in time  $T_s$  for the sample

$CPS_b$  → Counts in time  $T_b$  for background radiation

$T_b$  → Background counting time

$T_s$  → Sample counting time

The standard deviation  $\pm 1\sigma$  in cps was converted into activity in Bq/g according to the eq<sup>n</sup> (4.2) <sup>[93]</sup>.

Gross activity beta for samples collected from Rangpur and Dinajpur are given in Table 4.4-4.5.

Table 4.4: Total beta activity of the soil samples collected from different locations of Rangpur

Sample Identity	Location	Altitude and Longitude	Activity pCi/g
RS-1	Kaunia	25 <sup>0</sup> 3'5"E, 89 <sup>0</sup> 1'32"N	37.78 ± 4.41
RS-2		25 <sup>0</sup> 3'24"E, 89 <sup>0</sup> 1'30"N	40.31 ± 4.85
RS-3	Pirgacha	25 <sup>0</sup> 2'30"E, 89 <sup>0</sup> 1'37"N	37.85 ± 5.11
RS-4		25 <sup>0</sup> 1'34"E, 89 <sup>0</sup> 2'23"N	36.44 ± 3.90
RS-5	Pirgonj	25 <sup>0</sup> 1'27"E, 89 <sup>0</sup> 1'6"N	39.16 ± 4.93
RS-6		25 <sup>0</sup> 2'29"E, 89 <sup>0</sup> 2'15"N	50.42 ± 4.82
RS-7	Mithapukur	25 <sup>0</sup> 2'17"E, 89 <sup>0</sup> 1'1"N	30.17 ± 4.30
RS-8		25 <sup>0</sup> 2'14"E, 89 <sup>0</sup> 1'24"N	31.32 ± 4.64
RS-9	Gangacharda	25 <sup>0</sup> 3'14"E, 89 <sup>0</sup> 36"N	35.04 ± 4.58
RS-10		25 <sup>0</sup> 3'10"E, 89 <sup>0</sup> 1'12"N	39.23 ± 4.48
RS-11	Taragonj	25 <sup>0</sup> 3'9"E, 88 <sup>0</sup> 3'54"N	40.85 ± 4.23
RS-12		25 <sup>0</sup> 3'17"E, 88 <sup>0</sup> 3'22"N	37.26 ± 4.71
RS-13	Badorgonj	25 <sup>0</sup> 39"E, 89 <sup>0</sup> 2"N	36.54 ± 4.54
RS-14		25 <sup>0</sup> 30"E, 89 <sup>0</sup> 21"N	44.86 ± 4.72
RS-15	Rangpur	25 <sup>0</sup> 3'5"E, 89 <sup>0</sup> 1'3"N	41.94 ± 4.53
RS-16		25 <sup>0</sup> 3'7"E, 89 <sup>0</sup> 1'32"N	38.52 ± 4.09
Average			38.61 ± 4.55



Table 4.5: Total beta activity of the soil samples collected from different locations of Dinajpur

Sample Identity	Location	Altitude and Longitude	Activity pCi/g
DS-1	Biral	25°2'32"E, 88°1'57"N	45.20 ± 4.78
DS-2		25°2'30"E, 88°1'58"N	28.78 ± 4.36
DS-3	Botchagonj	25°3'14"E, 88°1'45"N	39.68 ± 3.10
DS-4		25°3'18"E, 88°1'43"N	40.74 ± 4.46
DS-5	Kaharol	25°3'13"E, 88°2'19"N	30.10 ± 4.41
DS-6		25°3'11"E, 88°2'28"N	28.32 ± 3.81
DS-7	Birgonj	25°3'36"E, 88°2'54"N	38.22 ± 4.16
DS-8		25°3'38"E, 88°2'51"N	29.28 ± 4.56
DS-9	Khansama	25°3'4"E, 88°2'50"N	45.66 ± 4.91
DS-10		25°3'12"E, 88°2'10"N	40.44 ± 4.01
DS-11	Chirirbandar	25°2'39"E, 88°3'28"N	29.25 ± 3.80
DS-12		25°2'32"E, 88°3'26"N	27.63 ± 4.18
DS-13	Ghodaghat	25°1'6"E, 89°1'1"N	36.97 ± 3.92
DS-14		25°1'8"E, 89°2'17"N	31.66 ± 4.53
DS-15	Hakimpur	25°1'16"E, 88°3'35"N	29.78 ± 4.24
DS-16		25°1'36"E, 88°3'24"N	35.12 ± 4.50
DS-17	Birampur	25°1'38"E, 88°2'48"N	28.08 ± 3.46
DS-18		25°1'24"E, 88°2'58"N	46.95 ± 4.60
DS-19	Nawabgonj	25°1'44"E, 89°7"N	32.73 ± 3.83
DS-20		25°1'37"E, 89°2'15"N	28.50 ± 3.93
DS-21	Phulbari	25°1'48"E, 88°3'36"N	28.18 ± 3.97
DS-22		25°1'9"E, 88°3'31"N	36.18 ± 4.29
DS-23	Parbatipur	25°2'36"E, 88°3'1"N	31.77 ± 4.69
DS-24		25°2'28"E, 88°3'10"N	27.10 ± 4.41
DS-25	Dinajpur	25°2'33"E, 88°2'21"N	34.65 ± 4.71
DS-26		25°2'35"E, 88°2'27"N	31.44 ± 3.80
Average			33.94 ± 4.21

#### 4.6 Efficiency of HPGe Detector

The efficiency of the HPGe detector was calculated for different energies i.e., different gamma emitting radionuclides by using the eq<sup>n</sup> which is given below<sup>1891</sup>:

$$Y=2358.2x^{-1.1941} \text{-----(4.5)}$$

where, x → Peak energy of gamma ray in KeV

The efficiencies of the detector for the specific energies are given in table 4.6.

Table 4.6: Efficiency calculation of High Purity Germanium (HPGe) detector for different energy.

Radionuclides	Energy (KeV)	%Efficiency
<sup>214</sup> Pb	352	2.146614
<sup>208</sup> Tl	583	1.175157
<sup>214</sup> Bi	609	1.115499
<sup>137</sup> Cs	662	1.009704
<sup>228</sup> AC	910	0.690541
<sup>228</sup> AC	968	0.641426
<sup>40</sup> K	1460	0.392669

#### 4.7 Activity of Gamma

The background radiation and the sample counts were taken for the duration of 5000 seconds after the proper setting of all parameters of the detector. The activities corresponding to the energy of 352 KeV, 583 KeV, 609 KeV, 662 KeV, 910 KeV, 968 KeV and 1460 KeV respectively of <sup>214</sup>Pb, <sup>209</sup>Tl, <sup>214</sup>Bi, <sup>137</sup>Cs, <sup>228</sup>Ac and <sup>40</sup>K were measured by using the detector counts. The activity of <sup>232</sup>Th was found by averaging the activities of <sup>208</sup>Tl (583 KeV), <sup>228</sup>Ac (910 KeV) and <sup>228</sup>Ac (968 KeV) for each sample. The activity of <sup>238</sup>U for each sample was found by averaging the activities of <sup>214</sup>Pb (352 KeV) and <sup>214</sup>Bi (609 KeV). The activities of <sup>137</sup>Cs (662 KeV) and <sup>40</sup>K (1460 KeV) were measured directly from the single channel energy counts. The formula used for the calculation of activity is given below

$$A = \frac{CPS}{\%efficiency \times P_{\gamma} \times weight(kg)} \text{ Bq / kg -----(4.6)}$$

where, A → Activity of the sample (Bq/kg)

CPS → Net counts per second (cps for sample-cps for background)

E → Counting efficiency of the specific nuclide's energy

$P_\gamma \rightarrow$  Absolute transition probability by gamma decay through the selected energy as for E.

$W \rightarrow$  Weight of the sample (kg).

Gamma activity of the soil samples collected from the Rangpur and the Dinajpur are given in Table 4.7-4.10.

Table 4.7: Activity concentration of different radionuclides in soil samples collected from different locations of Rangpur district.

Sample Identity	Location	Concentration (Bq.kg <sup>-1</sup> )						
		<sup>214</sup> Pb (352 KeV)	<sup>214</sup> Bi (609 KeV)	<sup>228</sup> Ac (910 KeV)	<sup>228</sup> Ac (968 KeV)	<sup>208</sup> Tl (583KeV)	<sup>137</sup> Cs (662KeV)	<sup>40</sup> K (1460 KeV)
Rs-1	Kaunia	63.15 ± 2.25	40.63 ± 2.75	69.80 ± 7.17	61.58 ± 7.77	24.86 ± 1.45		735.10 ± 53.24
Rs-2		84.83 ± 2.55	45.87 ± 2.84	23.75 ± 7.20	57.68 ± 7.67	21.40 ± 1.39		914.49 ± 55.15
Rs-3	Pirgacha	37.30 ± 1.99	38.10 ± 2.76	72.55 ± 7.05	29.62 ± 8.20	21.10 ± 1.46		706.12 ± 51.77
Rs-4		36.33 ± 1.97	35.72 ± 2.72	65.17 ± 6.90	18.51 ± 7.94	19.57 ± 1.43	6.75 ± 0.63	711.91 ± 51.83
Rs-5	Pirgonj	31.10 ± 2.02	28.18 ± 2.72	66.90 ± 6.72	55.35 ± 7.15	18.48 ± 1.39	7.08 ± 0.64	601.94 ± 51.77
Rs-6		47.21 ± 1.84	31.78 ± 2.37	93.03 ± 6.30	27.75 ± 6.61	21.69 ± 1.26		541.75 ± 41.78
Rs-7	Mithapukur	26.11 ± 1.62	26.36 ± 2.24	70.21 ± 5.72	65.64 ± 6.28	17.55 ± 1.16		458.40 ± 41.16
Rs-8		55.79 ± 2.03	31.11 ± 2.45	56.90 ± 6.29	42.79 ± 6.69	21.04 ± 1.27		622.52 ± 47.54
Rs-9	Gangacharda	36.32 ± 1.78	64.77 ± 2.79	90.24 ± 6.91	50.75 ± 6.35	21.02 ± 1.23		643.10 ± 46.19
Rs-10		31.52 ± 2.15	29.80 ± 3.10	65.91 ± 6.63	6.75 ± 7.62	16.98 ± 1.25		555.64 ± 47.49
Rs-11	Taragonj	83.60 ± 2.48	34.81 ± 2.64	68.50 ± 7.24	65.28 ± 7.40	19.91 ± 1.40		515.12 ± 52.98
Rs-12		33.27 ± 1.67	40.81 ± 2.50	93.07 ± 6.85	55.78 ± 7.08	23.09 ± 1.29	3.11 ± 0.40	637.95 ± 48.92
Rs-13	Badorgonj	43.12 ± 1.46	40.01 ± 3.08	89.21 ± 7.53	55.93 ± 8.05	21.13 ± 1.46	9.26 ± 0.73	758.21 ± 53.36
Rs-14		46.68 ± 2.10	44.73 ± 2.68	84.57 ± 7.45	60.41 ± 7.23	25.38 ± 1.41		764.01 ± 52.41
Rs-15	Rangpur	53.57 ± 2.31	37.17 ± 3.01	57.59 ± 7.84	15.81 ± 8.37	15.97 ± 1.49		575.48 ± 60.98
Rs-16		46.01 ± 1.86	38.95 ± 2.26	77.62 ± 6.43	45.91 ± 6.88	18.27 ± 1.25		704.84 ± 49.29
Average		47.24 ± 2.01	38.05 ± 2.68	71.56 ± 6.89	44.72 ± 7.33	20.47 ± 1.35	6.55 ± 0.6	652.91 ± 50.37

Table 4.8: Activity concentration of different radionuclides in soil samples collected from different locations of Dinajpur district

Sample Identity	Location	Concentration (Bq.kg <sup>-1</sup> )						
		<sup>214</sup> Pb (352 KeV)	<sup>214</sup> Bi (609 KeV)	<sup>228</sup> Ac (910 KeV)	<sup>228</sup> Ac (968 KeV)	<sup>208</sup> Tl (583KeV)	<sup>137</sup> Cs (662KeV)	<sup>40</sup> K (1460 KeV)
Ds-1	Biral	62.42 ± 2.23	43.51 ± 2.71	85.51 ± 7.01	59.39 ± 7.44	21.53 ± 1.38	5.05 ± 0.53	705.57 ± 51.59
Ds-2		45.13 ± 1.82	38.03 ± 2.17	45.08 ± 5.53	42.14 ± 5.97	13.03 ± 1.07		641.83 ± 43.88
Ds-3	Botchagonj	50.51 ± 1.91	43.07 ± 2.48	81.07 ± 6.33	56.53 ± 6.71	19.54 ± 1.24		499.25 ± 44.43
Ds-4		44.79 ± 1.79	27.45 ± 2.08	40.69 ± 5.97	39.76 ± 6.31	13.54 ± 1.08		524.89 ± 44.36
Ds-5	Kaharol	49.98 ± 1.92	38.48 ± 2.43	66.15 ± 6.11	41.41 ± 6.41	17.32 ± 1.21		547.67 ± 45.63
Ds-6		36.70 ± 1.59	28.80 ± 2.16	46.46 ± 5.51	20.11 ± 6.13	14.51 ± 1.11	3.12 ± 1.21	458.40 ± 42.59
Ds-7	Birgonj	48.07 ± 1.88	49.02 ± 2.59	79.49 ± 6.33	57.05 ± 6.75	20.29 ± 1.25		709.33 ± 46.94
Ds-8		21.33 ± 1.59	32.46 ± 2.19	44.02 ± 5.64	37.88 ± 6.01	14.19 ± 1.07		611.20 ± 44.61
Ds-9	Khansama	17.13 ± 1.24	33.96 ± 2.20	70.31 ± 5.78	46.01 ± 6.05	17.75 ± 1.16		553.82 ± 42.87
Ds-10		33.54 ± 1.61	30.49 ± 2.31	69.24 ± 6.31	26.10 ± 6.60	17.26 ± 1.23	2.95 ± 0.38	566.37 ± 46.50
Ds-11	Chirirbandar	36.01 ± 1.72	31.84 ± 2.10	51.27 ± 5.34	27.48 ± 5.99	15.44 ± 1.10		618.90 ± 42.76
Ds-12		32.25 ± 1.54	28.15 ± 2.13	71.48 ± 5.90	43.96 ± 6.10	15.14 ± 1.13		509.33 ± 43.14
Ds-13	Ghodaghat	33.04 ± 1.70	37.71 ± 2.51	93.75 ± 7.10	60.18 ± 7.70	26.31 ± 1.38		470.35 ± 47.55
Ds-14		33.10 ± 1.48	26.87 ± 1.10	69.12 ± 5.53	39.85 ± 5.64	13.51 ± 1.04		344.26 ± 38.68
Ds-15	Hakimpur	31.70 ± 1.95	37.63 ± 2.55	75.51 ± 6.94	51.20 ± 7.94	22.84 ± 1.41		483.76 ± 50.47
Ds-16		40.85 ± 1.87	41.87 ± 2.74	89.10 ± 7.49	101.71 ± 7.82	27.10 ± 1.46		457.52 ± 49.49
Average		38.53 ± 1.74	35.58 ± 2.28	67.39 ± 6.18	46.92 ± 6.60	18.10 ± 1.21	3.71 ± 0.71	543.90 ± 45.36

Table 4.9: Distribution of  $^{238}\text{U}$ ,  $^{232}\text{Th}$ ,  $^{137}\text{Cs}$  and  $^{40}\text{K}$  in soil samples collected from different locations of Rangpur.

Sample Identity	Location	Altitude and longitude	Concentration ( $\text{Bq.kg}^{-1}$ )			
			$^{238}\text{U}$	$^{232}\text{Th}$	$^{137}\text{Cs}$	$^{40}\text{K}$
Rs-1	Kaunia	$25^{\circ}3'5''\text{E}, 89^{\circ}1'32''\text{N}$	$51.59 \pm 2.5$	$52.08 \pm 5.46$		$735.10 \pm 53.24$
Rs-2		$25^{\circ}3'24''\text{E}, 89^{\circ}1'30''\text{N}$	$65.35 \pm 2.70$	$34.28 \pm 5.42$		$914.49 \pm 55.15$
Rs-3	Pirgacha	$25^{\circ}2'30''\text{E}, 89^{\circ}1'37''\text{N}$	$37.7 \pm 2.38$	$41.09 \pm 5.57$		$706.12 \pm 51.77$
Rs-4		$25^{\circ}1'34''\text{E}, 89^{\circ}2'23''\text{N}$	$36.03 \pm 2.35$	$34.42 \pm 5.42$	$6.75 \pm 0.63$	$711.91 \pm 51.83$
Rs-5	Pirgonj	$25^{\circ}1'27''\text{E}, 89^{\circ}1'6''\text{N}$	$29.64 \pm 2.37$	$46.91 \pm 5.09$	$7.08 \pm 0.64$	$601.94 \pm 51.77$
Rs-6		$25^{\circ}2'29''\text{E}, 89^{\circ}2'15''\text{N}$	$39.50 \pm 2.11$	$47.46 \pm 4.72$		$541.75 \pm 41.78$
Rs-7	Mithapukur	$25^{\circ}2'17''\text{E}, 89^{\circ}1'1''\text{N}$	$26.24 \pm 1.93$	$51.13 \pm 4.39$		$458.40 \pm 41.16$
Rs-8		$25^{\circ}2'14''\text{E}, 89^{\circ}1'24''\text{N}$	$43.45 \pm 2.24$	$40.24 \pm 4.75$		$622.52 \pm 47.54$
Rs-9	Gangacharda	$25^{\circ}3'14''\text{E}, 89^{\circ}36''\text{N}$	$50.55 \pm 2.29$	$54.01 \pm 4.83$		$643.10 \pm 46.19$
Rs-10		$25^{\circ}3'10''\text{E}, 89^{\circ}1'12''\text{N}$	$30.66 \pm 2.63$	$29.88 \pm 5.17$		$555.64 \pm 47.49$
Rs-11	Taragonj	$25^{\circ}3'9''\text{E}, 88^{\circ}3'54''\text{N}$	$59.21 \pm 2.56$	$51.23 \pm 5.35$		$515.12 \pm 52.98$
Rs-12		$25^{\circ}3'17''\text{E}, 88^{\circ}3'22''\text{N}$	$37.04 \pm 2.09$	$57.31 \pm 5.07$	$3.11 \pm 0.40$	$637.95 \pm 48.92$
Rs-13	Badorgonj	$25^{\circ}39''\text{E}, 89^{\circ}2''\text{N}$	$41.67 \pm 2.27$	$55.42 \pm 5.68$	$9.26 \pm 0.73$	$758.21 \pm 53.36$
Rs-14		$25^{\circ}30''\text{E}, 89^{\circ}21''\text{N}$	$45.71 \pm 2.39$	$56.79 \pm 5.36$		$764.01 \pm 52.41$
Rs-15	Rangpur	$25^{\circ}3'5''\text{E}, 89^{\circ}1'3''\text{N}$	$45.37 \pm 2.66$	$29.79 \pm 5.9$		$575.48 \pm 60.98$
Rs-16		$25^{\circ}3'7''\text{E}, 89^{\circ}1'32''\text{N}$	$42.48 \pm 2.06$	$47.27 \pm 4.85$		$704.84 \pm 49.29$
Average			$42.65 \pm 2.34$	$45.58 \pm 5.19$	$6.55 \pm 0.6$	$652.91 \pm 50.37$

Table 4.10: Distribution of  $^{238}\text{U}$ ,  $^{232}\text{Th}$ ,  $^{137}\text{Cs}$  and  $^{40}\text{K}$  in soil samples collected from different locations of Dinajpur.

Sample Identity	Location	Altitude and longitude	Concentration (Bq.kg <sup>-1</sup> )			
			$^{238}\text{U}$	$^{232}\text{Th}$	$^{137}\text{Cs}$	$^{40}\text{K}$
Ds-1	Biral	25 <sup>0</sup> 2'32"E, 88 <sup>0</sup> 1'57"N	52.97 ± 2.47	55.48 ± 5.28	5.05 ± 0.53	705.57 ± 51.59
Ds-2		25 <sup>0</sup> 2'30"E, 88 <sup>0</sup> 1'58"N	41.58 ± 2.0	33.42 ± 4.19		641.83 ± 43.88
Ds-3	Botchagonj	25 <sup>0</sup> 3'14"E, 88 <sup>0</sup> 1'45"N	46.79 ± 2.20	52.38 ± 4.76		499.25 ± 44.43
Ds-4		25 <sup>0</sup> 3'18"E, 88 <sup>0</sup> 1'43"N	36.12 ± 1.94	31.33 ± 4.45		524.89 ± 44.36
Ds-5	Kaharol	25 <sup>0</sup> 3'13"E, 88 <sup>0</sup> 2'19"N	44.23 ± 2.18	41.63 ± 4.58		547.67 ± 45.63
Ds-6		25 <sup>0</sup> 3'11"E, 88 <sup>0</sup> 2'28"N	32.75 ± 1.88	27.03 ± 4.25	3.12 ± 1.21	458.40 ± 42.59
Ds-7	Birgonj	25 <sup>0</sup> 3'36"E, 88 <sup>0</sup> 2'54"N	48.55 ± 2.24	52.38 ± 4.78		709.33 ± 46.94
Ds-8		25 <sup>0</sup> 3'38"E, 88 <sup>0</sup> 2'51"N	26.90 ± 1.89	32.03 ± 4.24		611.20 ± 44.61
Ds-9	Khansama	25 <sup>0</sup> 3'4"E, 88 <sup>0</sup> 2'50"N	25.55 ± 1.72	44.69 ± 4.33		553.82 ± 42.87
Ds-10		25 <sup>0</sup> 3'12"E, 88 <sup>0</sup> 2'10"N	32.02 ± 1.96	37.53 ± 4.71	2.95 ± 0.38	566.37 ± 46.50
Ds-11	Chirirbandar	25 <sup>0</sup> 2'39"E, 88 <sup>0</sup> 3'28"N	33.93 ± 1.91	31.40 ± 4.14		618.90 ± 42.76
Ds-12		25 <sup>0</sup> 2'32"E, 88 <sup>0</sup> 3'26"N	30.2 ± 1.84	43.53 ± 4.38		509.33 ± 43.14
Ds-13	Ghodaghat	25 <sup>0</sup> 1'6"E, 89 <sup>0</sup> 1'1"N	35.38 ± 2.11	60.08 ± 5.39		470.35 ± 47.55
Ds-14		25 <sup>0</sup> 1'8"E, 89 <sup>0</sup> 2'17"N	29.99 ± 1.29	40.83 ± 4.07		344.26 ± 38.68
Ds-15	Hakimpur	25 <sup>0</sup> 1'16"E, 88 <sup>0</sup> 3'35"N	34.67 ± 2.25	49.85 ± 5.43		483.76 ± 50.47
Ds-16		25 <sup>0</sup> 1'36"E, 88 <sup>0</sup> 3'24"N	41.36 ± 2.31	72.63 ± 5.59		457.52 ± 49.49
Average			37.06 ± 2.01	44.13 ± 4.66	3.71 ± 0.71	543.90 ± 45.36

## CHAPTER-V RESULTS AND DISCUSSION

### 5.1 Introduction

In this research work, the radioactive contents in soil samples collected from 42 different spots of Rangpur and Dinajpur were measured. The gross beta activities for the 16 samples of Rangpur and 26 of Dinajpur were calculated. The gamma activity concentrations of  $^{238}\text{U}$ ,  $^{232}\text{Th}$ ,  $^{137}\text{Cs}$  and  $^{40}\text{K}$  for the sixteen samples both from Rangpur and Dinajpur were estimated.

### 5.2 Gross Beta Activity of the Soil of Rangpur

The average gross activity was found to be  $38.61 \pm 4.55$  pCi/g with a range of  $30.17 \pm 4.30$  pCi/g to  $50.42 \pm 4.82$  pCi/g. The highest and the lowest of beta activities were found in Pirgonj and Mithapukur respectively.

### 5.3 Gross Beta Activity of the Soil of Dinajpur

The average beta activity was to be  $33.94 \pm 4.21$  pCi/g ranging from  $27.10 \pm 4.41$  pCi/g to  $46.95 \pm 4.60$  pCi/g. The lowest activity was shown in the site of Parbatipur and the highest at Birampur. These results are comparable to the beta activity found in USA<sup>126-271</sup>. Detail results were shown in chapter-4 on Table-4.4-4.5.

### 5.4 Gamma Activity for the Soil of Rangpur

#### Uranium-238 in soil:

The average concentration of  $^{238}\text{U}$  in soil samples was found to be  $42.65 \pm 2.34$  Bq/kg ranging between  $26.24 \pm 1.93$  Bq/kg and  $59.21 \pm 2.56$  Bq/kg. The highest value was found in Taragonj and the lowest was found in Mithapukur.

#### Thorium-232 in soil:

The average activity of  $^{232}\text{Th}$  was found to be  $45.58 \pm 5.19$  Bq/kg with a range of  $29.79 \pm 5.9$  Bq/kg to  $57.31 \pm 5.07$  Bq/kg. The highest activity was found in Taragonj and the lowest was at Rangpur.

#### Cesium-137 in soil:

The concentration of  $^{137}\text{Cs}$  was found only for four samples out of 16-sample. These were  $6.75 \pm 0.63$ ,  $7.08 \pm 0.64$ ,  $3.11 \pm 0.40$  and  $9.26 \pm 0.73$  Bq/kg. The average of these was  $6.55 \pm 0.6$  Bq/kg.



### **Potassium-40 in soil:**

The average activity of  $^{40}\text{K}$  was found to be  $652.91 \pm 50.37$  Bq/kg with a range of  $458.40 \pm 41.16$  Bq/kg to  $914.49 \pm 55.15$  Bq/kg. The lowest activity was found in Mithapukur and the highest in Kaunia.

A summarized result was shown in Ch-4 on Table-4.9.

### **5.5 Gamma Activity for the Soil of Dinajpur**

**Uranium-238 in soil:** The average activity of  $^{238}\text{U}$  was found to be  $37.06 \pm 2.01$  Bq/kg with a range of  $25.55 \pm 1.72$  Bq/kg to  $52.97 \pm 2.47$  Bq/kg. The lowest activity was found in Khansama and the highest in Biral.

**Thorium-232 in soil:** The average concentration of  $^{232}\text{Th}$  in soil samples was found to be  $44.13 \pm 4.66$  Bq/kg ranging between  $27.03 \pm 4.25$  Bq/kg and  $72.63 \pm 5.59$  Bq/kg. The highest value was found in Hakimpur and the lowest was found in Kaharol.

**Cesium-137 in soil:** The concentration of  $^{137}\text{Cs}$  was found only for three samples out of 16-sample. These were  $5.05 \pm 0.53$ ,  $3.12 \pm 1.21$  and  $2.95 \pm 0.38$  Bq/kg. The average of these was  $3.71 \pm 0.71$  Bq/kg.

**Potassium-40 in soil:** The average activity of  $^{40}\text{K}$  was found to be  $543.90 \pm 45.36$  Bq/kg with a range of  $344.26 \pm 38.68$  Bq/kg to  $709.33 \pm 46.94$  Bq/kg. The highest activity was found in Birgonj and the lowest was at Ghodaghat.

These findings were shown in Ch-4 on Table-4.10.

The concentrations of  $^{232}\text{Th}$  are comparable to the levels found in Egypt<sup>[61]</sup> and Taiwan<sup>[30,58]</sup> but higher than US<sup>[40]</sup> and lower than Greece<sup>[56]</sup>.

The average activities of  $^{238}\text{U}$  found in soil samples are comparable to the activities of soil in Taiwan<sup>[30,58]</sup>, Greece<sup>[56]</sup> and Spain<sup>[63]</sup> but higher than those of Egypt<sup>[75]</sup> and Louisiana<sup>[48]</sup> and lower than Hungary<sup>[36]</sup>.

The concentrations of  $^{40}\text{K}$  in the soil samples are similar to those of Spain<sup>[63]</sup> but higher than those of Egypt<sup>[75]</sup> and Hawaii<sup>[41]</sup> and lower than those of Hungary<sup>[36]</sup> and North Greece<sup>[50]</sup>.

The concentrations of  $^{137}\text{Cs}$  are comparable to the levels found in Taiwan<sup>[58]</sup> but higher than that of Montana, US<sup>[52]</sup> and lower than North Greece<sup>[50]</sup> and Hungary<sup>[36]</sup>.

## 5.6 Conclusion

The levels of radioactive concentration in the soil of our country are higher than the reported results of most of the countries in the world<sup>[16,28-31]</sup>. Over the last twenty years the elevated background radiation level had been known but the attributable cause was not ascertained. Effort has been made in this study to ascertain the cause of higher background radiation in Bangladesh.

Of the different fission products that are released and dispersed following nuclear accident, the radionuclides of  $^{90}\text{Sr}$ ,  $^{134}\text{Cs}$  and  $^{137}\text{Cs}$  may contribute varying degree of dose to the population depending on location, physical and chemical properties of the fission radionuclides and meteorological conditions prevailing during the accident. Both  $^{90}\text{Sr}$  and  $^{134}\text{Cs}$  with 2-3 y physical half-life emits a gamma ray of 0.60 MeV while  $^{137}\text{Cs}$  is a long-lived radionuclide (30y) and emits 0.662 MeV gamma of significant intensity through  $^{137}\text{Ba}$  in radioactive secular equilibrium. On the other hand,  $^{90}\text{Sr}$  also emits a beta radiation and requires extensive chemical separation for measurement. It may be mentioned that  $^{134}\text{Cs} + ^{137}\text{Cs}$  represent 66% of total dose from all fission products and the proportion of  $^{134}\text{Cs}$  to  $^{137}\text{Cs}$  is 1: 2 amounting to 44% by  $^{137}\text{Cs}$  alone. Therefore, for the control of radioactivity concentration in environmental samples  $^{137}\text{Cs}$  is used as an "Index Radionuclide" representing the entire fission products<sup>[15]</sup>. In this study, the concentration of  $^{137}\text{Cs}$  is negligible. So, the existence of  $^{90}\text{Sr}$  on soil is highly unlikely. This implies that there is no fallout effect on the environmental radioactivity due to nuclear explosion.

It can, therefore, be concluded that the geological structure of soil is the main cause of higher background radiation, but there may well be other reasons. Natural potassium ( $^{40}\text{K}$ ) could be the main source of beta-activity obtained in this work.

## REFERENCES

1. **Zbigniew Jaworowski**, "*Radiation Risk and Ethics*", *Physics Today*, Vol. 52 (9), P-24-29, 1999.
2. **D. Grabowski, M. Kurowski, W. Muszynski, B. Rubel, G. Smagala, J. Swietochowska**, "*Radioactive Contamination of Environment and Food in Poland in 1999*", Report CLOR NO 140, Central Laboratory for Radiological Protection, Warsaw, 2000.
3. **NRPB-W17**: "*The availability of soil-associated radionuclides for uptake after inadvertent ingestion by humans*", 1997.
4. **E. V. Domracheva, E. A. Aseeva, T. N. Obukhova, Y. N. Kobzev, Y. V. Olshanskaya, L. V. D'achenko, A. I. Udovichenko, A. V. Zakharova, G. I. Milyutina, V. V. Nechai and A. I. Vorobiov**, "*Cytogenetic features of leukaemias diagnosed in residents of areas contaminated after the Chernobyl nuclear accident*", *Applied Radiation and Isotopes*, Vol. 52 (5), P-1171-1177, 2000.
5. **Shadley J. D. & Dai G. Q.**, "*Cytogenic and survival adaptive responses in G-1 phase human lymphocytes*", *Mutat. Research*, Vol. 265, P-273-81, 1992.
6. **Cai L. & Liu S. J.**, "*Induction of cytogenic adaptive response of somatic and germ cells in vivo and in vitro by low dose X-irradiation*", *International Journal of Radiation Biology*, Vol. 58, P-187-94, 1990.
7. **Cardis E.**, "*Effects of low dose and low dose rates of external ionizing radiation: Cancer mortality among nuclear industry workers in three countries*", *Radiation Research*, Vol. 142, P-117-32, 1995.
8. **Davis H.G., Boice J. D., Hrubec Z. & Monson R. R.**, "*Cancer mortality in a radiation-exposed cohort of Massachusetts tuberculosis patients*", *Cancer Research*, Vol. 49, P-6130-6, 1989.
9. **Cohen B. L.**, "*The cancer risk from low level radiation*", *Health Physics*, Vol. 39, P-659-78, 1980.
10. **Rex Boyd**, "*Radioactivity, isotopes and radioisotopes from nature, nuclear reactors and cyclotrons for use in nuclear medicine*", An Occupational ANSTO Information Paper, ANSTO Research and Development, Radiopharmaceuticals Division, Royal Prince Alfred Hospital, Australia, 1997.

11. **NRPB Radiation Protection Bulletin # 167**, P-13-16, July 1995.
12. **Eric J Hall**, "*Radiation and Life*", Professor of Radiology, College of Physicians and Surgeons, Columbia University, New York, 2002.
13. **M. Sohrabi, J. U. A. M. Sohrabi, S. A. Durrani, eds.**, "*In high levels of natural radiation*", International Atomic Energy Authority, Vienna, Austria, P-39, 1990.
14. **P. C. Kesavan, L. Wei, T. Sugahara, Z. Tao, eds.**, "*In high levels of natural radiation*", Elsevier, Amsterdam, P-111, 1996.
15. **M. A. Rab Molla, A. Jalil, F. Nasreen, and S. F. Mahal**, "*Maximum units of radioactivity in foodstuffs in Bangladesh*", Nuclear Science and Applications; Bangladesh Atomic Energy Commission, Dhaka, Bangladesh. Vol. 1 (1), P-75, 1989.
16. **Shyamal Ranjan Chakraborty**, "*A study of radioactivity and radiation levels in Bangladesh for assessment of population exposure*", M. Phil. Thesis, Department of Physics, BUET, Dhaka, Bangladesh.
17. **Nuclear Issues Briefing Paper 17**, "*Radiation and the Nuclear Fuel Cycle*", Uranium Information Centre Ltd, Australia, 2001.
18. **A. P. Casarett. Radiation Biology**, Prentice Hall Inc., USA, P-76, 82-83, 1968.
19. **D. C. Lloyd, A. A. Edwards, J. E. Moquet and Y. C. Guerrero-Carbajal**, "*The role of cytogenetics in early triage of radiation casualties*", Applied Radiation and Isotopes, Vol. 52 (5), P-1107-1112, 2000.
20. **UNSCEAR (1982)**. "*Exposure from natural sources of radiation*", United Nations Scientific Committee on the Effects of Atomic Radiation, Report to the UN general assembly, 1982.
21. **Nicholas Dainiak**, "*Hematologic consequences of exposure to ionizing radiation*", Experimental Hematology, Vol. 30 (6), P-513-528, 2002.
22. **P. K. Roy**, "*Radioactivity in soil of Chittagong Hills*", M. Sc. Thesis, Department of Physics, University of Chittagong, Bangladesh.
23. **T. K. Saha**, "*Study of environmental radiation by TLD,  $\beta$ - $\gamma$  survey and  $\gamma$  - Spectrometry*", M. Sc. Thesis, Department of Physics, University of Chittagong, Bangladesh.
24. **Uttom Kumer Sarker**, "*Study of environmental radiation dose from the analysis of radioactivity in the soil of Bogra, Jaipurhat, Pabna and Sirajgonj*"

- district of Bangladesh*”, M. Sc. Thesis, Department of Physics, University of Rajshahi, Bangladesh.
25. **M. A. Karim**, “*Assessment of radiation dose from the analysis of natural and anthropogenic radionuclide concentrations in the soil of the Padma river of Rajshahi*”, M. Sc. Thesis, Department of Physics, University of Rajshahi, Bangladesh.
  26. **Michelle Huelskamp**, “*Background radiation in soil and water samples near Albuquerque*”, Sandia National Laboratories, Albuquerque, U.S.A, 1997.
  27. **D.S. Sill, C.W. Sill**, “*Simultaneous determination of the actinides in small environmental samples*”, Radioactivity & Radiochemistry, Vol. 5 (2), P-8-19, 1994.
  28. **M. A. Rab Molla and A. F. M. Salahuddin Chowdhury**, Annual Scientific Report, Health Physics Division, AECD, 1974-1976.
  29. **A. S. Mollah, S. Roy, A. F. Kuddus, K. Alam, and M. M. Rahman**, “*Environmental radioactivity monitoring*”, AERE, Technical Report 1990 and 1991, No. AERE/TR-3, Savar, Dhaka, P-45, June 1994.
  30. **Yu-Ming Lin, Pei-Huo Lin, Ching-Jiang Chen, and Ching-Chung Huang**, “*Measurement of terrestrial gamma-radiation in Taiwan*”, Republic of China, Health Physics, Vol. 52 (6), P-805-811, 1987.
  31. **Kiyoshi Shizuma, Kazuo Iwatani, Hiromi Hasai, Masaharu Hoshi, Takamitsu Oka, and Masaharu Okano**, “*<sup>137</sup>Cs concentrations in soil samples from an early survey of Hiroshima Atomic Bomb and cumulative dose estimation from the fallout.*” Vol. 71 (3), P-340-346, 1996.
  32. **Z. Papp\*, Z. Dezső, S. Daróczy**, “*Significant radioactive contamination of soil around a coal- fired thermal power plant*”, Journal of Environmental Radioactivity, Vol. 59, P-191-205, 2002.
  33. **S. Selvasekarapandian, R. Sivakumar, N. M. Manikandan, V. Meenakshisundaram, V. M. Raghunath, and V. Gajendran**, “*Natural radionuclide distribution in soils of Gudalore, India*”, Applied Radiation and Isotopes, Vol. 52 (2), P-299-306, 2000.
  34. **C. A. Papachristodoulou, P. A. Assimakopoulos, N. E. Patronis, and K. G. Ioannides**, “*Use of HPGe  $\gamma$ -ray spectrometry to assess the isotopic composition of uranium in soils*”, Journal of Environmental Radioactivity, Vol. 64 (2-3), P-195-203, 2003.

35. **J. Sannappa, M. S. Chandrashekara, L. A. Sathish, L. Paramesh, and P. Venkataramaiah**, "*Study of background radiation dose in Mysore city, Karnataka State, India*", Radiation Measurements, Vol. 37 (1), P-55-65, 2003.
36. **Z. Papp\*, Z. Dezső, S. Daróczy**, "*Measurement of radioactivity of  $^{238}\text{U}$ ,  $^{232}\text{Th}$ ,  $^{226}\text{Ra}$ ,  $^{137}\text{Cs}$ , and  $^{40}\text{K}$  in soil using direct Ge(Li)  $\gamma$ -ray spectrometry*", Journal of Radioanalytical and Nuclear Chemistry, Vol. 222 (1-2) P-171-176, 1997.
37. **M. A. Rab Molla**, Final Report, IAEA/BAEC research Contract No. 1325/RB AECD/HP/8, 1978.
38. **M. Asikainen and H. Kahlos**, "*Natural radioactivity of drinking water in Finland*", Health Physics, Vol. 39 (1), P-77-83, 1980.
39. **C. S. Chong and G. U. Ahmad**, "*Gamma activity of  $^{40}\text{K}$ ,  $^{226}\text{Ra}$ , and  $^{232}\text{Th}$  in building materials in Penang*", Health Physics, Vol. 43 (2), P-543-559, 1982.
40. **T. E. Myrck, B. A. Berven and F. F. Haywood**, "*Determination of concentrations of selected radionuclides in surface soil in the US*", Health Physics, Vol. 45 (3), P-543-559, 1983.
41. **Malcolm E. Cox and Barry L. Fankhauser**, "*Distribution of fallout of  $^{137}\text{Cs}$  in Hawaii*", Health Physics, Vol. 46 (1), P-65-71, 1984.
42. **J. G. Ackers, J. F. Den Boer, P. De Jong, and R. A. Wolschrijn**, "*Radioactivity and radon exhalation rates of building materials in the Netherlands*", The Science of The Total Environment, Vol. 45 (October), P-151-156, 1985.
43. **G. Keller and H. Muth**, "*Radiation exposure in German dwellings, some results and proposed formula for dose limitation*", The Science of The Total Environment, Vol. 45 (October), P-299-306, 1985.
44. **R. Van Dongen and J. R. D. Stoute**, "*Outdoor natural background radiation in the Netherlands*", The Science of The Total Environment, Vol. 45 (October), P-381-388, 1985.
45. **B. M. R. Green, L. Brown, K. D. Cliff, C. M. H. Driscoll, J. C. H. Miles, and A. D. Wrixon**, "*Surveys of natural radiation exposure in UK dwellings with passive and active measurement techniques*", The Science of The Total Environment, Vol. 45 (October), P-459-466, 1985.

46. **A. Rannou, C. Madelmont, and H. Renouard**, "Survey of natural radiation in France", *The Science of The Total Environment*, Vol. 45 (October), P-467-474, 1985.
47. **A. S. Mollah, G. U. Ahmad, S. R. Hussain, and M. M. Rahman**, "The natural radioactivity of some building Materials in Bangladesh", *Health Physics*, Vol. 43 (2), P-849-851, 1986.
48. **R. D. Delaune, G. L. Jones, and C. J. Smith**, "Radionuclide concentrations in Louisiana soils and sediments", *Health Physics*, Vol. 51 (2), P-239-244, 1986.
49. **P. Corvisiero, C. Salvo, P. Boccacci, G. Ricco, A. Pilot, G. Taccini, G. Scielzo, M. Corso, F. Valerio, and D. Bordo**, "Radioactivity measurements in north-west Italy after fallout from the reactor accident at Chernobyl", *Health Physics*, Vol. 53 (1), P-83-87, 1987.
50. **C. Papastefanou, M. Manolopoulou, and S. Charalambous**, "Cesium-137 in soils from Chernobyl fallout", *Health Physics*, Vol. 55 (6), P-985-987, 1988.
51. **Tieh-Chi Chu, Pao-Shen Weng, and Yu-Ming Lin**, "Changes in per capita and collective dose equivalent due to natural radiation in Taiwan (1950-1983)", *Health Physics*, Vol. 56 (2), P-201-217, 1986.
52. **Olafur Arnalds, Norman H. Cutshall and Gerald A. Nielsen**, "Cesium-137 in Montana soils", *Health Physics*, Vol. 57 (6), P-955-958, 1989.
53. **T. Yesin and N. Cakir**, "Caesium-137 and Caesium-134 levels in soil in a tea plantation in Turkey after the Chernobyl accident", *Applied Radiation and Isotopes*, Vol. 40 (3), P-209-211, 1989.
54. **S. E. Simopoulos**, "Soil sampling and <sup>137</sup>Cs analysis of the Chernobyl fallout in Greece", *Applied Radiation and Isotopes*, Vol. 40 (7), P-607-613, 1989.
55. **R. J. De. Meijer, F. J. Aldenkamp, M. J. A. M. Brummelhuis, J. F. W. Jansen, and W. Put**, "Radionuclide concentrations in the northern part of the Netherlands after the Chernobyl reactor accident", *Health Physics*, Vol. 58 (4), P-441-452, 1990.
56. **H. Florou and P. Kritidis**, "Natural radioactivity in environmental samples from an island of Volcanic origin (Milos, Aegean Sea)", *Marine Pollution Bulletin*, Vol. 22 (8), P-417-419, 1991.
57. **M. Brai, S. Bellia, R. Di Liberto, G. Dongarra, S. Hauser, F. Parello, P. Puccio, and S. Rizzo**, "Environmental gamma radiation measurements on the island of Pantelleria", *Health Physics*, Vol. 63 (3), P-356-359, 1992.

58. **Ching-Jiang Chen, Pao-Shan Weng, and Tich-Chi Chu**, “*Evaluation of natural radiation in houses built in black schist*”, Health Physics, Vol. 64 (1), P-74-78, 1993.
59. **P. Schuller, Ch. Lavengreen, and J. Handl**, “*<sup>137</sup>Cs concentration in soil, prairie plants, and milk from sites in southern Chile*”, Health Physics, Vol. 64 (2), P-157-161, 1993.
60. “*Ionizing radiation: sources and biological effects*”, United nations scientific committee on the effects of atomic radiation (UNSCEAR), 1982 Report to the general assembly, United nations, New York, 1982.
61. **N. M. Ibrahim, A. H. Abd El Ghani, S. M. Shawky, E. M. Ashraf, and M. A. Farouk**, “*Measurement of radioactivity levels in soil in the Nile Delta and Middle Egypt*”, Health Physics, Vol. 64 (6), P-620-627, 1993.
62. **A. P. Radhakarishna, H. M. Somashekarappa, Y. Narayana, and K. Siddappa**, “*A new natural background radiation area on the southern coast of India*”, Health Physics, Vol. 64 (4), P-390-395, 1993.
63. **L. S. Quindós, P. L. Fernández, J. Soto, C. Ródenas, and J. Gómez**, “*Natural radioactivity in Spanish soils*”, Health Physics, Vol. 66 (2), P-194-200, 1994.
64. “*Sources, effects, and risks of ionizing radiation*”, United nations scientific committee on the effects of atomic radiation (UNSCEAR), 1988 Report to the general assembly, United nations, New York, 1988.
65. **Man-Yin W. Tso, Chor-Yi Ng and John K. C. Leung**, “*Radon release from building materials in Hong Kong*”, Health Physics, Vol. 67 (4), P-378-384, 1994.
66. **Y. Narayana, H. M. Somashekarappa, A. P. Radhakrishna, K. M. Balakrishna, and K. Siddappa**, “*External gamma radiation dose rates in coastal Karnataka*”, Journal of Radiological Protection, Vol. 14 (3), P-257-264, 1994.
67. **John R. Meriwether, Scott F. Burns, Ronald H. Thompson, and James N. Beck**, “*Evaluation of soil radioactivities using pedologically based sampling techniques*”, Health Physics, Vol. 69 (3), P-406-409, 1995.
68. **Masayoshi Yamamoto, Tsuneo Tsukatani, and Yukio Katayama**, “*Residual radioactivity in the soil of the Semipalatinsk Nuclear Test Site in the former USSR*”, Health Physics, Vol. 71 (2), P-142-148, 1996.



69. **Shu-Ying Lai, Pao-Shan Weng, and The-Chi Chu**, "*Concentrations of  $^{137}\text{Cs}$  in soils and selected forest plants in Taiwan*", Applied Radiation and Isotopes, Vol. 47 (2), P-159-164, 1986.
70. **J. Uyttenhove, S. Pomme, B. Van Waeyenberge, F. Hardeman, J. Buysse, and J. P. Culot**, "*Survey of the  $^{137}\text{Cs}$  contamination in Belgium by in-situ gamma spectrometry, a decade after Chernobyl accident*", Health Physics, Vol. 73 (4), P-644-646, 1997.
71. **E. Gomez, F. Garcias, M. Casas, and V. Cerda**, "*Determination of  $^{137}\text{Cs}$  and  $^{90}\text{Sr}$  in calcareous soils: Geographical distribution on the island of Majorca*", Applied Radiation and Isotopes, Vol. 48 (5), P-699-704, 1997.
72. **F. K. Miah, S. Roy, M. Touhiduzzaman, and B. Alam**, "*Distribution of radionuclides in soil samples in and around Dhaka city*", Applied Radiation and Isotopes, Vol. 49 (1-2), P-133-139, 1998.
73. **N. N. Jibiri, and I. P. Farai**, "*Assessment of dose rate and collective effective dose equivalent due to terrestrial gamma radiation in the city of Lagos*", Radiation Protection Dosimetry, Vol. 76 (3), P-191-198, 1998.
74. **B. Baggoura, A. Noureddine, and M. Benkrid**, "*Level of natural and artificial radioactivity in Algeria*", Applied Radiation and Isotopes, Vol. 49 (7), P-867-873, 1998.
75. **R. H. Higgy, and M. Pimpl**, "*Natural and man-made radioactivity in soils and plants around research reactor of Inshass*", Applied Radiation and Isotopes, Vol. 49 (122), P-1709-1712, 1998.
76. **M. M. Rahman**, "*Fallout and natural radioactivity in the sand samples of costal areas and in the rock samples of north-eastern part of Bangladesh*", M.Sc. Thesis, Department of Physics, Jahangirnagar University, Dhaka, December-1991.
77. **Glenn F. Knoll**, "*Radiation Detection and Measurement*", 2nd Edition, John Wiley and Sons, Inc., USA, 1989.
78. **H. Bauser and W. Ronge**, "*The Electret Ionization Chamber: A dosimeter for long term personnel monitoring*", Health Physics; Vol. 34, P-97-102, 1978.
79. **Alan Martin and Samuel A. Harbison**, "*An Introduction to Radiation Protection*", 3rd Edition, Chapman and Hall, London, 1986.
80. **A. F. Mckinlay**, "*Thermoluminescence Dosimetry*", Medical Physics Handbooks 5, Adam Hilger Ltd, Bristol, Great Britain, 1981.

81. **Herman Cember**, "*Introduction to Health Physics*", 3rd Edition, Pergamon Press Ltd. UK, 1995.
82. **V. K. Mehta**, "*Principles of Electronics*", 5th Edition, S Chand & Company Ltd, New Delhi; 1993.
83. **William J. Price**, "*Nuclear Radiation Detection*", 2nd Edition, McGraw Hill Series in Nuclear Engineering, McGraw Hill Inc., USA, 1964.
84. **G5000 Automatic Low Level Counting System**, Gamma Products Inc.
85. **Q. He and D. E. Walling**, "*Calibration of a field-portable gamma detector to obtain in situ measurements of the <sup>137</sup>Cs inventories of cultivated soils and floodplain sediments*", Applied Radiation and Isotopes, Vol. 52 ( 4 ) , P-865-872, 2000.
86. **ORTEC Spectroscopy Amplifier Model-570**, Operating and Service Manual.
87. **High Voltage Power Supply: Nucleus Model- ORTEC 495**, Operating and Service Manual.
88. **Personal computer analyzer manual**, Aptec nuclear instruments Co. U. S. A.
89. **K. Abbas, F. Simonelli, F. D'Alberti, M. Forte and M. F. Stroosnijder**, "*Reliability of two calculation codes for efficiency calibrations of HPGe detectors*", Applied Radiation and Isotopes, Vol. 56 (5), P-703-709, 2002.
90. **A. Likar, and T. Vidmar**, "*Analysis of gamma-ray spectra from HPGe detectors field conditions without explicit energy calibration*", Applied Radiation and Isotopes, Vol. 57 (1), P-67-72, 2002.
91. **Eichrom Industries, Inc.** Procedure TCS01, Analytical Procedures Rev. 1.5, P-1-7, 1995.
92. **C.W. Sill, D.S. Sill**, "*Soiled standards for quality control in radiochemical analysis*", Radioactivity & Radiochemistry, Vol. 6(2), P-28-39, 1995.
93. **Sullivan, T.**, "*Determination of Technetium-99 in borehole waters using an extraction chromatographic resin*," 37th Annual Conference on Bioassay, Analytical and Environmental Radiochemistry. Ottawa, Canada. 1991.

## APPENDIX

### Units of Radiation, Radioactivity and their Relationships

Units are necessary for quantitative description of any physical concept. In radiological physics, units are defined by the International Commission on Radiation Units (ICRU).

The units of interest are:

- a. Radiation energy,
- b. Activity,
- c. Absorbed dose,
- d. Dose equivalent,
- e. Exposure-Air Kerma.

#### **Radiation energy:**

The unit of energy (in SI units) is the joule, but for radiation detection purposes, this unit is too large. Radiation energy is measured in electron volts (eV) and is defined as the energy attained by an electron while being accelerated through a potential of 1 volt.

The relationship between electron volts and joules is:

$$1 \text{ eV} = 1.6 \times 10^{-19} \text{ J}$$

For the case of gamma and x-ray work, energy is usually expressed as kiloelectron volts (keV) and megaelectron volts (MeV).

#### **Activity:**

The activity of a radioactive material signifies its spontaneous disintegration process. The activity of a source is defined in terms of the number of disintegrations it undergoes in one second. The unit of activity is Becquerel (Bq). One Becquerel corresponds to one disintegration per second. Formerly, the unit of activity was expressed in Curie (Ci) corresponding to  $3.7 \times 10^{10}$  disintegrations per second.

$$\begin{aligned} 1 \text{ Ci} &= 3.7 \times 10^{10} \text{ disintegrations / sec} \\ &= 3.7 \times 10^{10} \text{ Bq} \\ &= 37 \text{ GBq} \end{aligned}$$

Submultiples of Curie viz., 1 mCi (1/1000Ci) and 1 uCi (1/10<sup>6</sup>Ci) are occasionally used.

**Absorbed dose:**

The absorbed dose is the energy imparted to matter by the ionizing radiation per unit mass of the material at the place of interest.

The unit of absorbed dose is Gray (Gy).

If one joule of energy is imparted by any radiation in one kilogram of that material, the absorbed dose is 1 Gray.

Formerly, the unit of absorbed dose was rad.

1 rad = 100 ergs/gm of material.

1 Gy = 100 rad

= 10<sup>7</sup> ergs/kg or 10<sup>4</sup> ergs/gm

1 rad = 0.01 Gy.

The concept of absorbed dose applies to any medium for all types of radiation and energies. The dose is an index of energy released by the radiation of irradiated material. Dose rate in terms of rad/h or rad /year, etc. are occasionally used.

**Dose equivalent:**

The biological damage suffered by the tissue exposed to different radiation may be different. That the biological damage due to 1 Gy of alpha dose would be different from the damage due to 1 Gy of gamma dose. This is because the energy loss per unit path length for different types of radiation is different. Alpha particles, because of their larger charge and mass cause greater ionization per unit path length than gamma. Hence, 1 Gy of alpha dose is approximately 20 times more effective in causing biological damage compared to 1 Gy of gamma dose. To account this variation due to various types of radiation, a term known as the quality factor (QF) is used to modify the absorbed doses from one type to the other types of radiation.

For any type of radiation,

Quality Factor

(QF)=

Dose of reference radiation (200kV x - rays) to cause a certain amount of damage.

Dose of test radiation to cause same amount of damage.

The quality factors for various types of radiation are shown in Table-A<sup>[79]</sup>.

Table-A. Quality factors of various types of radiation.

Type of radiation	Quality Factor (QF)
X-, gamma and beta rays	1
Thermal neutrons	5
Fast neutrons	20
Alpha particles and heavy recoil nuclei	20

It is now apparent from biological damage point of view that 1 Gy of alpha dose would be equivalent to 20 Gy of gamma dose. This equivalence is calculated by multiplying the absorbed dose with the quality factor.

The unit of dose equivalence is Sievert (Sv).

Dose equivalent in Sv = Dose in Gy x QF.

Formerly, the unit of dose equivalent was rem

Dose equivalent in rem = Dose in rad x QF

1 Sv = 100 rem or

1 rem = 0.01 Sv

The concept of dose equivalent enables us to state that how much dose of alpha radiation is equivalent to the beta radiation for the cause of same biological damage. Thus, dose equivalent is an index of biological damage caused by radiation.

### **Exposure- air kerma:**

In order to obtain information about quantity of x or gamma radiation present at a place of interest the concept of exposure is utilized, which characterizes the ability of radiation to produce ionization in air.

The unit of exposure is Coulomb per kg (C/kg), which is defined as the quantity of charge either sign in Coulombs produced in 1 kg of air.

The earlier unit of exposure is Roentgen (R) which is used for x or gamma rays up to 3 MeV. This is defined as the amount of exposure due to x or gamma radiation of energy upto 3 MeV which would cause ionization which would result in 1 esu of charge of either sign in 1 cc of air at STP (Standard Temperature and Pressure.)

The two units are related thus

$$1 \text{ R} = 2.58 \times 10^4 \text{ C/kg}$$

For practical convenience, the concept of air kerma is used to specify the radiation quantity instead of exposure. Air kerma gives an idea about the energy transferred to air.

The unit of air kerma is Gray (Gy)

1 air kerma Gy = 114 R.

The usefulness of air kerma can be extended to the determination of the radiation output at a specified distance from a radiation source in terms of mGy per hour.

When a radiation source is supplied to a user, its activity is specified by the supplier in terms of GBq or Curies or their fractions. In future, air kerma rate at 1 metre distance from gamma source may be used to indicate the activity of a source. The air kerma rate at 1 metre and the activity of a gamma source can be correlated using exposure rate constant applicable for that source. For example: 37 GBq (1Ci) of Cobalt-60 gives an Air-kerma output of 11.4 mGy/h at 1 metre.

1 GBq of Cobalt-60 gives an air-kerma output of 0.31 mGy/h.

Hence, the activity of a gamma emitting radionuclide can be expressed directly terms of its radiation output in mGy/h at 1 meter from the source (Table-B) <sup>[79]</sup>.

Table –B: Radiation output in mGy/h at 1 meter from the source of gamma emitting radionuclide.

Source and activity	Air-kerma rate at 1 meter (mGy/h)	Exposure rate at 1 meter (mR/h)
Cesium – 137 1 GBq	0.077	8.86
Cobalt- 60 1 GBq	0.31	35.3
Cesium - 137 1 Ci	2.86	328
Cobalt - 60 1 Ci	11.4	1307

In addition a relationship of some biological quantities between their old and new units is shown in Table –C.

Table- C: Relationship between radiation units.

Radiological quantity	Old unit	SI unit	Relationship between units
Activity of a radioactive material	The Curie $1 \text{ Ci} = 3.7 \times 10^{10}$ dis/ sec	The Becquerel $1 \text{ Bq} = 1 \text{ dis/sec}$	$1 \text{ Bq} = 2.7 \times 10^{-11}$ Ci
Exposure	The Roentgen $1 \text{ R} = 2.58 \times 10^{-4}$ C/kg (of air)	No special named unit for exposure but the unit of ionization is C/kg	
Absorbed dose	The rad $1 \text{ rad} = 0.01 \text{ J/kg}$	The gray $1 \text{ Gy} = 1 \text{ J/kg}$	$1 \text{ Gy} = 100 \text{ rad}$
Dose equivalent	The rem $1 \text{ rem} = 1 \text{ rad} \times \text{QF}$	The Sievert $1 \text{ Sv} = 1 \text{ Gy} \times \text{QF}$	$1 \text{ Sv} = 100 \text{ rem}$

### Protection from Radiation

Because exposure to high levels of ionising radiation carries a risk, we should attempt to avoid it entirely. Even if we wanted to, this would be impossible. Radiation has always been present in the environment and in our bodies. However, we can and should minimise unnecessary exposure to significant levels of man-made radiation.

Radiation is very easily detected. There is a range of simple, sensitive instruments capable of detecting minute amounts of radiation from natural and man-made sources. There are four ways in which people are protected from identified radiation sources:

**Limiting time:** For people who are exposed to radiation in addition to natural background radiation through their work, the dose is reduced and the risk of illness essentially eliminated by limiting exposure time.

**Distance:** In the same way that heat from a fire is less the further away you are, the intensity of radiation decreases with distance from its source.

**Shielding:** Barriers of lead, concrete or water give good protection from penetrating radiation such as gamma rays. Radioactive materials are therefore often stored or handled under water, or by remote control in rooms constructed of thick concrete or lined with lead.

**Containment:** Radioactive materials are confined and kept out of the environment. Radioactive isotopes for medical use, for example, are dispensed in closed handling facilities, while nuclear reactors operate within closed systems with multiple barriers which keep the radioactive materials contained. Rooms have a reduced air pressure so that any leaks occur into the room and not out from the room.

### Measuring Ionizing Radiation

Grays and Sieverts

The human senses cannot detect radiation or discern whether a material is radioactive. However, a variety of instruments can detect and measure radiation reliably and accurately.

The amount of ionising radiation, or 'dose', received by a person is measured in terms of the energy absorbed in the body tissue, and is expressed in gray. One gray (Gy) is one joule deposited per kilogram of mass.

Equal exposure to different types of radiation expressed as gray do not however necessarily produce equal biological effects. One gray of alpha radiation, for example, will have a greater effect than one gray of beta radiation. When we talk about radiation effects, we therefore express the radiation as effective dose, in a unit called the sievert (Sv).

Regardless of the type of radiation, one sievert (Sv) of radiation produces the same biological effect.

Smaller quantities are expressed in 'millisievert' (one thousandth) or 'microsievert' (one million) of a sievert. We will use the most common unit, millisievert (mSv), here <sup>[12]</sup>.

